2

NUREG/IA-0018




# International Agreement Report

# RELAP5/MOD2 Assessment, OECD–LOFT Small Break Experiment LP–SB–03

Prepared by
S. Guntay

Paul Scherrer Institute
CH–5303 Wurenlingen, Switzerland

**Office of Nuclear Regulatory Research**
**U.S. Nuclear Regulatory Commission**
**Washington, DC 20555**

**April 1990**



Prepared as part of
The Agreement on Research Participation and Technical Exchange
under the International Thermal-Hydraulic Code Assessment
and Application Program (ICAP)

Published by
U.S. Nuclear Regulatory Commission

---

Available from

Superintendent of Documents
U.S. Government Printing Office
P.O. Box 37082
Washington, D.C. 20013-7082

and

National Technical Information Service
Springfield, VA 22161

NUREG/IA--0018

TI90 010669

# International Agreement Report

# RELAP5/MOD2 Assessment, OECD–LOFT Small Break Experiment LP–SB–03

Prepared by
S. Guntay

Paul Scherrer Institute
CH-5303 Wurenlingen, Switzerland

**Office of Nuclear Regulatory Research**
**U.S. Nuclear Regulatory Commission**
**Washington, DC 20555**

**April 1990**

Prepared as part of
The Agreement on Research Participation and Technical Exchange
under the International Thermal-Hydraulic Code Assessment
and Application Program (ICAP)

Published by
U.S. Nuclear Regulatory Commission

NOTICE

This report is based on work performed under the sponsorship of the Swiss Federal Office of Energy. The information in this report has been provided to the USNRC under the terms of the International Code Assessment and Application Program (ICAP) between the United States and Switzerland (Research Participation and Technical Exchange between the United States Nuclear Regulatory Commission and the Swiss Federal Office of Energy in the field of reactor safety research and development, May 1985). Switzerland has consented to the publication of this report as a USNRC document in order to allow the widest possible circulation among the reactor safety community. Neither the United States Government nor Switzerland or any agency thereof, or any of their employees, makes any warranty, expressed or implied, or assumes any legal liability of responsibility for any third party's use, or the results of such use, or any information, apparatus, product or process disclosed in this report, or represents that its use by such third party would not infringe privately owned rights.

# RELAP5/MOD2 Assessment. OECD-LOFT Small Break Experiment LP-SB-3

S. Guntay

ABSTRACT

An analysis of the experimental results and post-test calculations using RELAP5/MOD2 carried out for OECD-LOFT small break experiment LP-SB-3 are presented. Experiment LP-SB-3 was conducted on March 5, 1984 in the Loss-of-Fluid Test (LOFT) facility located at the Idaho National Engineering Laboratory (INEL). The experiment simulated a small cold leg break, with concurrent loss of high pressure injection system, and cooldown and recovery by feed and bleed of the steam generator secondary side and accumulator injection, respectively.

The analysis was under taken as a part of a program at EIR aimed at developing experience in using the latest generation of best estimate Loss of Coolant Accident (LOCA) analysis computer codes, and to improve understanding of Small Break LOCA transients and as well as a part of a program aimed at assessing the RELAP5/MOD2 code The latest available version (Cycle 33 to 36.1) of the code was used. The particular test selected for the analysis included several phenomena potentially relevant to any PWR plant operating in Switzerland.

This report documents a short post-test analysis of the experiment emphasizing the results of additional analysis performed during the course of this task. RELAP5/MOD2 input model and results of the post-test calculation are documented. Included in the report is the results of a sensitivity analysis which show the predicted thermal-hydraulic response to a different input model.

## SUMMARY

This report documents the post-test calculation of OECD-LOFT Experiment LP-SB-3 using the RELAP5/MOD2 computer code.

Experiment LP-SB-3 simulated a hypothetical loss-of-coolant accident (LOCA) which resulted from a 4.67 cm diameter single-ended break in the cold leg of a large commercial pressurized water reactor (PWR) with a concurrent loss of high pressure emergency core coolant injection capability. The experiment was initiated from conditions which were scaled to be representative of the design operating conditions of a large PWR; reactor power of 50 MWe, core temperature rise of 20 K, and system pressure of 14.95 MPa. The experiment provided data on (a) core heat transfer characteristics when core uncovery occurs during relatively slow boil-off conditions, (b) effectiveness of steam generator feed and bleed to depressurize and cool a highly voided system, (c) effectiveness of the accumulator injection in establishing core cooling in a highly voided system.

Results of Experiment LP-SB-3 showed that decay heat removal from the 4.66 cm diameter equivalent small break LOCA was dominated by the break flow and heat transfer to the secondary side. It was believed that during the boil-off phase, reflux condensation took place for most of the period. The possibility of condensed liquid draining back through the hot leg and into the core was supported by the asymmetrical fuel cladding temperature developments. The feed and bleed of the steam generator secondary side was effective depressurizing the system. The accumulator injection established core cooling.

The RELAP5/MOD2 computer code was shown to be valuable in understanding the physical phenomena in the experiment. Although differences in detail were observed between the calculational results and experimental data, the code generally performed well, predicting all the key events in the correct sequence and with reasonable timing.

TABLE OF CONTENTS

TABLES



FIGURES

# 1. INTRODUCTION

The Loss-of-Fluid Test (LOFT) experimental facility is a 50 MW test reactor at the Idaho National Engineering Laboratory (INEL) used for the study of Loss of Coolant Accidents, and other reactor transients. The LOFT reactor system, in particular the primary coolant system and reactor core, is a fully operational (scaled) representation of a commercial pressurized water reactor (PWR). It has a nuclear powered core and a single active (the normally intact loop), containing a U tube Steam Generator (SG) and two reactor coolant pumps in parallel branches in the cold leg. A second loop (the normally broken loop), containing passive hydraulic resistances to simulate the steam generator and pumps, is also connected, primarily for use in large break LOCA simulations.

LOFT experiment LP-SB-3[1] simulated a 4.66 cm (1.84 in) break in the cold leg of a commercial PWR. Additional features simulated were the failure of high pressure emergency core cooling injection system, and feed and bleed of the steam generator secondary side. The experiment was conducted on March 5, 1984 for the Organization for Economic Corporation and Development (OECD) consortium. This report reviews briefly the post test analysis carried out at INEL together with additional post test analysis carried out during this study and the post test calculations performed using the RELAP5/MOD2[2] (Cycles 33 to 36.1). The data deck used for the analysis was based on pre-test prediction deck used by the INEL to produce Best Estimate Prediction Document (EPD)[3]. Several improvements and corrections on the pre-test deck were done (a) to convert the deck to the RELAP5/MOD2 format, (b) to eliminate some minor errors, (c) to tune various operations (such as opening or closure of valves) according to the experimental data, (d) to apply cross cross flow junction model.

The analysis was undertaken to assess the RELAP5/MOD2 computer code, in displaying a wide range of thermal-hydraulic phenomena. These includes:

a- Primary-secondary relationship — Single and two phase forced convection
Reflux natural circulation

b-Slow boil-off
c-Core heat transfer
d-Single and two phase break flow
e-Pump performance, degradation
f-Cooldown and recovery of the plant by steam generator feed and bleed and accumulator injection

Section 2 of this document presents a short description of Experiment LP-SB-3 and discusses briefly the post-test analysis of the experiment emphasizing the new findings during the conduction of this study. The RELAP5/MOD2 code is introduced in Section 3 along with the nodalization used in the base case calculation. Section 4 discusses the results of post-test calculation and compares the results of the calculation with the data. Section 5 discusses the sensitivity study performed and compares the base and sensitivity case results. Section 6 discusses run statistics. Conclusions and recommendations are discussed in Section 7. A description of the LOFT facility is presented in Appendix A. Appendix B contains details of the input data for the base and sensitivity analyses.

## 2. DESCRIPTION AND DISCUSSION OF EXPERIMENT LP-SB-3

OECD-LOFT experiment series LP-SB-3 was designed to investigate the system thermal-hydraulic response under (a) slow coolant boil-off leading to core uncovery at high system pressure, (b) steam generator feed and bleed operation, and (c) plant recovery with accumulator injection.

A short description of Experiment LP-SB-3 and discussion of post-test analysis of the experiment beyond what was already presented in the Quick Look Report (QLR)[1] are presented in the following subsections.

### 2.1 Description of Experiment LP-SB-3

Experiment LP-SB-3 simulated a small cold leg break loss-of-coolant transient, with a scaled break size corresponding to a 4.66 cm (1.84 in.) pipe diameter in a reference commercial PWR. The experiment was initiated from conditions representative of those in a commercial PWR by opening a valve in the normally intact loop cold leg break piping. The scram was initiated on low pressure in the intact loop hot leg. The primary system depressurized rapidly until fluid saturation conditions were reached in the hot leg at about 100s, which resulted in a decrease in the primary system depressurization rate. As a result, a reduction of the break mass flow rate occurred with void formation in the coolant. Since the primary system energy loss from the break due to the size of the break was not enough to remove the decay heat energy, the heat transfer to the secondary side resulted in a higher pressurization of the secondary side which caused the main steam valve to cycle four times and to relieve the energy of the system. The primary coolant pumps continued operation until the system mass inventory was reduced to approximately 2800 Kg. Single phase forced convection before the system reached saturated conditions and two phase forced convection until the pump trip were observed. Following the pump trip, reflux condensation occurred depending on the primary-secondary relationship. The pumps during the two phase system coolant condition delivered a relatively homogeneous mixture of liquid and

steam to the intact loop cold leg and the piping upstream of the break nozzle. The primary and secondary system pressures became almost the same after the primary system reached saturation coolant conditions and remained coupled during the rest of the transient. A top to bottom slow core uncovery was observed after the system mass inventory was reduced to approximately 1750 Kg. Steam generator feed and bleed operation was initiated when the peak cladding temperature reached 987 K which let to a rapid cooldown and depressurization of the secondary side followed closely by the primary side. A partial rewet of the core from below followed the initiation of the feed and bleed. Primary pressure dropped below the accumulator set point shortly after this, causing a further pressure reduction. The accumulator injection caused core rewet from the bottom upwards and quenched the core quickly to the coolant saturation temperature. Low pressure emergency core cooling injection system (LPIS) became operational after the complete core quench at a system pressure of 1.03 MPa and provided long term cooling. The experiment was terminated one minute after the LPIS injection.

The chronology of various events for Experiment LP-SB-3 is presented in Table 1. For details of the experiment description, Reference 1 should be referred.

### 2.2 Discussion of the Experimental Results

Experimental results have already been presented in the QLR of this experiment. In order to perform the post-test analysis and compare with the data, additional post test analysis was performed to identify primary-secondary relationship and its implications. A summary of the post-test analysis emphasizing the new findings will be discussed in the following subsections.

The experiment is discussed in there sections covering (a) mass depletion, (b) core boil-off, and (c) core cooldown and recovery phases.

#### 2.2.1 Mass Depletion Phase

This phase refers to the duration of the transient between the break

initiation and primary coolant pumps trip at 1600 s.

Figure 1 and 2 present the short (150 s) and long (7000 s) term primary and secondary system pressures. The primary system depressurization under the control of subcooled break flow until about 100 s. The depressurization rate increased slightly when the pressurizer emptied at about 70 s. The primary system depressurized to saturation conditions in the break piping upstream of the break at about 100 s after the break initiation and the primary-secondary pressure coupling was established. The core reached saturation at about 200 s. Energy addition to the primary system from the decay heat and primary pump heat was mainly removed by the break flow and by heat transfer to the steam generator secondary side. The heat input to the secondary side was relieved by periodic cycling of the main steam control valve (MSCV) during the first 1030 s of the transient. Figure 3 presents the steam generator secondary pressure with the opening and closure set points. It appears that instrument noise caused the valve to open or close exceeding or without actually reaching the valve set point. The valve did not seat 100 % nor did it seat the same closure, yielded different leakage from the steam generator during different periods of the experiment. After the last closure of the valve, the steam generator pressure showed a similar pressure increase to the pressure rise rates occurred during the earlier closures. After it reached a pressure some where between the opening and closure set points, the pressure increase ceased and started dropping. Two different mechanism might be responsible for this. The first is that the steam valve's fourth closure position let more steam leakage than the previous closure positions. And the second is that the heat generation in the primary side was not enough to cope with the energy loss from the system, which could also be related to the first mechanism. The primary and secondary systems showed a continuous pressure drop after the fourth MSCV cycling until the break was isolated.

After the saturation coolant condition was established in the break line at about 100 s, the fluid density at the break continued to decrease due to voidage of the fluid in the break line was increased. Figure 4 and 5 present the break line density and mass flow rate. Increased voidage in the primary coolant system decreased the break flow.

Fluid densities in the intact loop hot and cold legs are presented in Figures 6 and 7. As a result of MSCV cycling, increased cooling in the steam generator tube bundle affected the intact loop cold leg density and the intact loop hot leg fluid velocity which is shown in Figure 8. The differential pressure across the pump continuously decreased as the primary coolant voidage increased. Oscillation in the pump differential pressure started at around 700 s at a vapor fraction at the primary coolant pump inlet of 40 %. The oscillations seen in Figure 9 continued until 875 s. Although pump operation caused a homogeneous density in the intact loop cold leg, onset of fluid stratification as indicated by the density measurements in the intact loop hot leg (Figure 6) occurred shortly after the abrupt drop in pump differential pressure at 875 s. The pump operation continued until 2800 Kg mass in the system remained. The actual remaining inventory was 800 Kg more than the desired 2000 Kg as specified in Experiment Specification Document (ESD)[4].

### 2.2.2 Core Boil-Off Phase

This section discusses the core boil-off phase which refers to the duration of the transient between the primary coolant pump trip at 1600 s and the steam generator feed and bleed operation.

Cessation of the pump operation caused also fluid stratification in the intact loop cold leg as seen from the cold leg density measurements as illustrated in Figure 7. This stratification caused the break plane to become uncovered. Thereafter, the break flow was high quality steam. Consequently, the primary system depressurization rate was increased. The other affect of the pump trip was on the pump seal density and mass inventory. Since the fluid in the suction and as well as in the discharge piping collapsed with the pump coastdown, the liquid collected in the loop seal caused immediate density increase in the loop seal as presented in Figure 10. The loop seal remained covered afterwards and prevented natural loop circulation. The secondary system pressure followed the primary response, and both pressures decreased at 0.8 kPa/s rate.

A slow boil-off process was taking place in the reactor vessel governed by (a) decay heat energy addition to the fluid, (b) break mass flow, and (c) primary-secondary heat transfer rate. The upper portion of the core showed dryout at about 3800 s, when the primary system mass inventory fell to approximately 1750 Kg. The dryout progressed towards bottom of the core. Based on the dryout times indicated by the cladding thermocouples, the rate of core uncovery rate was about 1.8 mm/s when the dryout level was within the upper 1/3 of the core, and was reduced to 1.1 mm/s when the dryout level was between 2/3 and 1/3 of the core height. The boil-off rate decreased as the core become uncovered because less energy was transferred into the fluid from the lower portion of the core below the peak-power region which is 0.68 m above the core inlet. The cladding temperature measurements below 0.13 m elevation indicated that the core was not completely uncovered. Figure 11 presents the fuel cladding temperatures in the center bundle. Figures 12 presents the fuel cladding radial temperature response at the 1.14 m elevation. Differences in the heat up rates at (a) different axial elevations and (b) at different radial locations were observed. The QLR suggested that a small amount of entrained water carried up into the core slowed the heat up rate at higher elevations. The difference in the heat up rate in the radial direction was explained with the difference in the radial power factors. Further analysis of the primary-secondary relationship indicated that the indicated differences were more likely as a result of liquid drainback from the hot leg, generated due to reflux condensation in the steam generator tubes and its re-evaporation in the core. Detailed discussion of the primary and the secondary relationship is given in the following subsections.

### 2.2.3 Discussion of Primary-Secondary Relationship During Experiment LP-SB-3

Post-test examination of the measured pressures and temperatures in the primary and secondary sides and the conditions existing in the inlet and outlet plena provided that reflux condensation was occurring when the primary side pressure and/or temperature was higher than the secondary pressure and/or temperature during the boil-off phase. This conclusion was further supported by the RELAP5/MOD2 post-test calculations and will be presented in Section 3. The possibility of drainback of the

condensed liquid through the hot leg into the core and interpretation of various data providing evidence to this conclusion are discussed in the following two subsections.

2.2.3.1 Reflux Condensation and Heat Transfer to the Secondary Side

Pressure differential between the primary and secondary systems is presented in Figure 13. As the core uncovery progressed, due to lesser energy transfer to the fluid, and at the same time due to continuous energy loss from the break, the primary side pressure dropped below the secondary side pressure at about 4300 s. The primary side pressure remained below the secondary level until about 4900 s, slightly after the break isolation at 4750 s. During this time period the secondary temperature was higher, as illustrated in Figure 14, than the saturation temperature of the hot leg. Outside of this period it was believed that condensation was taking place in the steam generator tubes below the secondary liquid level, especially close to the tube sheet and forcing the primary pressure to follow that of the secondary pressure. The condensation heat transfer in the steam generator tubes was the additional heat removal mechanism in the primary side besides the heat removal via the break flow. After the break was isolated, it became the only heat removal mechanism in the primary system other than the heat loss to the environment. The sharp change in the slope of the pressure differential suggests that the condensation heat transfer was reestablished just after the break isolation, presumably increased in magnitude to compensate the loss of the primary side energy outflow via the break flow. Therefore, the condensation heat transfer became an essential factor in the overall heat balance existing in the primary system.

The heat transfer from from the primary to secondary side was estimated to be 50 to 150 kW in the QLR with the lower bound attained which the pressure differential was negative. On an approximate basis, the actual heat transfer can be excepted between zero to 100 kW with a 50 kW offset to eliminate the heat from the metal work ( which was not taken into consideration in the QLR) and the instrument (which indirectly measures

the steam generator level) uncertainties. A heat transfer of probable 50 kW is equivalent to a condensation rate of 30 g/s[5] in the primary tubes.

2.2.3.2 Liquid Drainback and its Effect on Fuel Rod Temperature Some of the condensate that formed in the upside might have probably drained back into the vessel. The indirect evidences of this drainback outside of the 4300-4900 s period were (a) the thermocouples in the steam generator plena showed that saturation conditions persisted in those regions during the entire period except from 4200 s to 5000 s, when superheat was measured (the steam superheat shown in Figure 15 was due primarily to hot wall effects), (b) the upper end box thermocouples which showed typically 200 K lower temperature in fuel module 4 (which is the nearest to the intact loop hot leg) than in equivalent ones in modules 2 and 6, (c) cladding temperatures in modules 4 were asymmetrically lower than in modules 2 and 6; by 60 K at 1.14 m, by 50 K at 0.76 m, and approximately equal at 0.28 m above the core inlet, and (d) the fuel heat up rate, as seen in Figure 12, considerably decreased after 4900 s with the reestablishment of the reflux condensation, and (e) corner module liquid level probes, as illustrated in Figure 16, showed that the probe at 1.77 m elevation above the core inlet was wet outside of the negative pressure differential period (4300 to 4900 s) although the dryout level was well in progress in the core.

2.2.4 Core Cooldown and Recovery Phase

This phase refers to the duration of the transient starting with the initiation of the feed and bleed operation at 5415 s and with experiment termination at 6845 s.

The feed and bleed operation was initiated at 5415 s when the peak cladding temperature in the core reached 987 K. The feed and bleed operation was affective as anticipated to depressurize the system at an increased rate and to terminate the cladding heatup and even caused the lower section (below 0.38 m elevation) of the core quenched as seen in Figure 11. The primary system pressure dropped to the accumulator injection set point in about 140 s. The fuel cladding cooling induced by the

steam generator feed and bleed operation was enhanced by the initiation of the accumulator. The core was completely quenched and refilled in 242 s after the accumulator injection started.

## 3. RELAP5/MOD2 COMPUTER CODE SIMULATION OF EXPERIMENT LP-SB-3

The RELAP5/MOD2 computer code was used for the post-test calculation of Experiment LP-SB-3. RELAP5/MOD2 is an advanced, best estimate computer program developed at the Idaho National Engineering Laboratory (INEL) for the analysis of Loss-of-Coolant Accident (LOCA) and other PWR transients. The specific application of the code to the experiment LP-SB-3 post-test simulation is discussed in this section.

### 3.1 RELAP5/MOD2 Description

RELAP5/MOD2 employs a finite-difference fluid cell representation of the primary and secondary coolant systems. The six-equation hydrodynamic formulation employs separate equations to describe the conservation of mass, momentum and energy for liquid and steam within each fluid cell. The description of the hydrodynamics is essentially one dimensional within each fluid cell. The inclusion of a simplified treatment of the conservation of momentum in the direction perpendicular to the main stream flow, where cross flow occurs between parallel volumes and in branches, brings a special treatment of two-dimensional effects.

Description of the hydrodynamics of choked flow, stratified flow, and abrupt area changes are carried out with special process models. Special models are included for simulation of particular components, such as pumps and accumulators. Flow-regime-dependent constitutive equations and heat transfer packages are incorporated to complement the hydrodynamic description. Conduction of heat within metalwork or fuel rods is calculated with one-dimensional (two-dimensional in fuel cladding for reflooding simulation) finite difference formulation. A powerful control and trip logic capability is built into the code.

## 3.2 RELAP5/MOD2 Nodalization and Input Model for Experiment LP-SB-3

The nodalization used for the base case calculation was based on the RELAP5/MOD1 input deck that was used for the planning and prediction of the experiment at the INEL. The deck was first converted to the RELAP5/MOD2 format and following changes were applied :

a- to utilize cross flow junction model at the pressurizer connection to the hot leg to obtain an improved pressurizer drainage,

b- to correct minor errors in the main steam valve flow area, and in some of the control variables mainly calculating heat loss, mass etc,

c- to tune various valve opening and closure timing.

Figure 17 presents the nodalization diagram used for the base case calculation. Some more updates were done during the steady state calculations and early phase of the transient in order to:

a-match the by pass leak flows between the downcomer and upper plenum and through the reflood assist piping valve with the experience,

b-tune drainage timing of the pressurizer by increasing flow loss coefficients of the surge line,

c-tune MSCV leak to match the first MSCV cycling time,

d-reorientate the by-pass flow junction connecting the downcomer upper annulus to upper plenum upper volume to avoid subcooled state being calculated in the upper two volumes of the upper plenum. The final connection was between the downcomer upper annulus and the upper plenum nozzle area.

The final version of the input data listing is supplied in Appendix B.

The input model consists a total of 32 fluid cells for the vessel and 100 cells for the remainder of the primary, secondary and ECC systems. Characteristics of the model are as follows :

a- a split downcomer upper annulus was used with the cross flow connections,

b- filler gap was separately modeled,

c- core was modeled by a average channel approach and represented by

six equal length heat slabs,

d- reactor vessel internals and loop piping, pressurizer and steam generator walls were simulated with heat slabs. Heat losses from the piping to the environment was modeled,

e- steam leak through the steam valve was specially modeled,

e- one velocity break flow model was used at the break. Discharge coefficients for the subcooled and saturated flows were 0.93 and 0.81, respectively.

## 4. RESULTS OF RELAP5/MOD2 POST-TEST CALCULATION

This section presents the thermal-hydraulic results of Experiment LP-SB-3 post-test calculation. Prior to performing the post-test calculation, a steady state calculation was performed to obtain the initial conditions measured during the experiment. Following the steady state calculation, transient calculation was started with the trip set points taken from the experiment. The following subsections discuss the steady state and transient calculations.

### 4.1 Calculation of the Steady State

Using a steady state controller package the simulated LOFT system was brought to the required initial conditions. At first, steady state option of RELAP5/MOD2 was used to automatically terminate the calculation when the required steady state was achieved. However, this option terminated the calculation at a time when various key parameters were too far off from their steady state values. Therefore, the steady state calculation was performed with the transient option. The calculation was continued until the observed variations of the calculated values of these parameters from their desired values were acceptable. The key parameters controlled using the control variables were the primary system pressure, pressurizer level, cold leg temperature, primary system mass flow rate and steam generator secondary level. The behaviors of the secondary side feed and steam flows, pump speed and head, pressurizer heater power, pressurizer spray valve and steam generator main steam valve positions, and primary side charge or let down flows were the other parameters checked for the

steady state.

The system pressure was controlled by the pressurizer spray which injected cold leg fluid to the pressurizer to reduce the pressure if the pressure was calculated to be greater than the measured value. The second controller on the system pressure was the pressurizer heaters. These heaters were charged if the pressure was lower than the set point. These heaters, although in reality were located close to the bottom of the pressurizer, were placed at the mixture level in the RELAP5 model to increase the boiling. The pressurizer level was controlled by two controllers. One controller which charged fluid at the cold leg temperature to the cold leg if the pressurizer level was lower than the set point. The second controller dumped the system fluid to a time dependent volume if the pressurizer liquid level was higher than the set point. The final values of the primary pressure and pressurizer level were calculated to be almost the same as their measured values. The final valve positions controlling the pressurizer spray, primary system charge or let down flows were zero. The final pressurizer heater power was zero. The pressurizer surge line flow was negligible at the end of the steady state calculation.

The primary loop flow was adjusted by using a proportional/integral controller based on loop flow error to control pump speed. The steady state intact loop flow was calculated to be the same as the experimental equivalent. The pump speed and head were in agreement with the measured initial values. The broken loop flow (from the vessel to the cold leg and via the reflood assist valve to the hot leg and back to the vessel) was small and based on the leak flow through the reflood assists by-pass valve. The total by-pass leak flow based on the flow loss coefficients used in the INEL deck was calculated to be about 2% of the total loop flow. This value compared with the generally accepted 7% of the loop flow was considered to be too low.

The cold leg temperature was controlled by the main steam valve position with a proportional/integral control system. Based on the steam flow rate and heat transfer to the secondary side, the code calculated the secondary system pressure. Another control logic was used to adjust the feed flow to control the steam generator required level. This controller

was also coupled to the main steam flow. The steam generator level, main steam and feed water flows were calculated to be the same as measured. Although the steam and feed water flow rates were correctly calculated, the steam generator secondary side pressure was the only parameter being calculated offset by 0.35 Mpa from the measured equivalent.

After about 300 s of calculation the steady state was considered acceptably stable. Two 150 s long steady state calculations as a continuation to the previous run were performed:

a-to increase the total by-pass leak flows by decreasing the flow loss coefficients of the two leak junctions,

b- to increase the secondary side pressure.

The system reached steady state condition and become stable during the first 150 s long transient and the total by-pass leak flow was calculated to be 4.5% of the total loop flow. Further trials to increase the by-pass leak to the generally accepted level were not done due to the computer cost. The final value was accepted to be adequate. Despite of the trials done to increase the steam generator secondary pressure, no success was reached. The complex geometry and atypical internal structure of the steam generator with rather simple nodalization were possible causes of the problem.

### 4.2 Transient Calculation

After the steady state was considered stable, various steady state controllers associated with the pressurizer heaters, pressurizer spray, primary system mass charger and let down, pump speed, and various valve position were removed. The trips for various actions were defined based on the measured data. Table 2 compares the calculated and the measured steady state values. The transient calculation was started from time zero and using the last restart record in the steady state plot-restart file. The complete transient was calculated in three major restarts. Each restart used the recent code version available at the time of the run. These were the cycles 33, 35, and 36.

The course of the calculated simulation is discussed in the same phases that were analyzed in Section 2, namely : (a) mass depletion, (b) core boil-off, and (c) core cooldown and recovery phases. Table 1 compares the timing of various events calculated and measured.

4.2.1 Mass Depletion Phase

This phase begun with the opening of the break, defined as time zero. Reactor scram followed rapidly (measured at 9.21 s, calculated at 10.746 s) when the hot leg pressure fell to the scram setpoint of 14.19 MPa. The steam generator main steam control valve was closed and feed was isolated upon scram. Primary system coolant pumps were left running until the primary system inventory fell to 2800 Kg from an initial inventory of 5600 Kg.

4.2.1.1 Primary and Secondary System Pressure Behavior Calculated and measured intact loop hot leg and steam generator pressures during the mass depletion phase are shown respectively in Figure 18 and 19 Primary pressure dropped rapidly under the control of the subcooled blowdown. After the pressurizer level dropped below its indicating range (corresponding to approximately 8 cm of the calculated level at this time), the calculated and measured system pressures showed an increased depressurization rate. This trend continued until saturation condition was reached at 99 s in the break line upstream of the break during the experiment, but ceased in the calculation about 15 s after the pressurizer became empty. This reduction in the calculated depresurization rate caused the simulated system to reach the end of blowdown condition at about 200 s. The difference between the depressurization rates measured between 70 and 99 s and calculated between 77 and 200 s was believed to be associated with (a) poor modeling of the pressurizer surge line and (b) the water remaining below the surge line entrance after the pressurizer level showed below its indicating range and effect of flashing of this water on the system pressure response. It was doubtful that flow loss coefficients representing the entrance effects and also the bends in the line and the nodalization of the 7 meter line with three fluid cells were adequately modeled. However, for a long experiment having major phenomena occurring a couple of thousand seconds later, it was believed

that this time shift did not affect the subsequent thermal-hydraulic phenomena. The calculated primary system pressure was controlled thereafter by the secondary side pressure as in the experiment.

After the main steam control valve was closed and the feed water was isolated, the secondary side pressure reached the cycling pressure of 7.12 MPa (measured at 87.5 s, and calculated at 76.5 s). The first cycle was followed by three more cycles, the last one being measured at 1030 s and calculated at 1175 s. The difference between the measured and calculated cycle times were associated with the different opening and closure set points observed during the measurement. After the last cycling, the calculated secondary pressure continued to increase further, although the measured pressurize increase ceased shortly after the valve was (supposedly ) closed. This difference was believed to be either as a result of improper valve seat position which resulted in more leak then calculated or more energy transfer calculated to the secondary side. Calculated primary and secondary pressures were overall in agreement with the data except with small deviations due to main steam valve cycling behavior.

4.2.1.2 Break Flow Calculated and measured break flows are shown in Figure 20. The break flow rose from from zero rapidly to a peak of 6.4 Kg/s in the calculation and to 6.7 Kg/s in the experiment than fell to 2.5 Kg/s at the end of the subcooled break flow period and to 1.3 Kg/s just prior to the pump trip. The break flow calculation except with minor differences associated with the pressure behavior was in excellent agreement with the data.

4.2.1.3 Density Comparison of the measured and calculated densities in the intact loop hot and cold legs are shown respectively in Figure 21 and 22. Similar comparison in the break piping is shown in Figure 23. Overprediction of the density in the hot leg was a result of the difference between the calculated and measured secondary system pressures after the fourth main steam valve cycle and its consequent effect on the primary system pressure. The calculated beak line density was surprisingly well in agreement with the data.

3.6.1.4 Pump behavior Calculated and measured pump pressure differential are displayed in Figure 24. After the subcooled blowdown ended the pump pressure differential showed a continuous decrease. The code calculated the pump degradation indicated in Section 2 slightly later The oscillations seen in the data were also observed in the calculated pump performance but being small in magnitude. The pump homologous curves (mainly were developed based on the Semiscale pumps[6] and partially modified using LOFT L3-6 experimental data[7]) used for this calculation was responsible for this difference. An excellent agreement between the calculated pump differential pressure and the data existed after about 1300 s in the transient.

4.2.1.5 System Mass Inventory Figure 25 presents a comparison of the primary system mass inventories. An excellent agreement was reached as a result of a good break mass flow calculation. The 2800 Kg inventory was calculated at 1618 s and measured at 1600 s.

4.2.2 Core Boil-Off Phase

This phase starts with the pump trip and continues until the peak cladding temperature reaches 987 K to initiate feed and bleed operation.

4.2.2.1 Primary and Secondary System Pressure Behavior Comparisons of calculated and measured primary and secondary pressures are presented in Figures 26 and 27, respectively. The primary side was depressurizing as the break discharged almost pure steam. The data (Figure 13) showed that the primary side pressure fell below the secondary level only after the core uncovery was started. The code calculated similar trend except between 2300 and 3000 s. when the secondary side pressure was higher than the primary side as illustrated in Figure 28. This discrepancy was related to a trip logic which did not activate the steam valve leak although the main steam valve was close. The leak was designed to be activated whenever the steam generator pressure fell below the main steam valve closure set point. After the last cycle, in absence of this leak, it took quite a long time until the secondary pressure fell below the valve closure set point and then the leak was activated.

The primary pressure was not calculated to fall below the secondary pressure after the heat up started. This was due to late core uncovery calculation, which caused the simulated primary system received slightly more heat from the core. The core begun to uncover (measured at 3800 s, calculated at 4008 s) and hence the heat transfer to primary fluid was reduced. This increased the depressurization rate and the hot leg saturation temperature fell below the secondary temperature (measured at 4300 s, calculated at 4325 s) as presented in Figure 29 and 14 where the calculated and measured primary secondary temperature differences are presented. The sign of the calculated temperature difference reversed, as in the experiment, shortly after the break isolation at about 4905 s. The calculated primary secondary pressure difference was much smaller than the measured difference. As a result of this, the primary secondary temperature difference was less than the measured difference. Figure 30 presents the condensation rate (negative vapor generation rate) in the steam generator upright (Volume 115020000). Figure 31 presents the liquid flow flowing into the steam generator inlet plenum. The code calculated condensation in the steam generator tubes. The amount of total condensate was generated at an approximately 40 g/s rate. A reasonable condensation axial distribution was calculated in the steam generator tubes, with maximum condensation rate being calculated in the cells next to the tube sheet and no condensation being calculated in the cells of which outside pipe surface was uncovered. The condensation ceased in the steam generator tubes except in the very lower cell at about the initiation of the core uncovery. The amount of condensation calculated might be smaller than what actually occurred during the experiment due to the calculation of smaller primary-secondary temperature difference. Figure 32 presents the steam and liquid flow rates in the intact loop hot leg (Volume 100010000). The code also calculated condensation in the hot leg due to the heat transfer to the environment. For a very long transient, the piping inner wall should be at the saturation temperature of the system couple of thousand seconds in the transient and act as a heat sink. Since there was no data taken to indicate the transient heat loss from the piping, it was not possible to verify the calculated condensation rate. The other important conclusion from Figure 32 is that the liquid and steam flow rates were the same indicating that the heat and mass transfer and

resultant mass balance were calculated properly. The calculated reflux condensation in the steam generator upright was restored after the break isolation. Although the code was not able to calculate the primary secondary pressure crossover due to different core uncovery timing, the primary and secondary pressures and continuation of reflux condensation were satisfactorily calculated.

4.2.2.2 Density Figures 33 and 34 present a comparison of the measured and calculated densities in the intact loop hot and cold legs, respectively. After the pump trip the liquid in the system fell to the lower part of the loop, e.i, to the reactor pressure vessel and loop seals, therefore, a sharp reductions in the densities in the hot and cold leg was calculated similar to the measured reductions. The code calculated the liquid build up in the loop seal, as illustrated in Figure 35, and the reactor vessel, as illustrated in Figure 36 where the collapsed liquid level in the reactor vessel is shown. The recoveries seen in the measured hot and cold leg densities immediately following the indicated drops were very well calculated by the code.

4.2.2.3 Break Flow As noted above, the break flow was of single phase throughout the boil-off phase, and was very accurately calculated, as presented in Figure 37.

4.2.2.4 Core Dryout and Thermal Response Figure 38, adopted from the OLR, presents the measured core dryout information based on the thermocouples and liquid level probes and also overlaid are the RELAP core heat slab nodalization and calculated dryout times. RELAP5/MOD2 calculated the dryout initiation in the core approximately 200 s later then earliest measured dryout based on the thermocouple readings. This figure shows that the dryout time at 1.397 m (55 in) elevation (which corresponds to the bottom of the top most heat slab) occurred sometime between 3830 s (implied by fuel cladding thermocouple reading) and 4032 s (implied by the corner module level probe) (possibly later as will be explained below). The center bundle thermocouples showed dryout earlier than the dryout indicated by the center bundle liquid level probes and much earlier than the dryout indicated by the corner bundle liquid probes.

The code (due to the heat transfer logic) waited until the void fraction in a volume associated with a heat slab reached a critical void fraction (which is 0.99999 ) after which it could pass to post-dryout heat transfer mode. Therefore, the calculated dryout times were more relevant to the dryout indicated by the liquid level probes than the dryout times of the center bundle cladding thermocouples. The late dryout indicated by the corner channel liquid probe was believed to be a result of the liquid drainback from the hot leg before 4300 s or after 4900 s. Since this corner probe was located under the broken loop hot leg, it could be arguable that the condensed liquid draining back from the intact loop hot leg was more effective on the dryout of the fuel moduls 7,4 and 8 which were just under this leg. Since the code considered homogeneous distribution of the drained liquid in the nozzle area, which was believed not to be the case, and homogenous downward liquid flow, the net effect of this drained liquid postponed the dryout of the core. There were three more uncertain areas which might be responsible for this late dryout. These are: (a) not accurate mass distribution in the primary system, (b) over estimation of the amount of condensation occurring in the hot leg, and (c) smaller pressure differential between the hot and cold legs.

Since the code predicted a correct mass inventory in the system as seen in Figure 25, the distribution of the mass in the system might be wrong due to artificial liquid hold up in the hot leg before the dryout begun and afterwards excessive liquid draining back to the core prevented the dryout. Because of the center of gravity of the simulated hot or cold legs are at a different elevation than the center of gravity of the connected volume in the vessel, liquid hold up might be a problem due to improper connection simulation. A sensitivity analysis in which the cross flow connection of the legs to the vessel was planned to investigate the effect of the cross flow junction model on the dryout initiation.

Since there was no data available to indicate the amount of heat loss from the hot leg which determines the amount of condensation, no further analysis was planned.

These junctions might have created a lower back pressure in the upper plenum than might have consequently caused the liquid to be hanging in the core longer and resulted in late dryout. Since the flow loss

coefficients of the by-pass junctions were decreased during the early phase of the calculation to increase the by-pass leak flow, another sensitivity was not planned.

Although the code calculated slightly late initiation of the dryout and slightly higher core uncovery rate, initiation and progress of the dryout was successfully calculated. The calculation indicated that the core was never completely dryed out, as was in the experiment.

Figures 39 to 44 present a comparison of the thermocouple data with the calculated temperatures at levels 1 to 6. Calculated temperatures at adiabatic boundary condition are also overlaid. It can be seen that the initial heat up was almost adiabatic, both in the calculated (except at the sixth elevation) and measured data. As significant cladding to coolant temperature difference was established more heat transferred to the steam and the heat up rate, although being higher in the calculation, fell below the adiabatic rate.

The measured heat up rate at the top of the core was greater than the adiabatic as the steam temperature was above the cladding temperature and heat was transferred to the fuel. The calculated cladding temperature response at the highest core elevation was different than the measured response due to the followings:

a- the draining liquid was avoiding the heat up of this slab until the reflux condensation in the steam generator upright ceased at about 4500 s. After this time the heat up rate was approximately the same as the measurement,

b- the reflux condensation in the steam generator upright started again at about 4930 s in the calculation and caused an affective cooling at this elevation.

Since the incoming liquid was considerably evaporated in the sixth core volume, the liquid draining back to the lower core elevations did not affect the other heat slabs. However, in the experiment, the draining liquid was probably more effective on the fuel rods in the fuel modules 7,4 and 6 after 4900 s. It reduced the cladding and the steam temperatures and created considerable radial temperature differential between the center

of the core and the filler blocks. Since the LOFT core is a small core where center to filler block distance only 23 times the fuel pitch, this temperature differential considerably increased the radiation (especially above 700 K) and convective heat transfers especially from the rods in the center bundle, which in turn reduced the heatup rate extensively as seen in Figures 39 to 41. Since three dimensional behavior of the liquid drainback into the core was not modeled and the code did not have the radiation heat transfer model, the calculated temperature excursion rates at the second to the fifth core elevations were much higher than the measured rate. Therefore, the time at which the maximum core temperature of 816 K was reached (to initiate the closure of the break valve) was calculated only 163 s later than the measured 4742 s, although the dryout was calculated approximately 200 s later at the hot temperature elevation.

4.2.3 Core Cooling and Recovery Phase

At a peak core cladding temperature of 987 K, the main steam valve was opened to blow the steam generator and at the same time the feed water flow was restored. This commenced the feed and bleed phase of the experiment, the time was 5415 s in the experiment and 5186 s in the calculation. The feed and bleed operation caused the system to depressurize to the accumulator injection set point at 5558 s in the experiment and at 5360 s in the calculation. Accumulator injection enhanced the cooling of the system and the system pressure was further reduced to LPIS injection set point at 6785 s in the experiment and at 6222 s in the calculation. The experiment was terminated at 6845 s while the calculations was stopped at 6560 s.

4.2.3.1 Primary and Secondary System Pressure Behavior. Feed and bleed in the steam generator caused a rapid drop in the secondary side pressure, followed closely by the highly voided primary system, showing that secondary feed and bleed operation was an effective recovery procedure from a small break LOCA with no HPIS injection. Figures 45 and 46 present a comparison of the measured calculated primary and secondary system pressures, respectively. The rate of depressurization was very well predicted, except with a slight time shifting caused by the

calculated core thermal response during the boil-off phase.

4.2.3.2 Core Thermal Behavior With the feed and bleed operation, the increased condensation in the steam generator caused an increase in the steam velocity, and therefore entrainment in the core. This, coupled with the level swell caused by the reduction in the pressure resulted in a partial rewet of the core from bottom up ( Figure 40). The rewet at the core level below 0.38 m above the core inlet was followed by a re-dryout. This re-dryout seen was not calculated. The upper section of the core above 0.38 m above the core inlet started to decrease in temperature. The code properly calculated the increase in the steam velocity in the core This was evident from the increase in the temperature of the upper most heat slab (Figure 44). But this increase ceased and temperature of this heat slab decreased with the increased cooling in the core. The other core elevations showed a sharp decrease in temperature until accumulator injection. The indicated temperature decrease was further enhanced by the accumulator injection as in the experiment. The difference between the calculated and measured temperature reduction rates during the period between the feed and bleed operation and accumulator injection was due to:

a- entrainment calculation,
b- steam condensation calculation in the steam generator upright and its drain back to the core,
c- calculated heat transfer coefficient.

The code might have possibly calculated more entrainment which increased the cooling excessively at elevation higher than 0.38 m In the experiment, possibly most of the entrained water evaporated before reaching the higher elevations for about 200 s after the initiation of the feed and bleed. This was then followed by a higher entrainment which caused a very sharp reduction in the temperatures.

The code might have calculated more steam to be condensed in the steam generator tubes and drained back to the core.

The code might have over predicted the heat transfer coefficient when

the flow contained less than approximately 20 % liquid void fraction

A split core channel approach might have improved the core behavior, provided with a detailed upper plenum nodalization, especially in the nozzle area which should simulate the 3-dimensional liquid drainback behavior. However, the difficulty in detailed modeling the LOFT upper plenum which required precise information about the geometry, flow loss coefficients (especially in the radial direction) did not encourage a sensitivity study on this issue.

After the accumulator injection started, the core was completely quenched as in the experiment. The quench progress and temperature, and rate of temperature drop were well in agreement with the data.

4.2.3.3 Accumulator and LPIS Injection The calculated feed and bleed operation successfully brought the system pressure, first to the accumulator injection point, and shortly after to the LPIS injection point (Figures 45) as in the experiment. The calculation went smoothly during both injection periods and no noticeably oscillations were observed.

4.2.3.4 Accumulator and LPIS Flow Figure 47 overlays the calculated and the measured ECC flows Figure 48 overlays the integrated ECC flows, with a time shift applied to the RELAP calculated flow for a better comparison. As seen from these figures, except very small underprediction during the first 500 s of the accumulator injection, the calculated accumulator flow was in agreement with the data. The slight overprediction of the LPIS flow was observed.

## 5. SENSITIVITY CALCULATION

A sensitivity study was performed to assess hot and cold leg connections to the vessel using cross flow junctions. At the time when the base case calculation was initiated, the original connections of these legs to the vessel were kept the same since the standard RELAP5 LOFT deck has been extensively used using "down connection" of the legs. This connection scheme created an artificial elevation difference between the center of the gravities of the volumes representing the legs and those of the

volumes to which these legs were connected. This unphysical boundary condition used by the code might have caused a different hydraulic behavior during the period when liquid from the hot legs was slowly draining into the vessel. The cross flow junction model was developed especially for the flow paths where there are no gravity effects involved. Since, a late core dryout behavior was calculated, remodeling of the leg connections using cross flow junctions was tried to see whether any improvement could be gained.

In order to use the cross flow junction connections, the upper downcomer annulus, and upper plenum volumes were remodeled. The final nodalization diagram is presented in Figure 49. The base case calculation was repeated with the new nodalization from 3200 s to 5000 s.

The following subsections compare various system parameters calculated using two different types of the leg connections.

### 5.1 Pressures

The system pressures in the primary and secondary systems were calculated to be the same as the ones presented earlier. This was expected and also was a good indication that the model was functioning properly.

### 5.2 Core Uncovery

Figure 50 and 51 compare the calculated fuel cladding temperatures at the fifth and third core levels. The dryout was calculated earlier by about 40 s with the cross flow junction connected legs. Since the calculation was repeated from 3200 s, another approximately 40 s could be gained if the calculation would have been repeated from the time of the pump trip. This argument was based on the fact that cross flow junction connection should have to have effect during the period when the hot legs and the steam generator tubes contained considerable amount liquid inventory. And it should have negligible effect during the time when very small amount of condensed liquid was present in the hot leg. This was verified with the fact that there was no difference observed between the calculated heat up rates as seen in Figure 50 and 51.

In Section 4.2.2.4, it was indicated that the code predicted the dryout late by about 200 s. Application of the cross flow junction model at the hot and the cold legs to vessel connections from the beginning of the transient would bring this time to approximately to 100 s. This remaining time difference was believed due to the decreased flow loss coefficients of the junctions representing the two leak paths which created less pressure differential between the downcomer and the upper plenum. An evidence to this conclusion is that as the level progressed into the core, the pressure differential got smaller and the calculated and the measured dryout times got closer to each other.

## 6. RUN STATISTICS

CPU time versus transient time was shown in Figure 52. The mass depletion phase and early core uncover phases consumed considerable amount of CPU time. The total CPU time was 7.5 hr on CYBER 176 system for a total of 6560 s of problem time. Wherever Courant limit dominated the time step size (such as Volume 107), an attempt was made to renodalize that particular volume during the next restart. This problem mainly occurred when the flow in the hot leg started to become stratified. The code was forced to run faster by assigning relatively larger time step size as the maximum time step size. This caused the code to violate the Courant limit for most of the time. The criteria in selection of the maximum and minimum time step sizes were that number of repeated time steps was under a reasonable value. During the base case analysis, 10389 time steps were repeated out of a total 114065 time steps. The grind time[a] was achieved to be 1.7931 ms. The run time of the sensitivity study was practically the same as the base case calculation.

---

a The grind time is the total CPU time diveded by the total number of volumes and total number of time steps. A total of 26998 s of CPU seconds was used for 132 volumes and 114065 time steps.

## 7 CONCLUSIONS and RECOMMENDATIONS

This LOFT-OECD LP-SB-3 analyses showed that RELAP5/MOD2 correctly calculated many major system variables in a small break LOCA, such as primary and secondary system pressures, break flow, density and timing and progression of the dryout. Reflux condensation was calculated in the steam generator tubes and in the intact loop hot leg.

The major problem encountered was the core heat thermal behavior. The initial heatup rate was properly calculated except at the highest core elevations. The deviations started above 600-700 K at the core elevations between 2 and 5. The heatup rate at the six elevation was more in agreement with the data after the reflux condensation ceased. Although, calculated peak cladding temperature was in agreement, the timing was different. This agreement was due to the termination of the temperature excursion with feed and bleed initiation based on the peak cladding temperature. The heat up rate in the experiment was controlled by a strong cooling which was believed as a result of the draining of the condensed liquid into the vessel. The condensation was evidently taking place in the steam generator. Some of the condensed liquid generated in the upright drained into the vessel. The resultant downword liquid flow was not uniform across the vessel. Since the LOFT was not instrumented to provide detailed information on reflux condensation occurring in the steam generator tubes and possibly in the hot legs, it was not possible to assess the code models such as interfacial heat and mass transfer and surface transfer, controlling the reflux condensation and its reevaporation on route to core. The other constraint was that the non homogeneous liquid distribution in the upper plenum and its asymmetrical fall back into the core could not properly be modeled with a one dimensional code, even with series of cross flow junction connected volumes which simulate upper plenum and core in detail. The lack of of radiation heat transfer model increased the overprediction of the heat up rate in addition to the lack of proper cooling due to the drained liquid. Therefore, it should not be expected any better results from the code on the core thermal response The code properly calculated the cooling induced by the feed and bleed operation but the amount of it was overpredicted between the third and fifth elevations. Although the partial quench seen in the experiment below 0.38 m elevation was reproduced, the code extracted all the stored heat from the fuel, and could not calculate the re-dryout at this elevation. The

core behavior (quench progression, temperatures) during the accumulator injection period was very good agreement with the measured data.

The pump degradation was properly modeled. The differences observed between the calculated and the measured pressure differential across the pumps were as a result of the pump homologous curves used. These curves were basically developed using the Semiscale pumps and were partially modified using LOFT Small Break Experiment L3-6 data.

The problem seen in the calculated heatup behavior associated with improper simulation of the cooling due to the drained liquid and lack of the radiation heat transfer calculation is believed to be more pronounced in the small LOFT core. For a large PWR simulation, it is believed that, the RELAP5/MOD2 code will provide a better simulation of a small break LOCA occurring under similar conditions, provided that an appropriate representation of the physical systems should be provided.

In general, the RELAP5/MOD2 code is adequate to predict the transient thermal-hydraulic behavior of a reactor system undergoing a small break LOCA. However, the code performance was not only depending on the its models capabilities, but equally depending on how the physical system was modeled. The representation of the complicated systems where complex phenomena are occurring has always given the problem of in what detailed a particular component must be modeled. Attempts to represent every detail may even create problems due to lack of accurate information such as geometry, flow loss coefficients etc. Experience developed by using the same code and the same system for different simulations and assessing with the experimental data is probably the only guidance on this issue.

## 8. REFERENCES


1. W. B. Grush et al., Quick Look Report on Oecd LOFT Experiment LP-SB-3 OECD LOFT-T-3604, March 1984
2. V. H. Ransom et al., RELAP5/MOD2 Code Manual, EGG-SAAM-6377, April 1984.
3. W. B. Grush et al., Best Estimate Prediction for OECD LOFT Small Break Experiment LP-SB-3, OECD-LOFT-T-3603. February 1984
4. M. Tanaka, M. Peters, OECD LOFT Experiment Specification Document

Cold Leg Small Break Experiment LP-SB-3, OECD-LOFT-T-3602, December 1983.

5. Private communication with J. Birchley who was UK delegate to the LOFT-OECD program, May 1985.
6. D. L. Peeder, LOFT System and Test Description, NUREG/CR-0247, TREE-1208, July 1978.
7. P. D. Bayless and J. M. Carpenter, Experiment Data Report for LOFT Nuclear Small Break Experiment L3-6 and Severe Core Transient Experiment L8-1, NUREG/CR-1868,EGG-2075, January 1981.

TABLE 1 CHRONOLOGY OF EVENTS FOR EXPERIMENT LB-SB-3

| Event | Time After Experiment Initiation (s) | |
|---|---|---|
| | Measured Data | Post-Test Calculation |
| Small break valve opened | 0.0 | 0.0 |
| Reactor scrammed on low pressure in intact hot leg | 9.21 | 10.746 |
| Main feedwater pump shut off on scram signal | 9.41 | 10.746 |
| MSCV started to close | 9.5 | 10.746 |
| Pressurizer level below indicating range | 67. | 94. |
| First time MSCV cycled open | 87.5 | 75.6 |
| Subcooled blowdown ended | 98.5 | 201. |
| Pump differential pressure degradation observed | 700-875. | 800-1250. |
| Last time MSCV cycled open | 1030. | 1155. |
| Primary coolant pumps tripped | 1600. | 1618. |
| Break uncovered | 1612. | 1630. |
| Start of core heatup | 3800. ±50 | 4008. |
| Break isolated | 4742. | 4905. |
| Steam generator feed and bleed initiated | 5415. | 5186. |
| Maximum cladding temperature reached | 5422. | 5198. |
| Accumulator injection initiated | 5558. | 5360. |
| Core quenched | 5800. | 5570. |
| Low pressure injection initiated | 6785. | 6222. |
| Experiment terminated | 6845. | 6560. |

TABLE 2. INITIAL CONDITIONS FOR EXPERIMENT LP-SB-3

| Parameter | Measured value | RELAP-steady state |
|---|---|---|
| Primary Coolant System | | |
| Power level (MW) | 50.3 ±1.2 | 50.3 |
| Primary coolant mass flow rate (kg/s) | 482.6±2.6 | 482.6 |
| Pressurizer pressure (MPa) | 15.26±0.1 | 15.24 |
| Pressurizer liquid level (m) | 1.115±0.06 | 1.094 |
| Cold leg temperature (K) | 556.6±1 | 556.6 |
| Hot leg temperature | 576.6±1 | 576.12 |
| Secondary Coolant System | | |
| Steam generator liquid level[a] (m) | 0.21 | 0.21 |
| Pressure (Mpa) | 5.58 ±0.06 | 5.21 |
| Mass flow rate (kg/s) | 26.67±0.77 | 27.05 |

a. The level is defined as 0.0 at 2.95 m above the top of the tube sheet

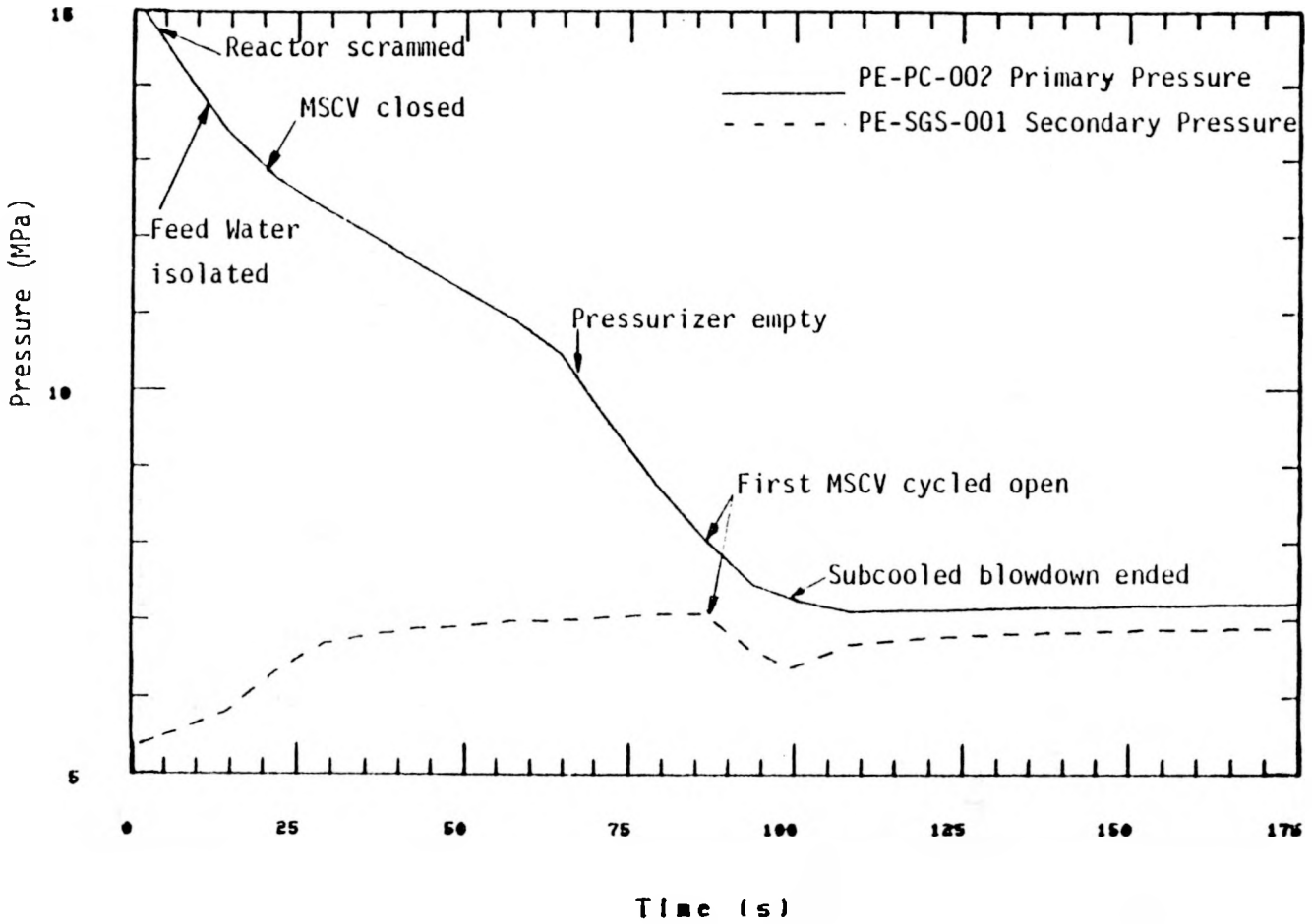


Figure 1. Primary and secondary system pressures (0 - 150 s)

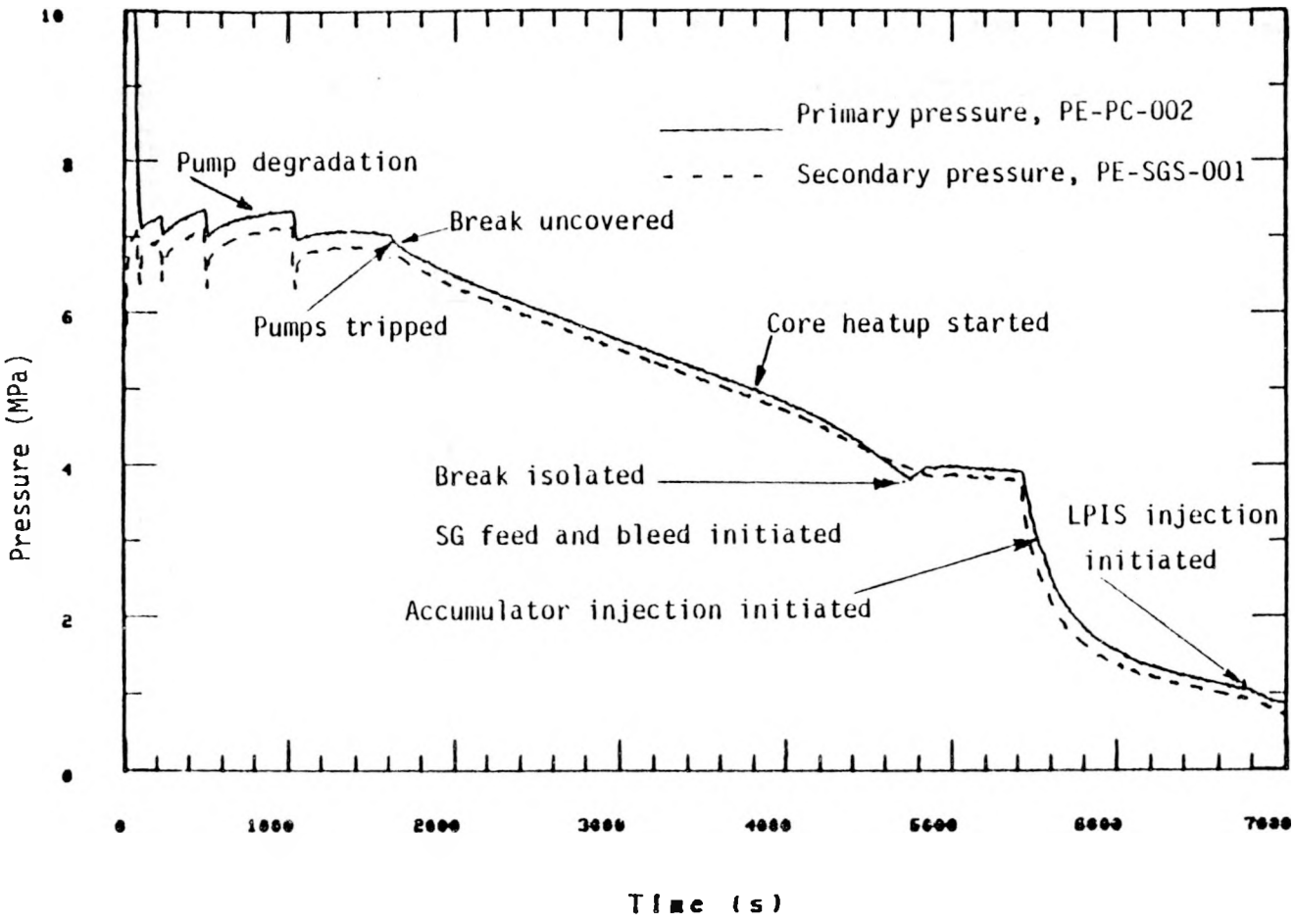


Figure 2. Primary and Secondary system pressures (0 - 7000 s)

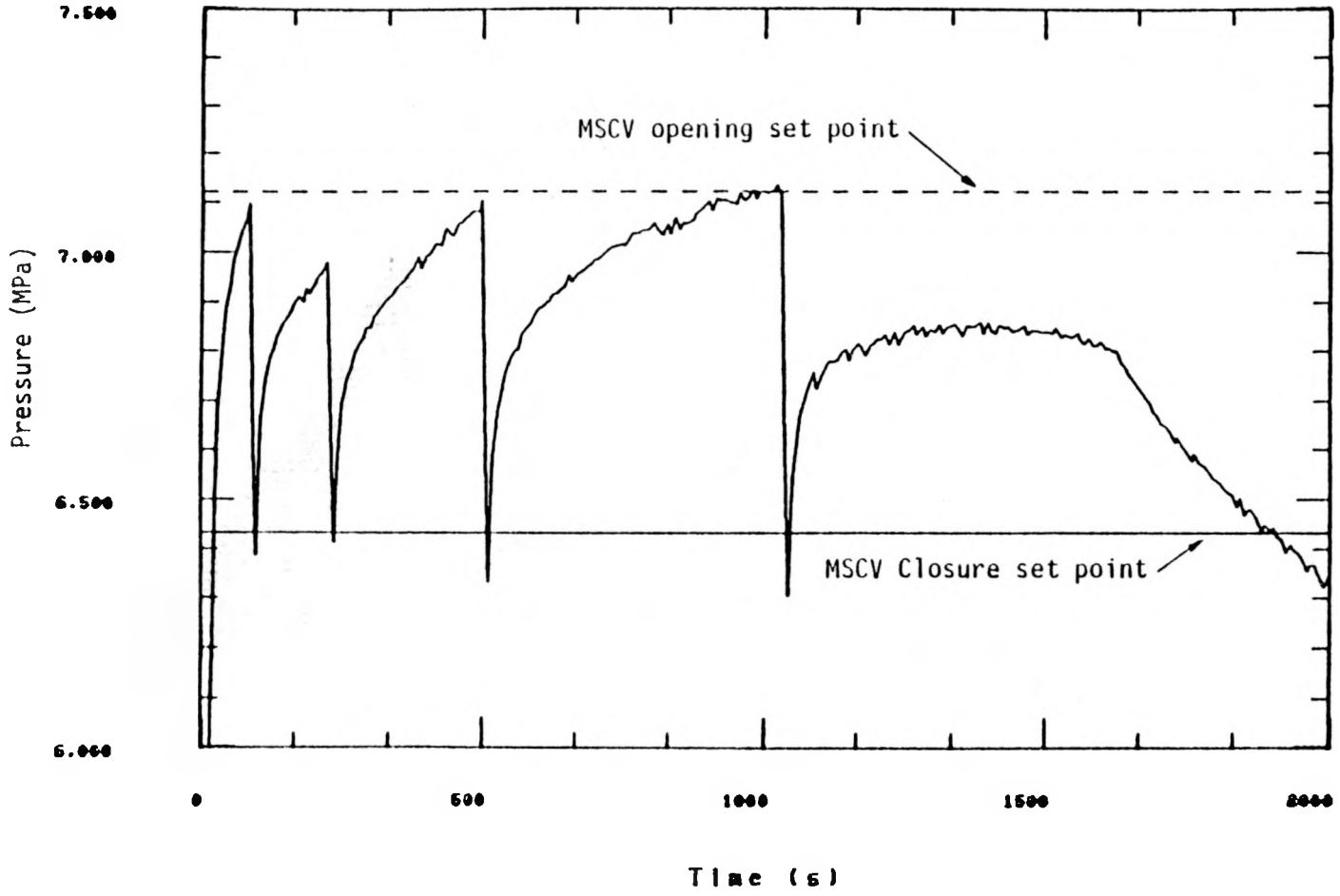


Figure 3. Steam generator secondary pressure and MSCV cycling set points

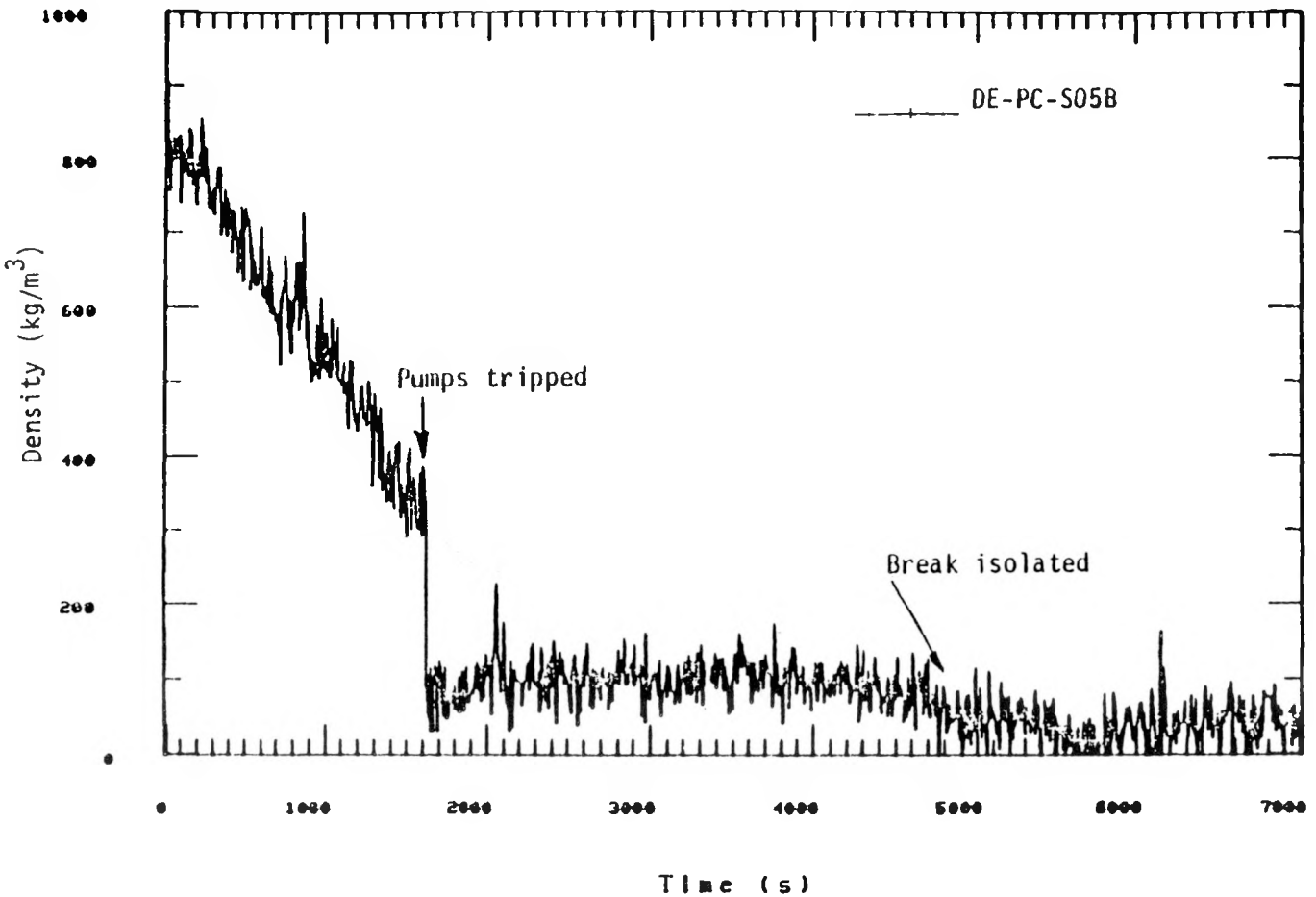


Figure 4. Fluid density in the break piping

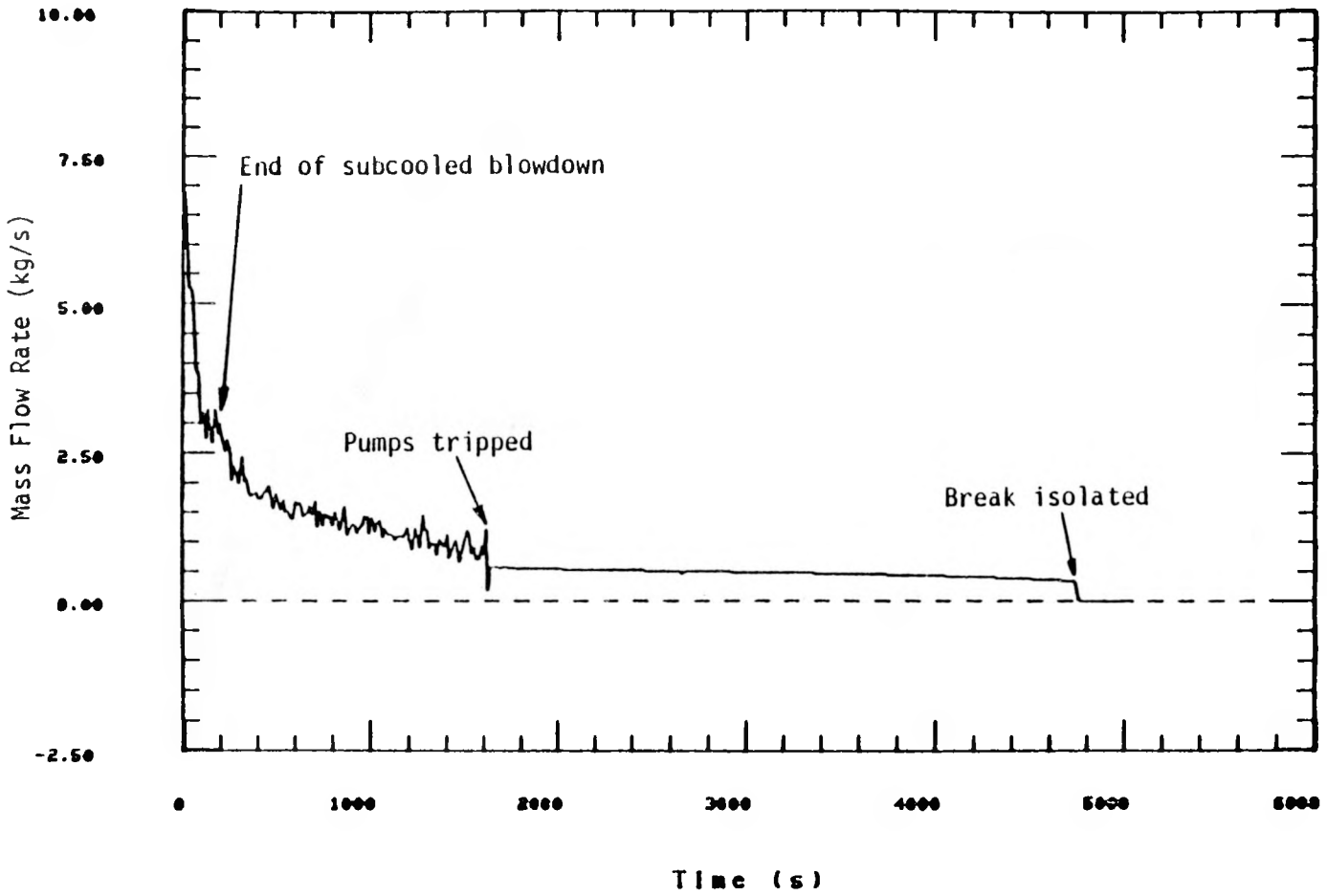


Figure 5. Break flow

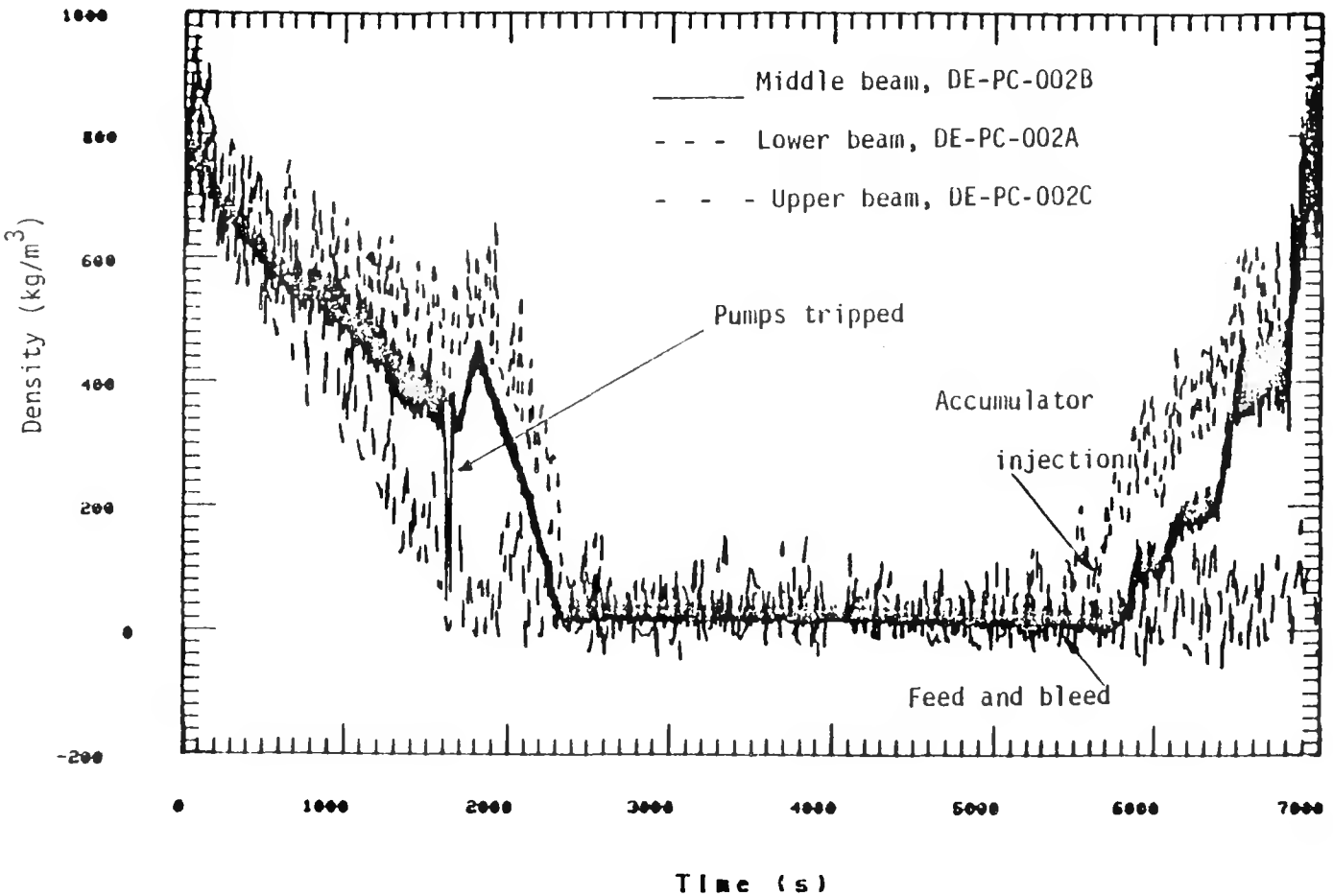


Figure 6. Fluid density in the intact loop hot leg

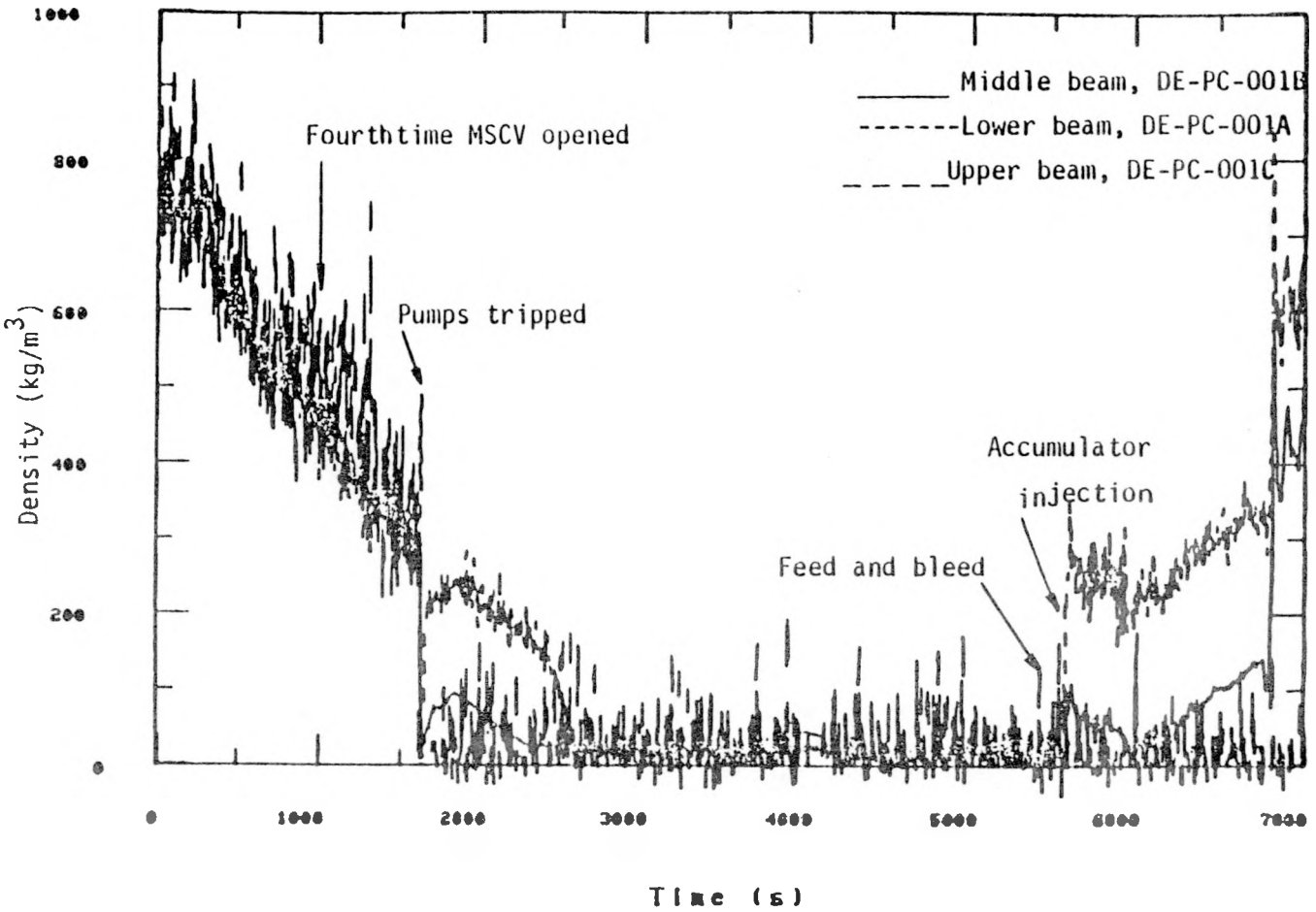


Figure 7. Fluid density in the intact loop cold leg

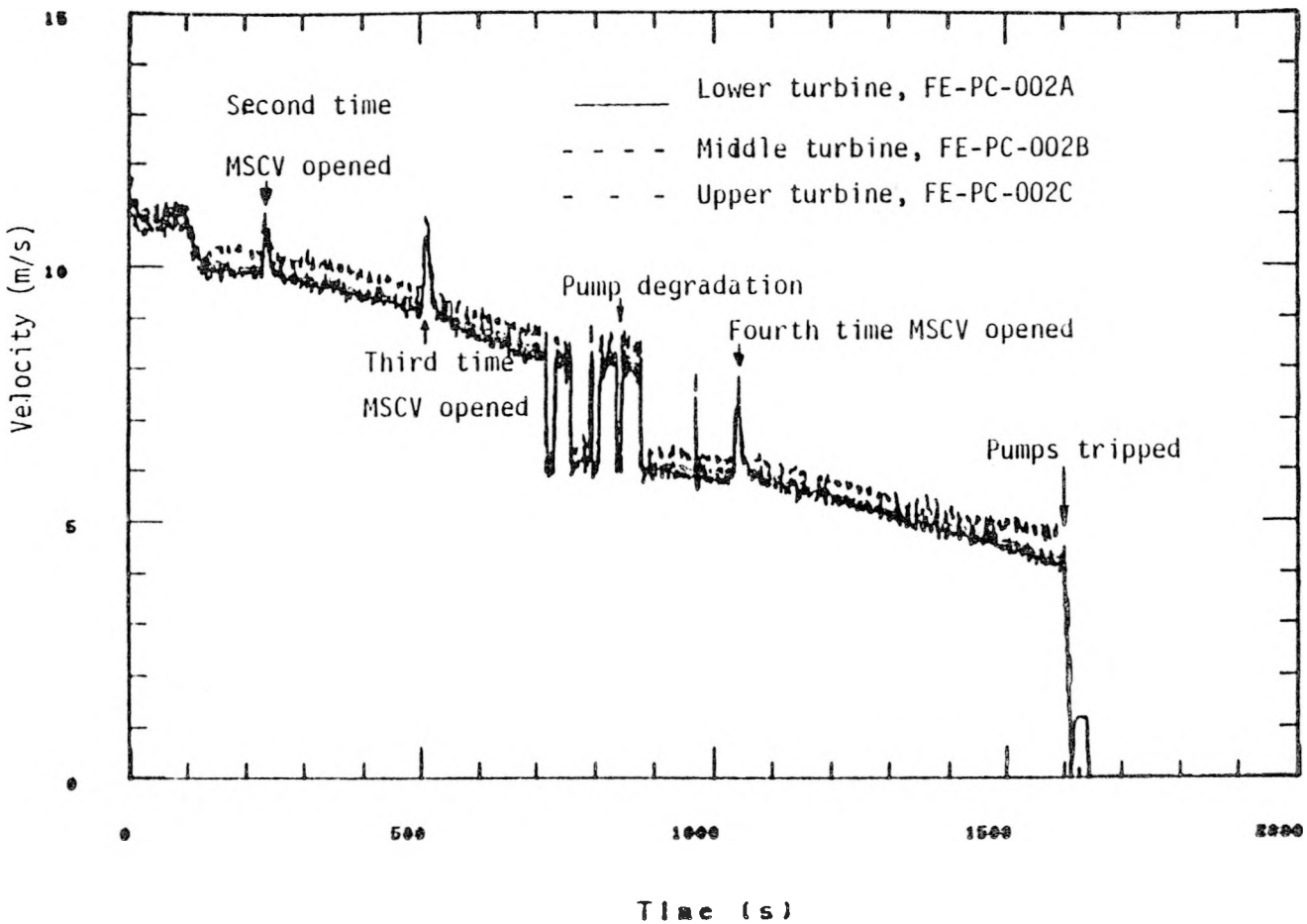


Figure 8. Fluid velocity in the intact loop hot leg

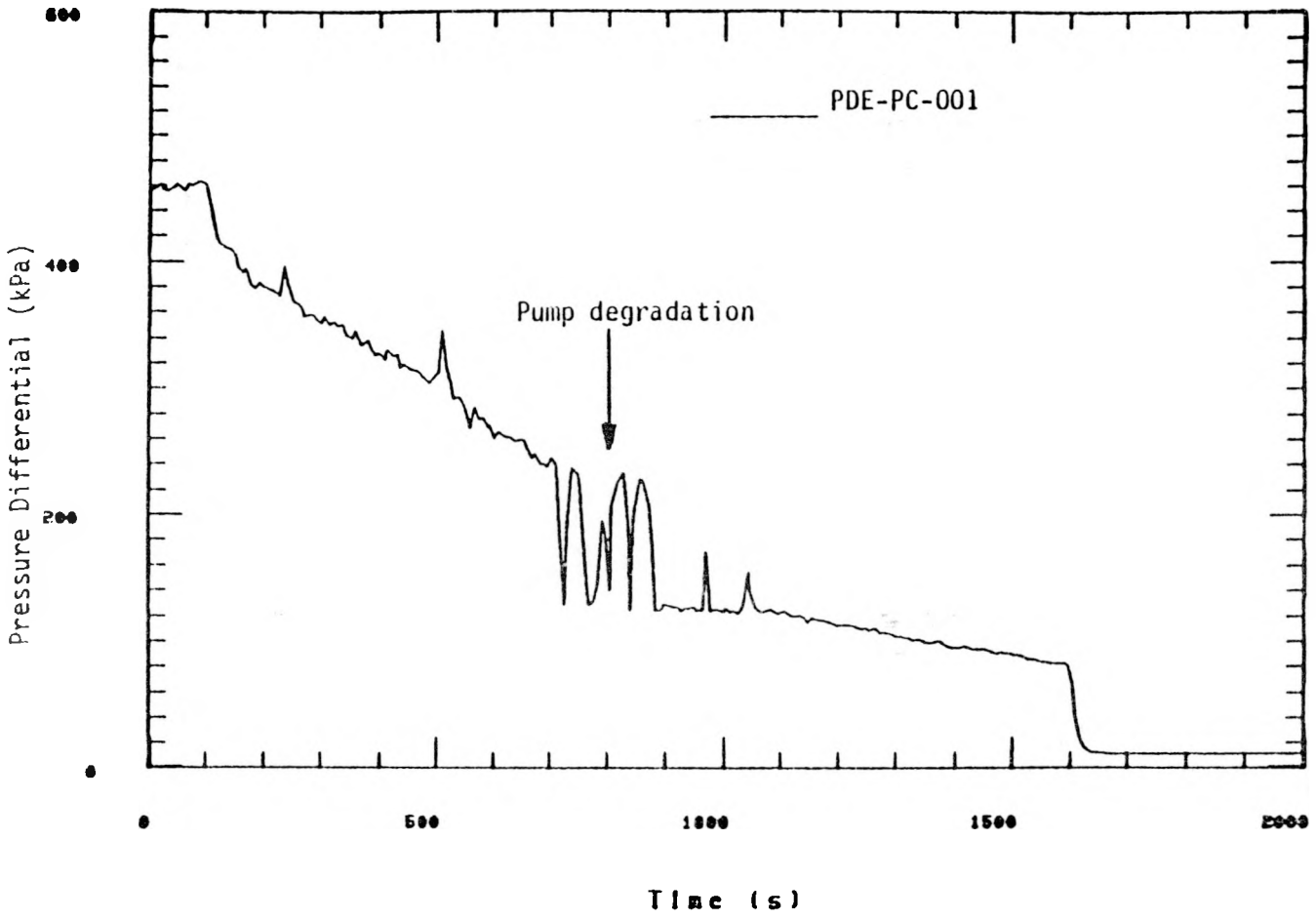


Figure 9. Pressure rise across the primary coolant pumps

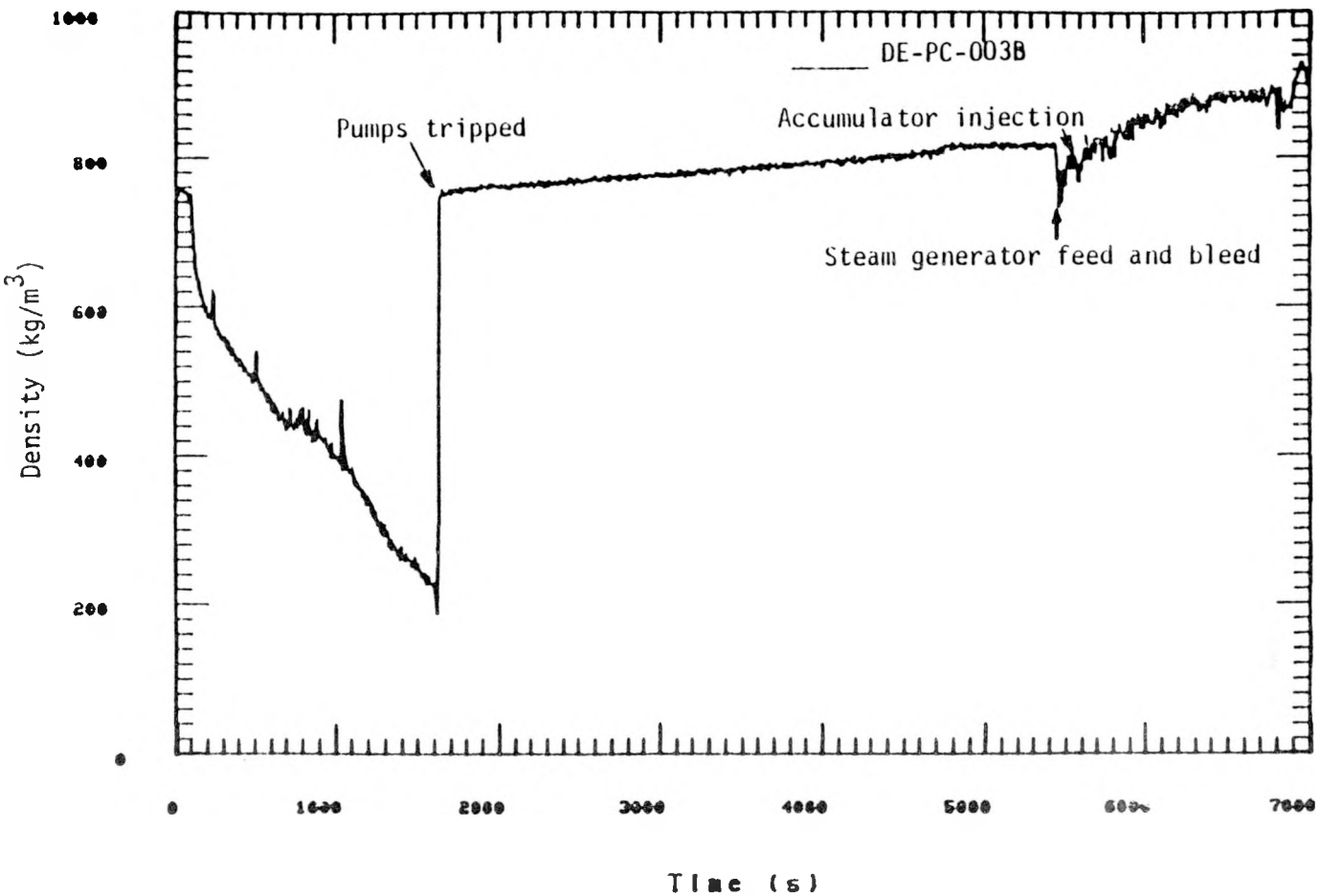


Figure 10. Fluid density in the intact loop seal

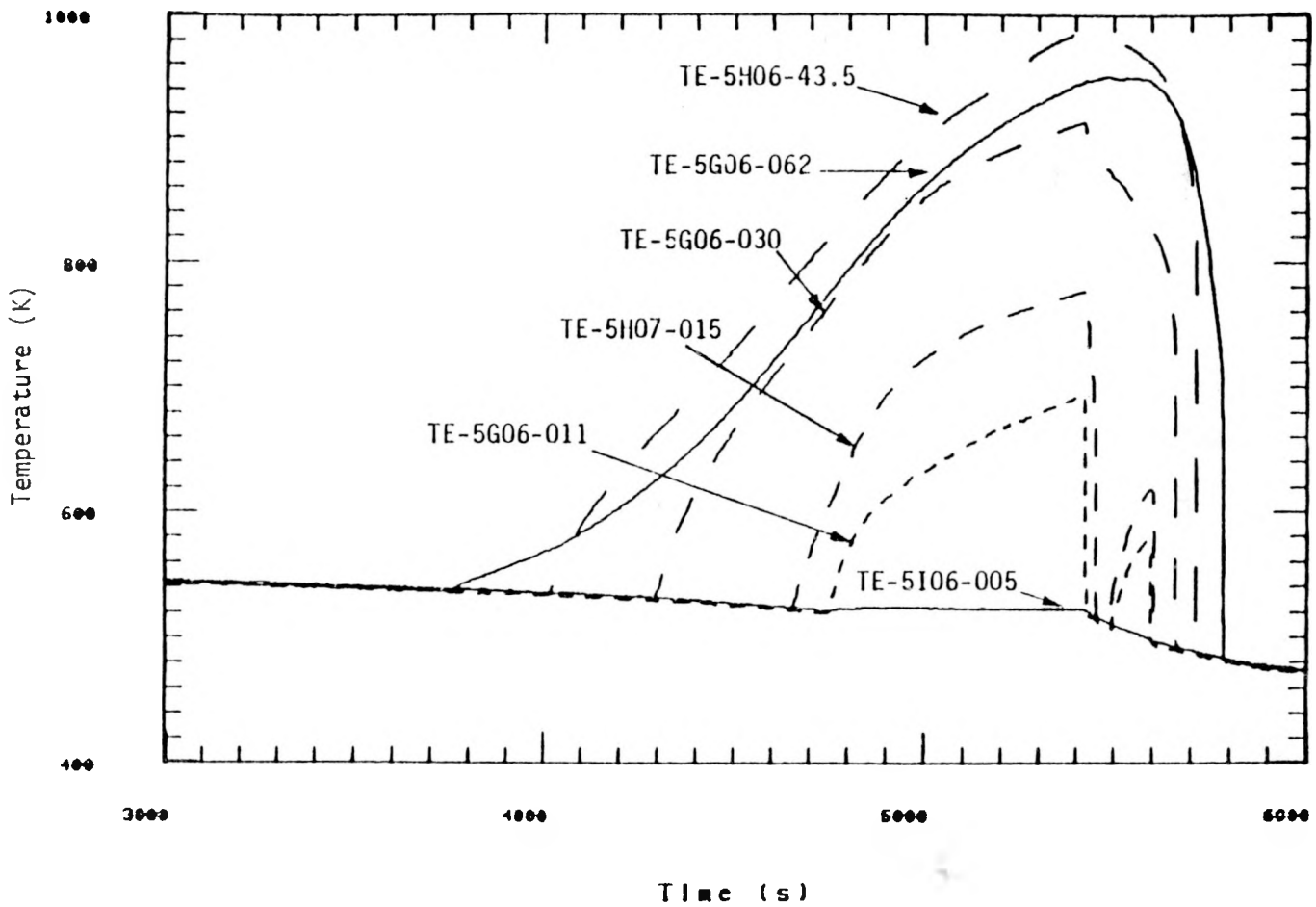


Figure 11. Fuel cladding temperatures in the center bundle

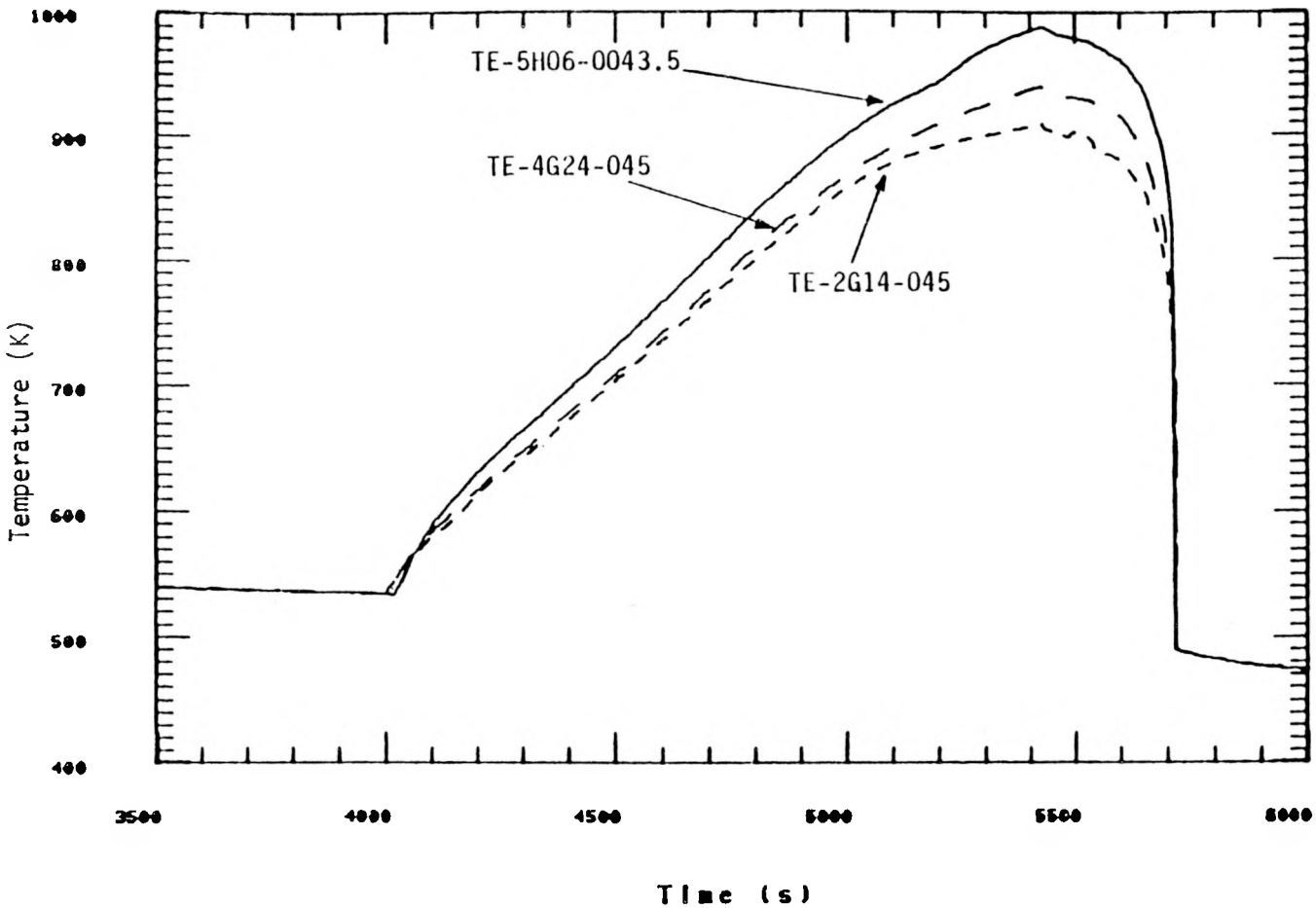


Figure 12. Cladding temperatures at different radial positions

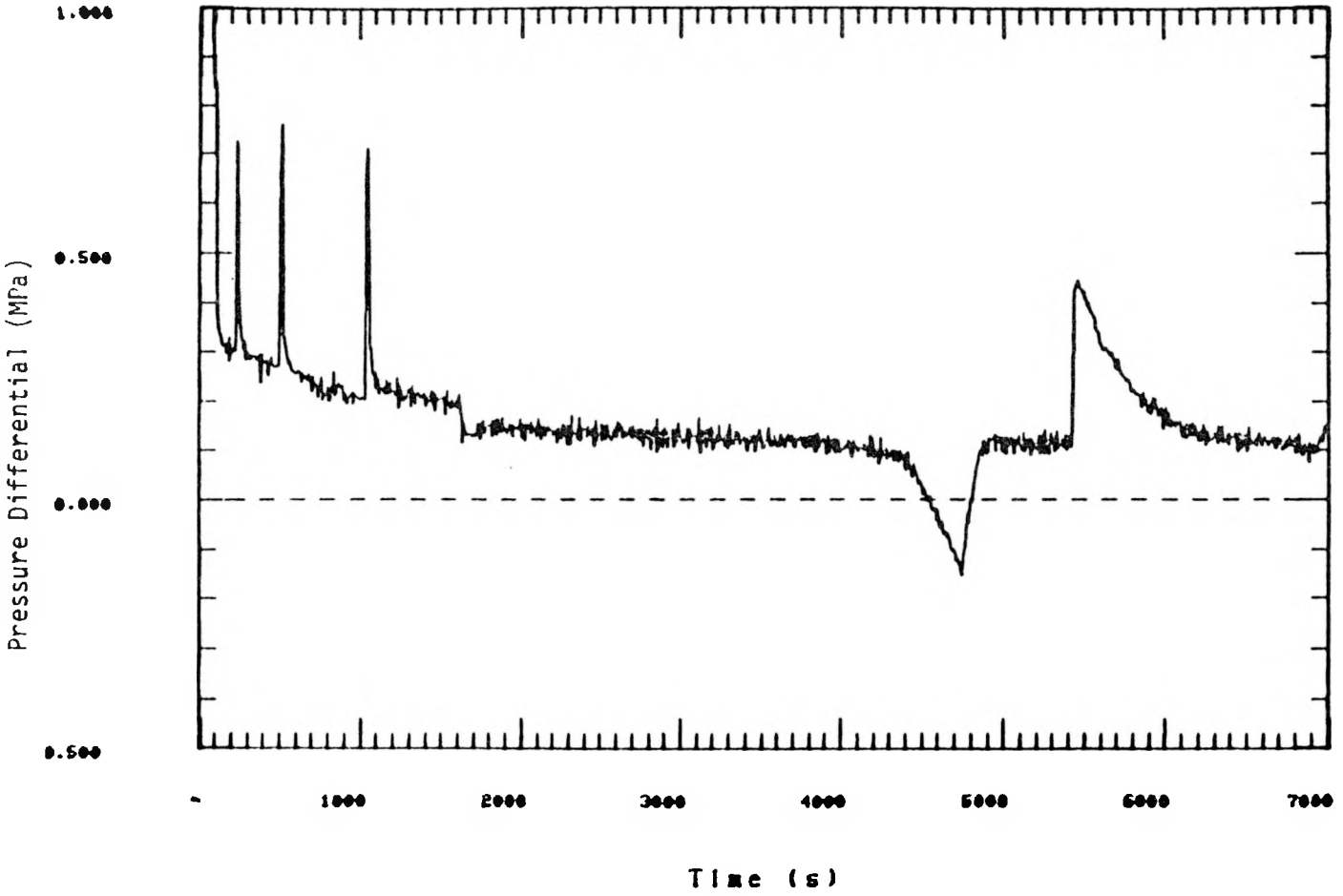


Figure 13. Primary-secondary pressure differential

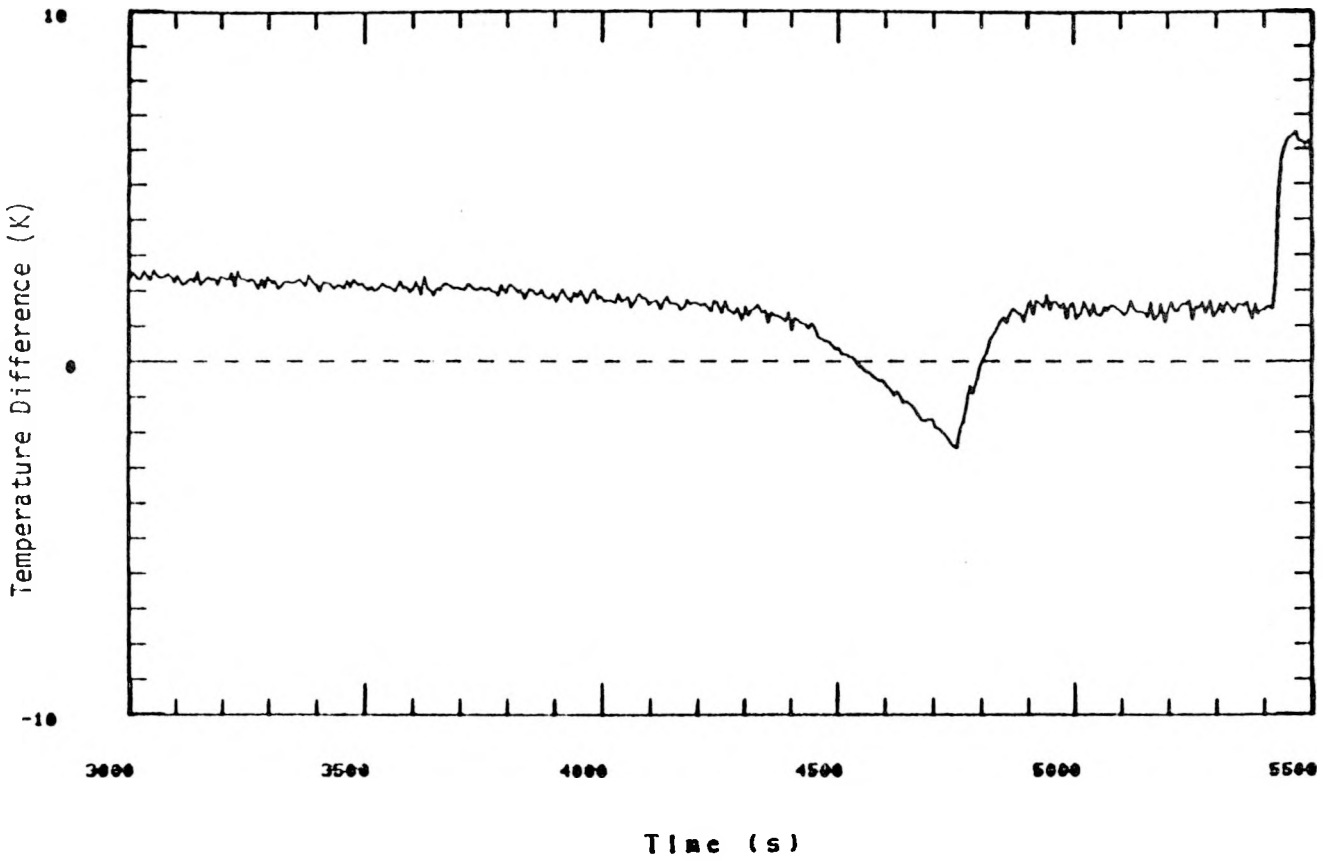


Figure 14. The temperature difference between the saturation temperature of the primary system and the temperature of the secondary system

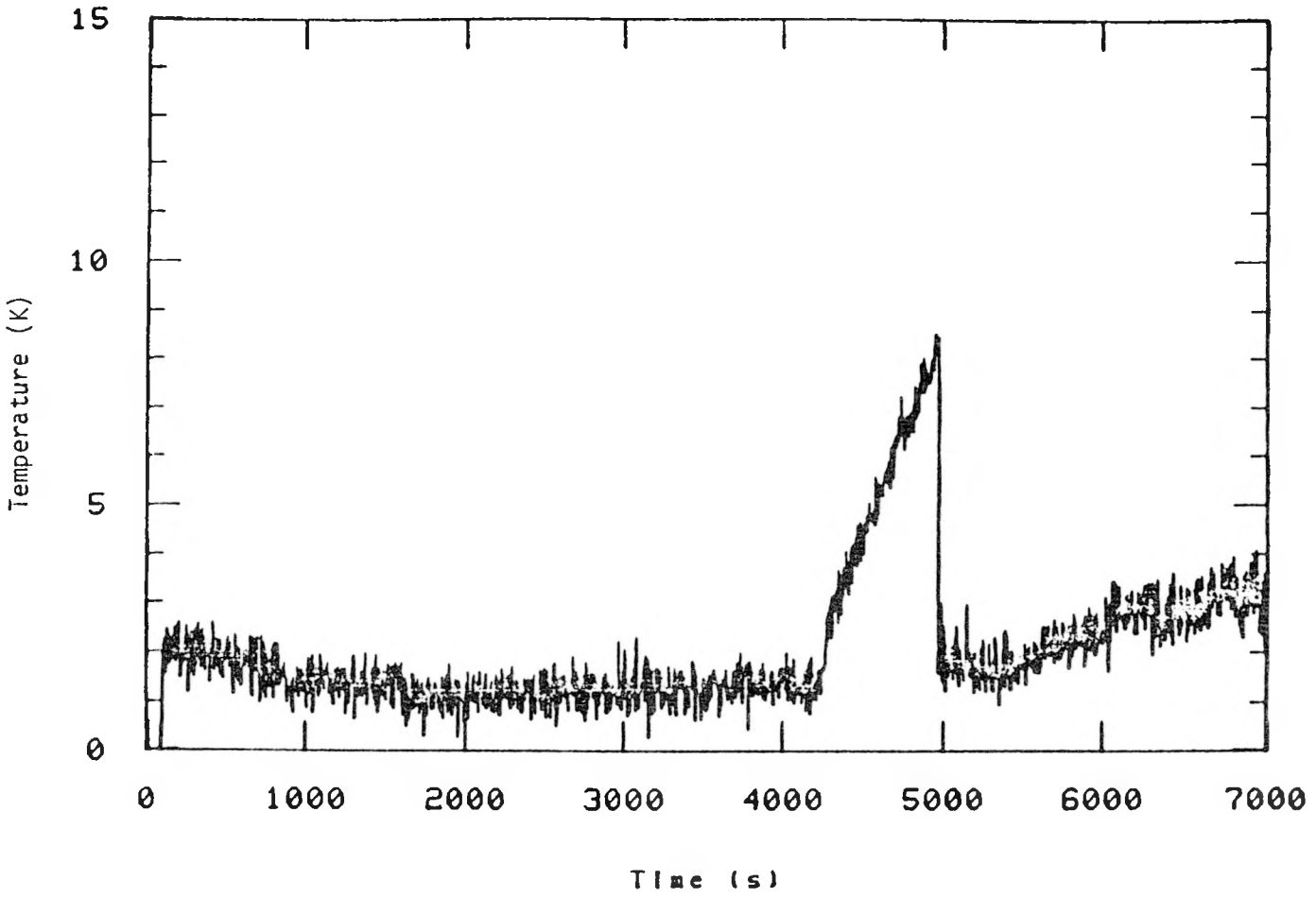


Figure 15. Steam superheat in the steam generator inlet plenum

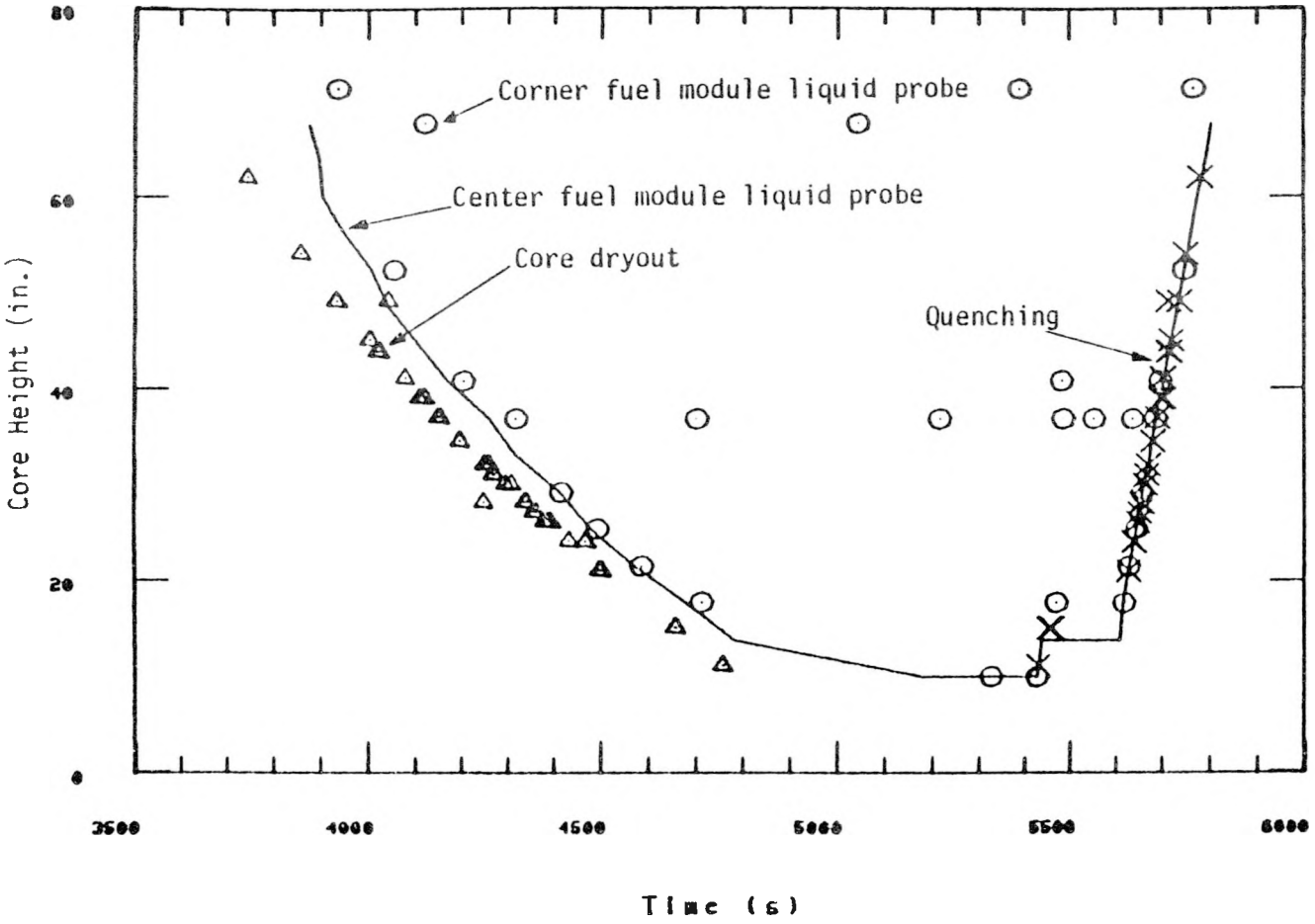


Figure 16. Response of reactor vessel liquid level probes, core dryout and quench data

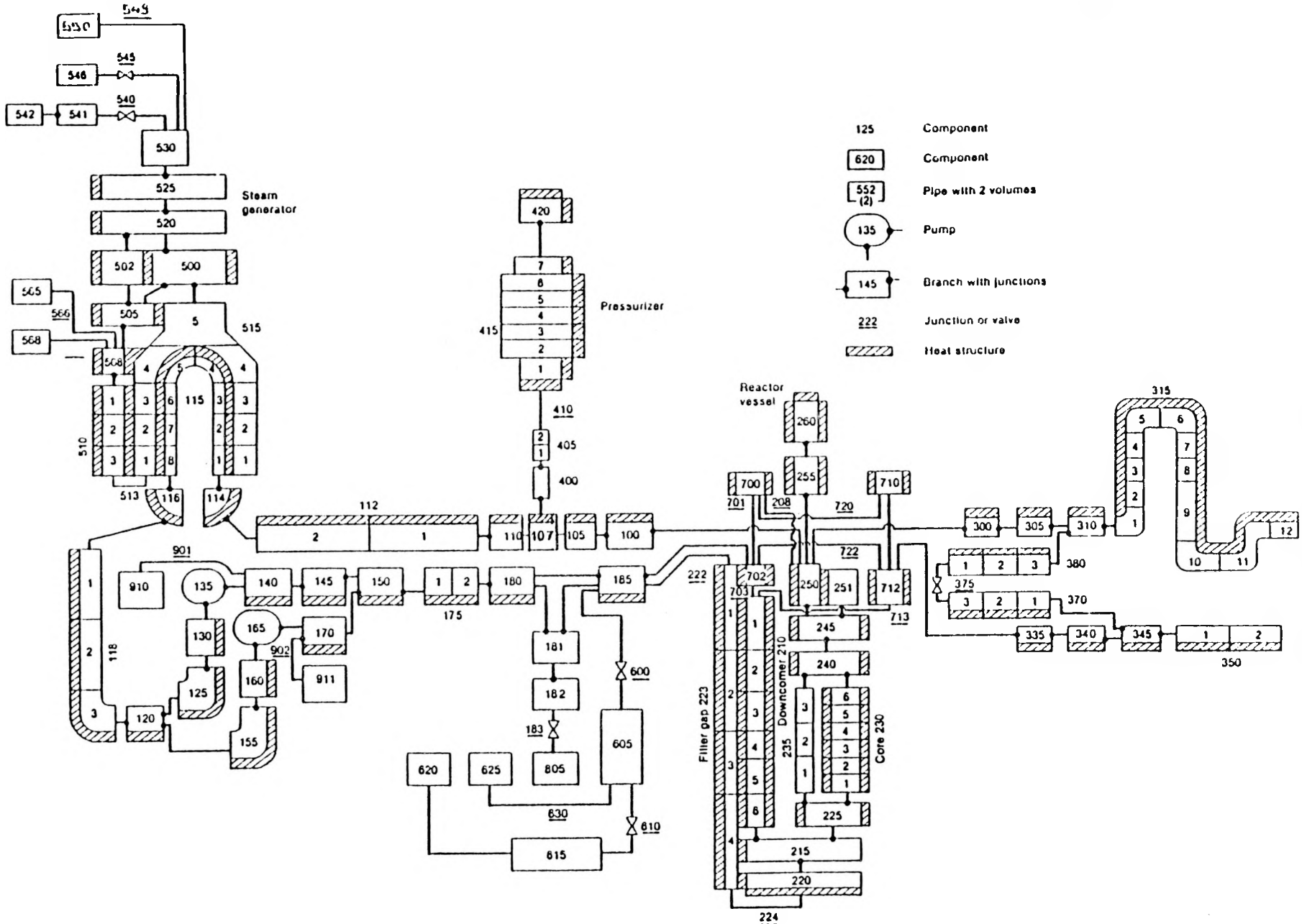


Figure 17. RELAP5/MOD2 Nodalization for Experiment LP-SB-3

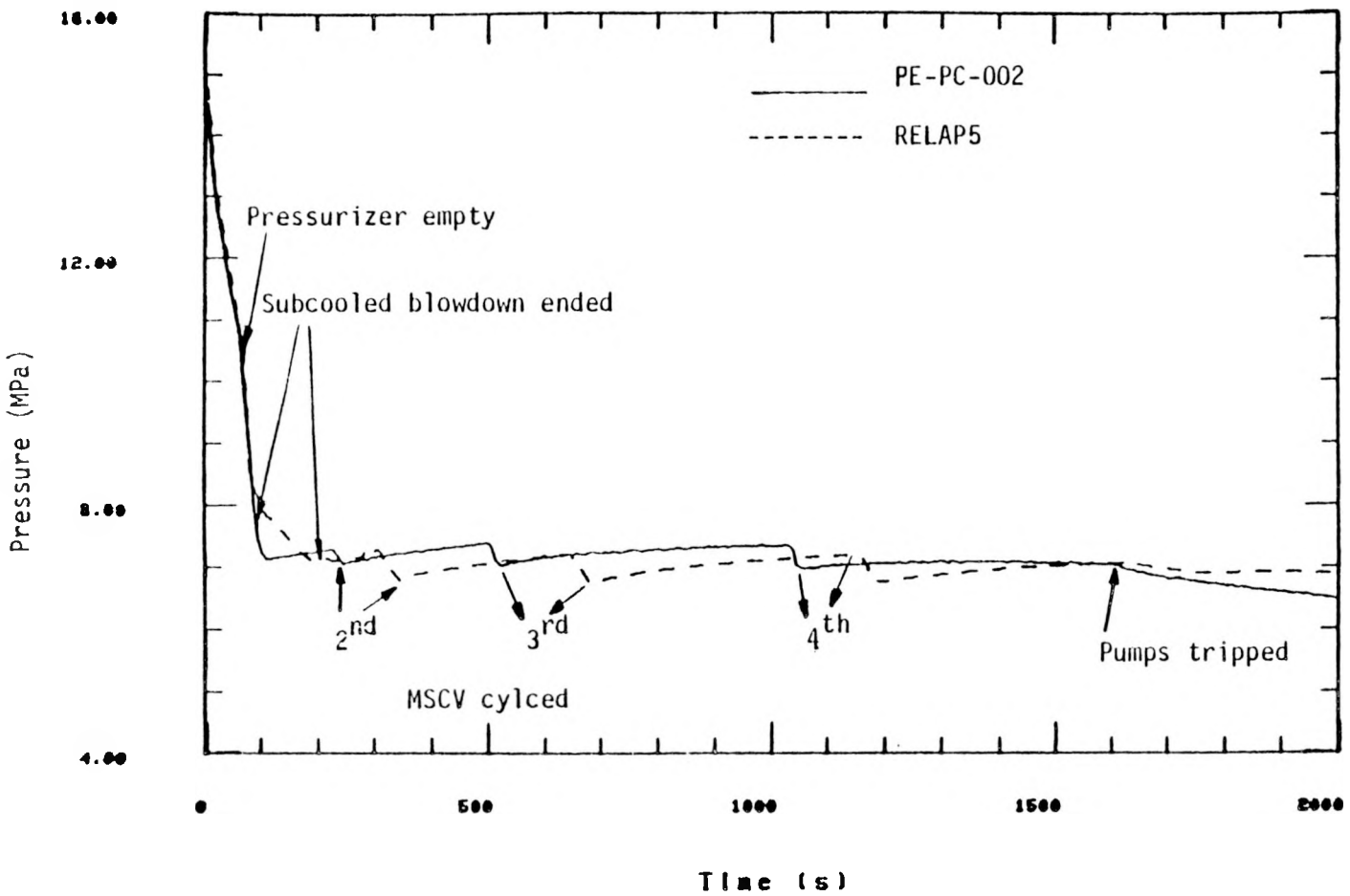


Figure 18. Comparison of pressures in the intact loop hot leg

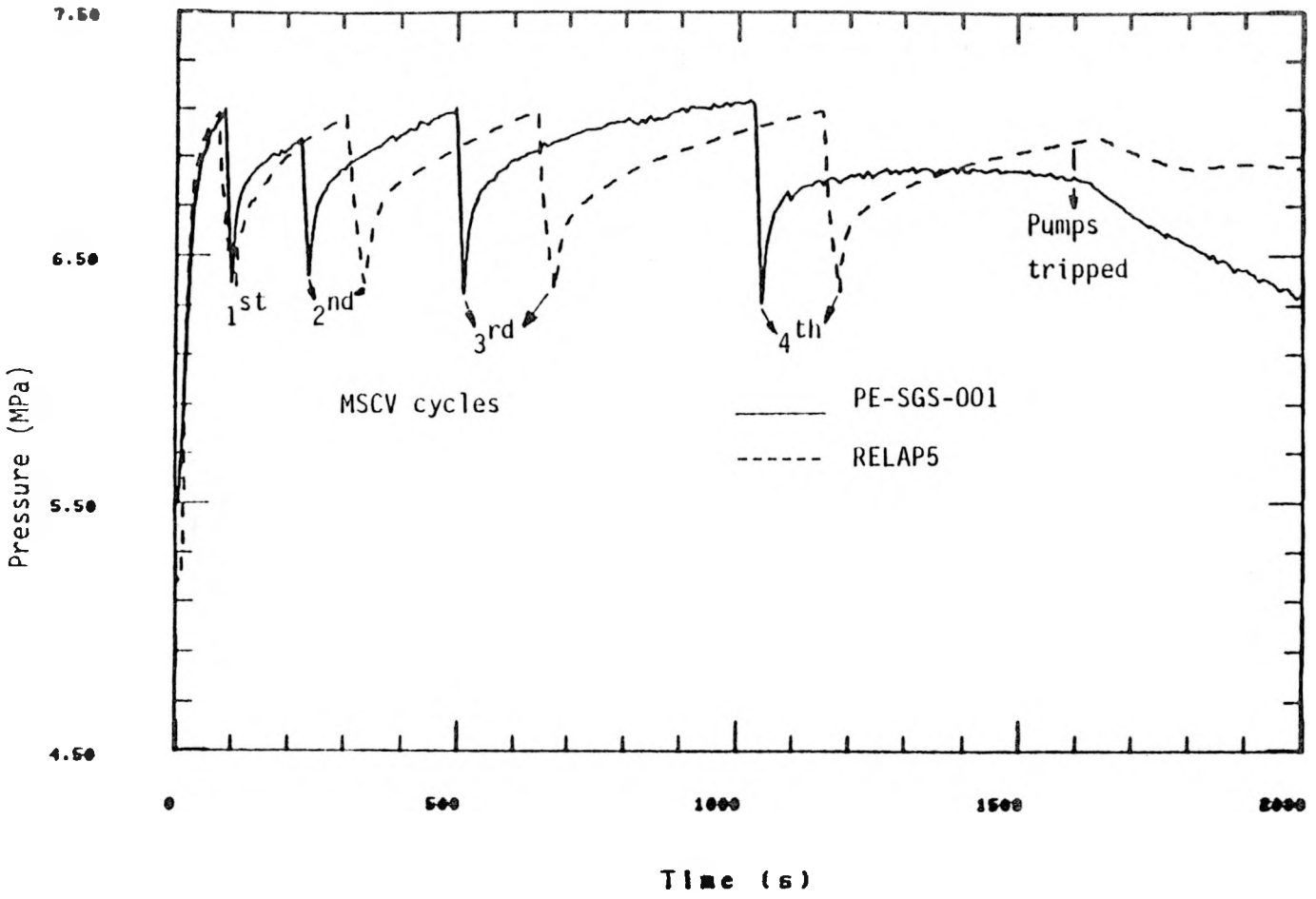


Figure 19. Comparison of pressures in the steam generator secondary side

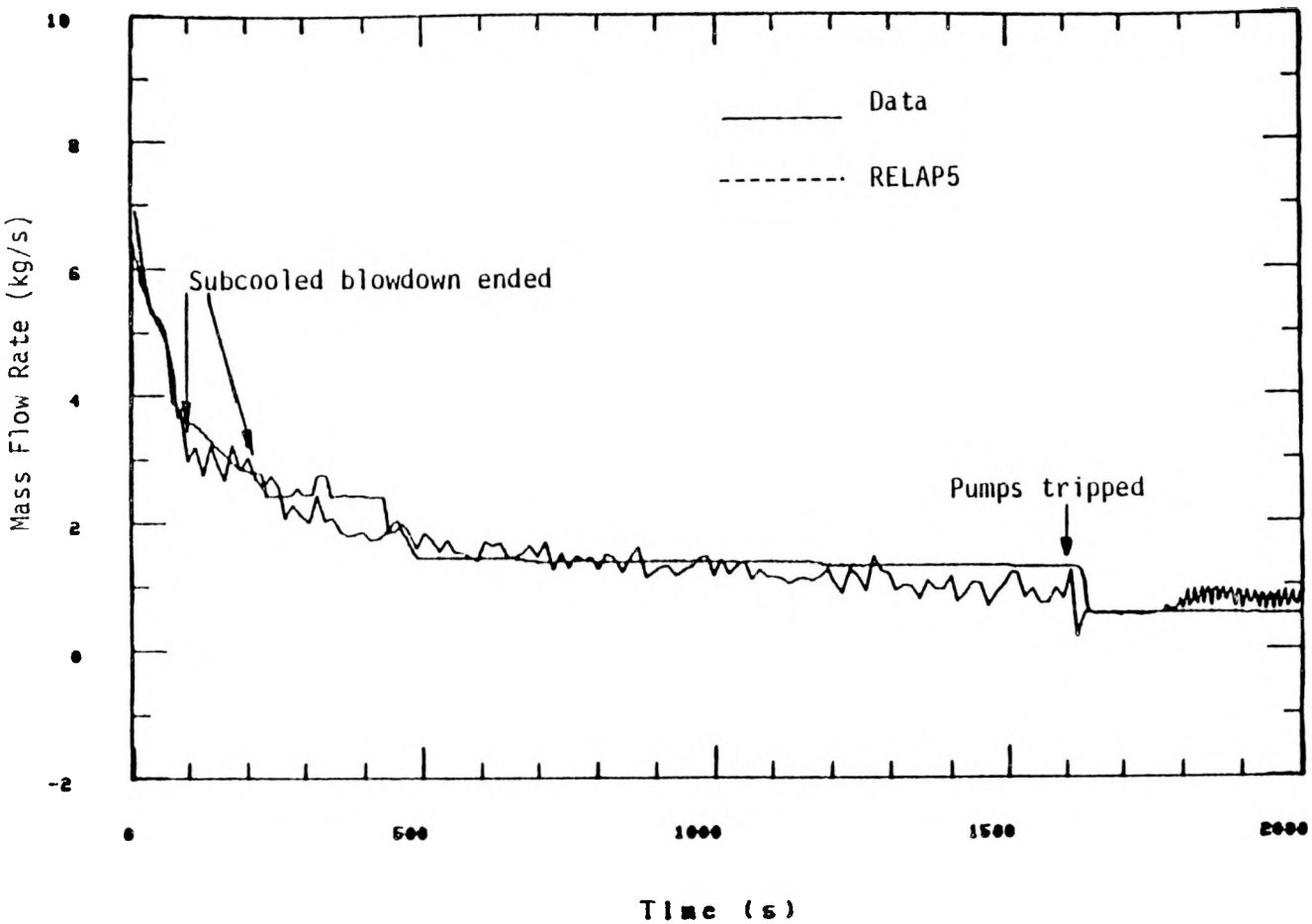


Figure 20. Comparison of break flows

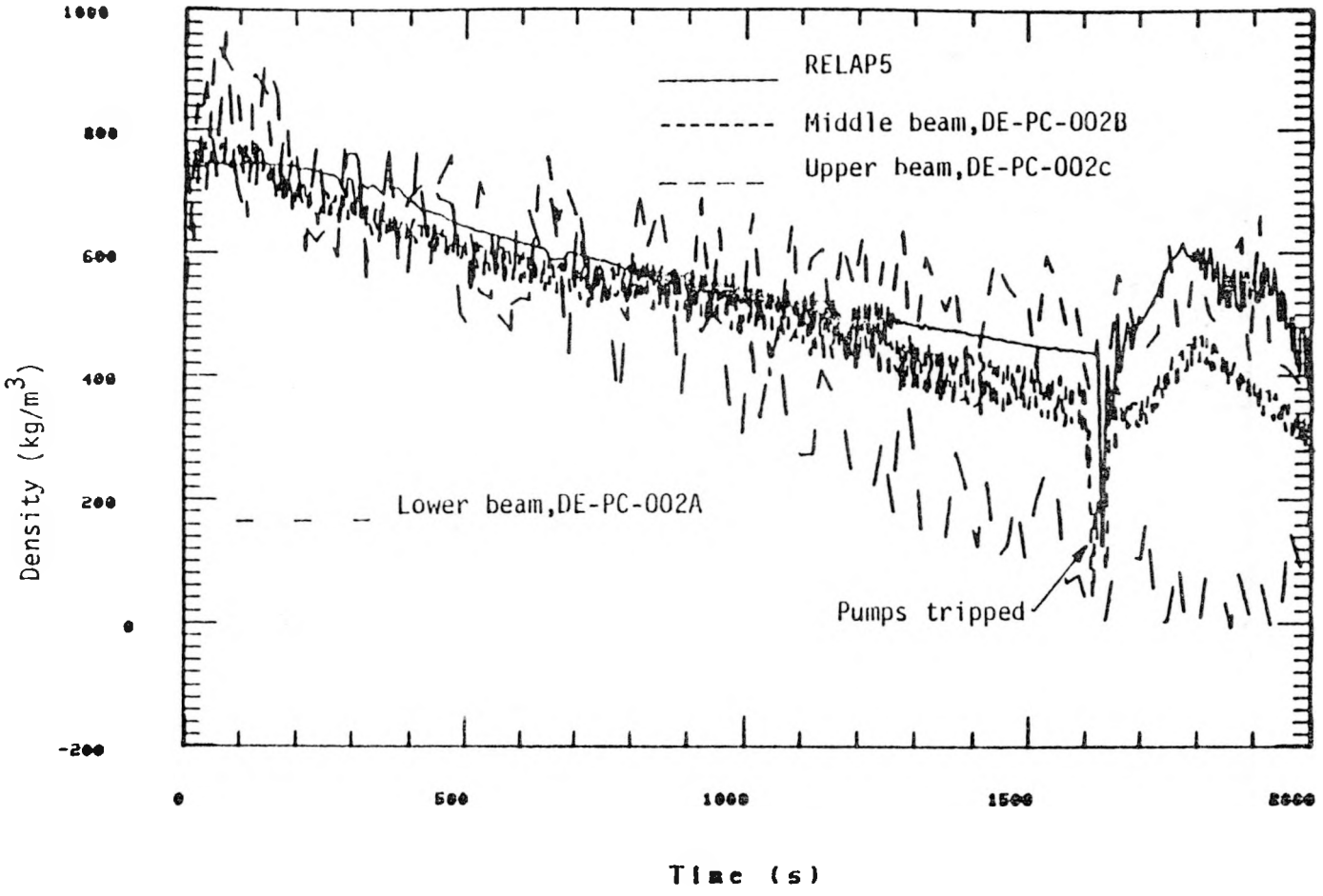


Figure 21. Comparison of densities in the intact loop hot leg

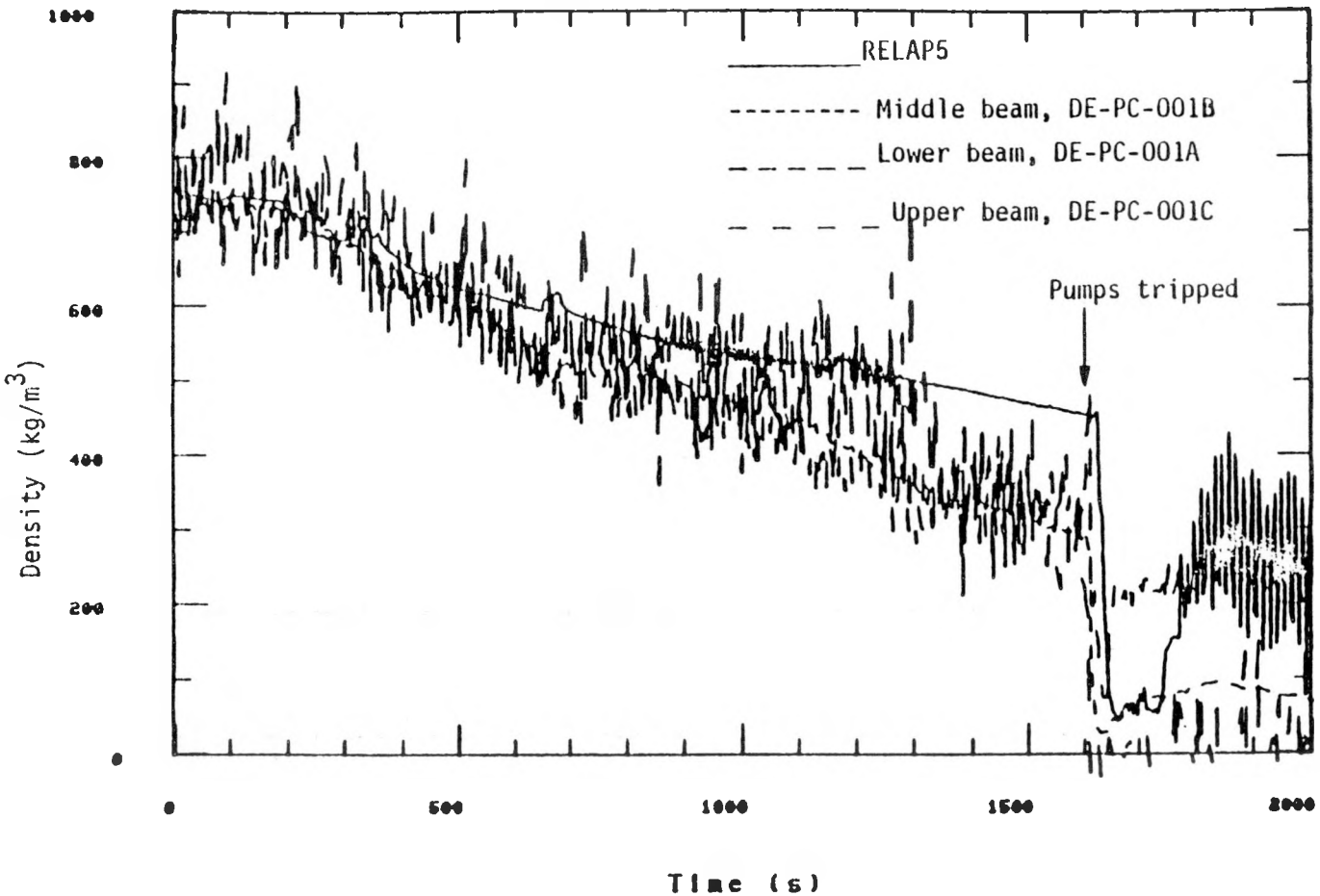


Figure 22. Comparison of densities in the intact loop cold leg

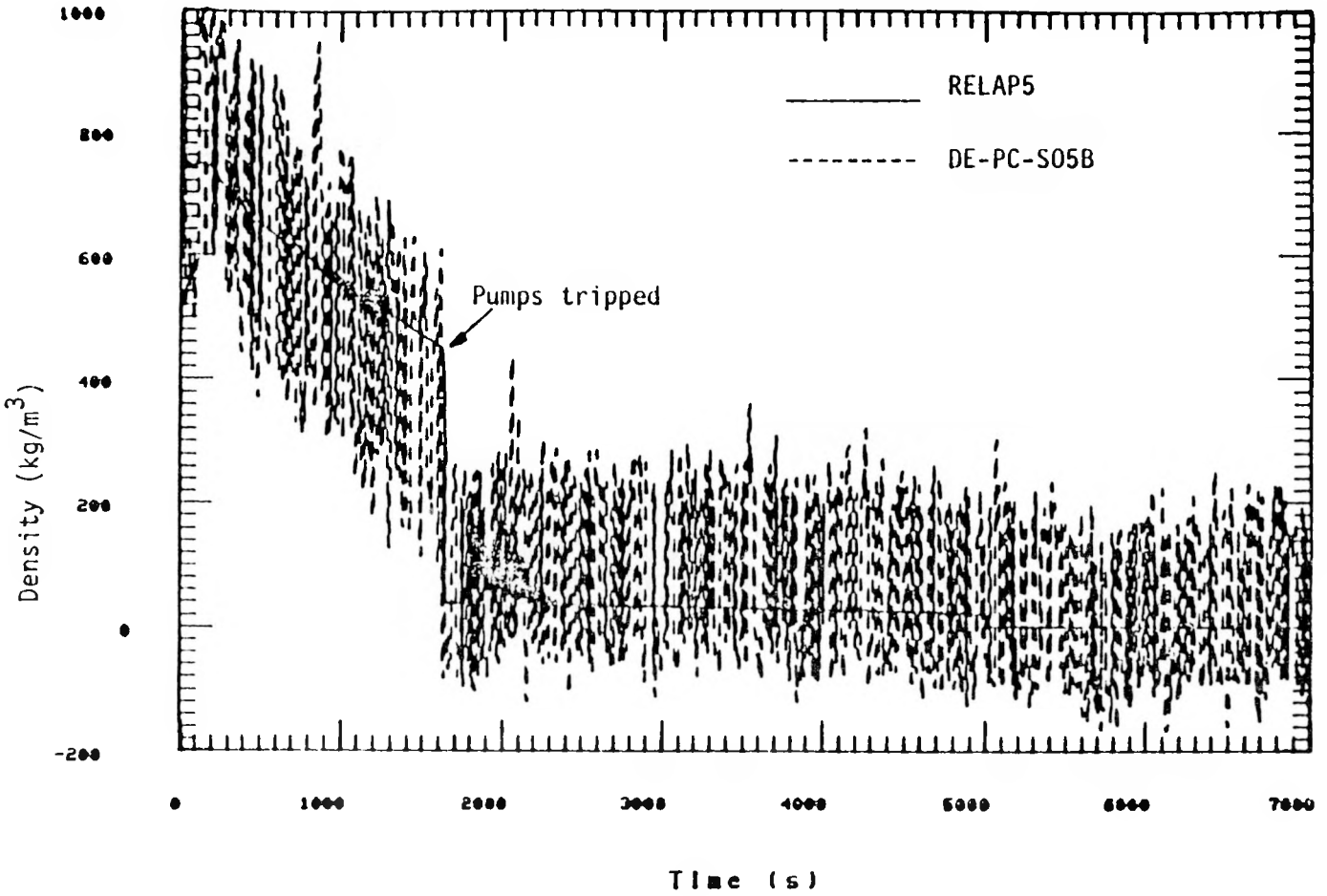


Figure 23. Comparison of densities in the break line

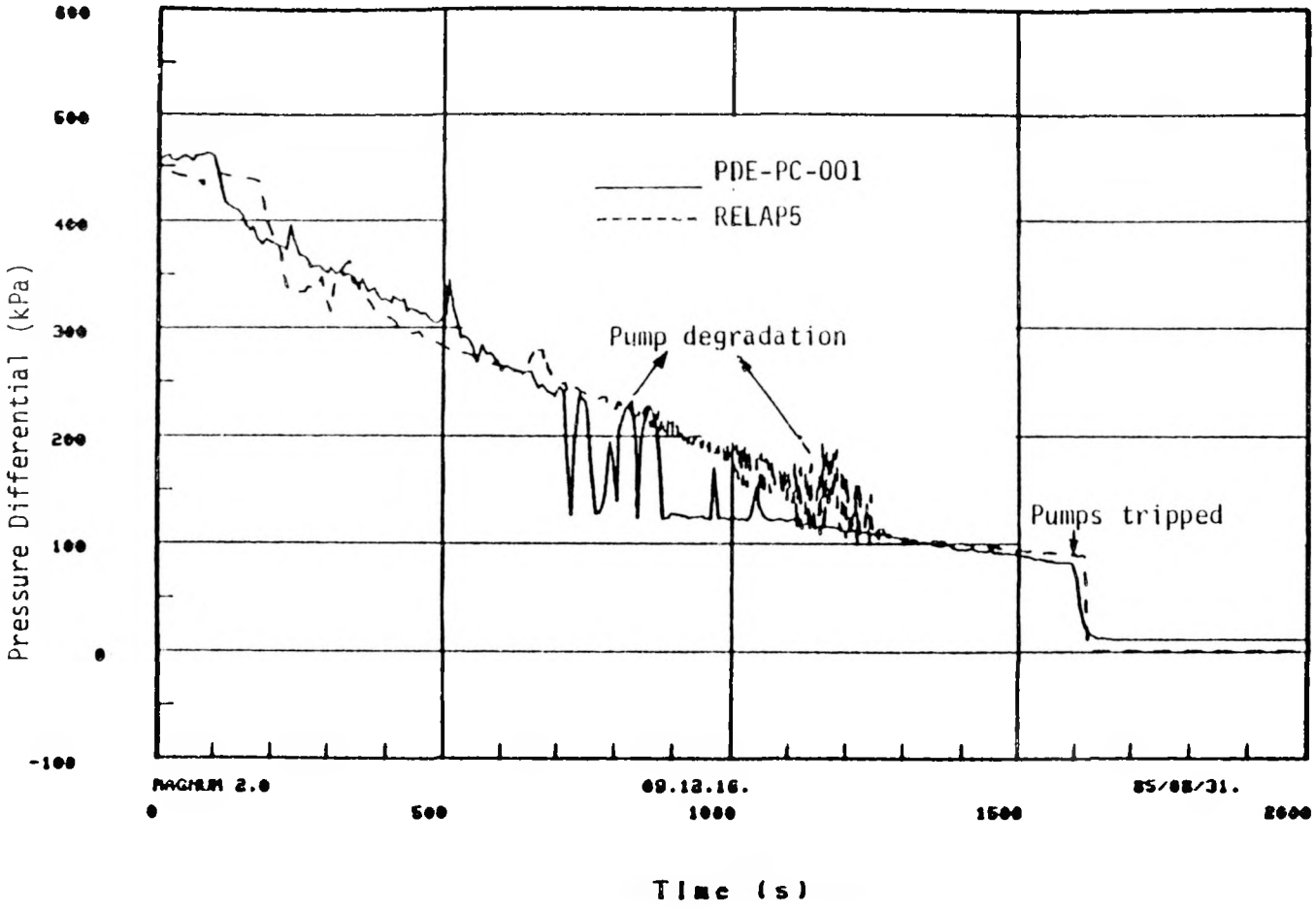


Figure 24. Comparison of pressure differentials across pump

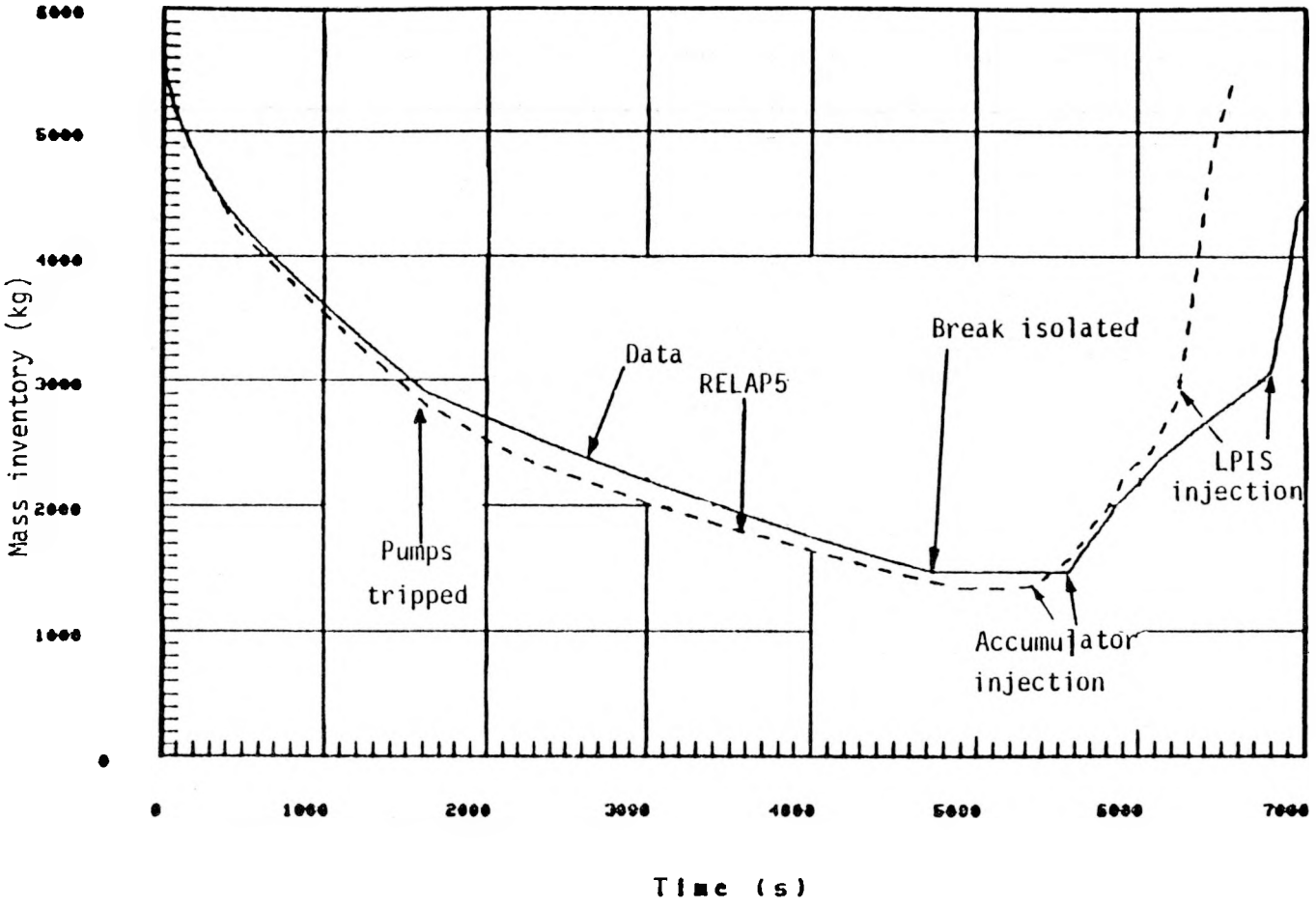


Figure 25. Comparison of primary system mass inventories

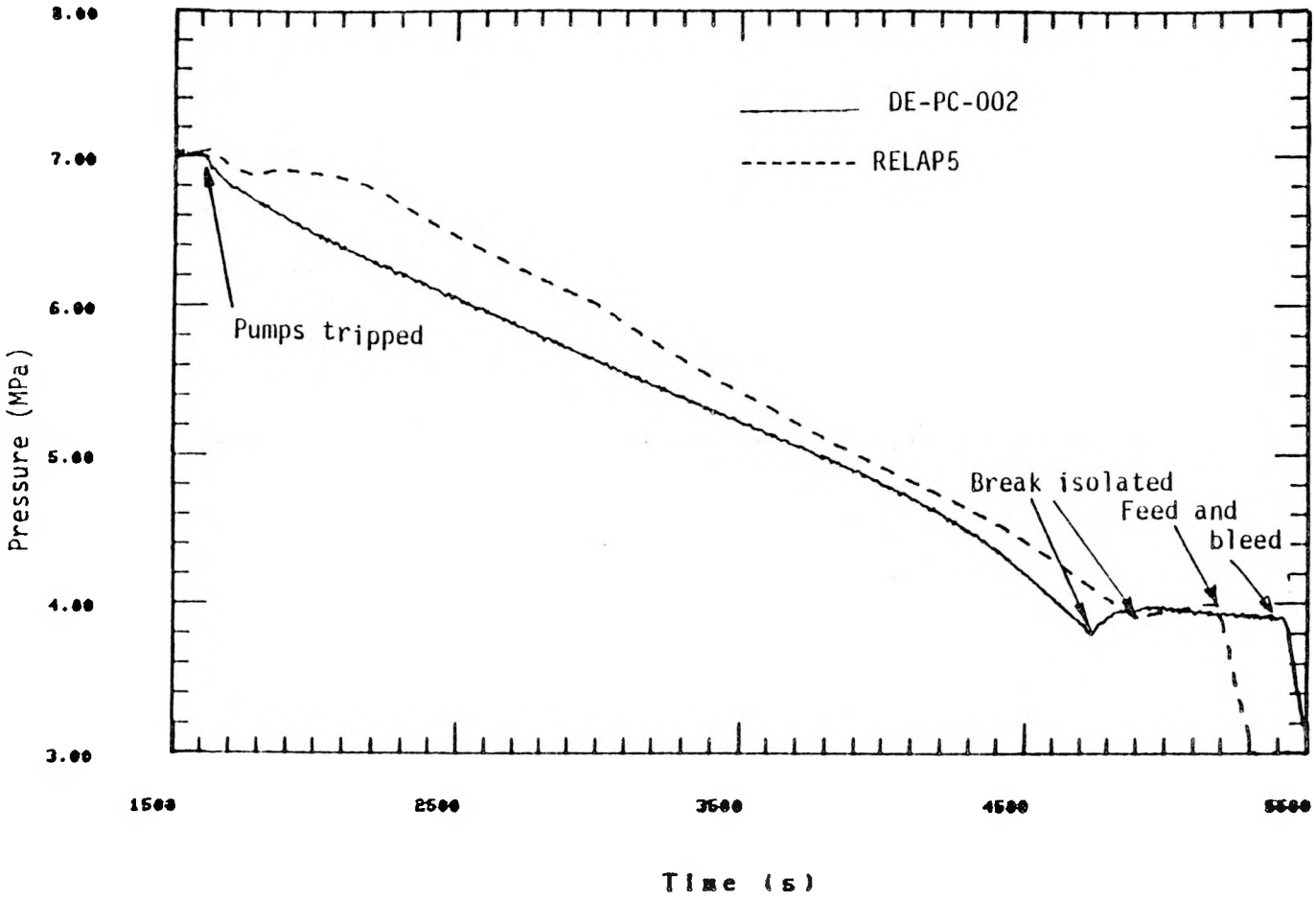


Figure 26. Comparison of pressures in the intact loop hot leg

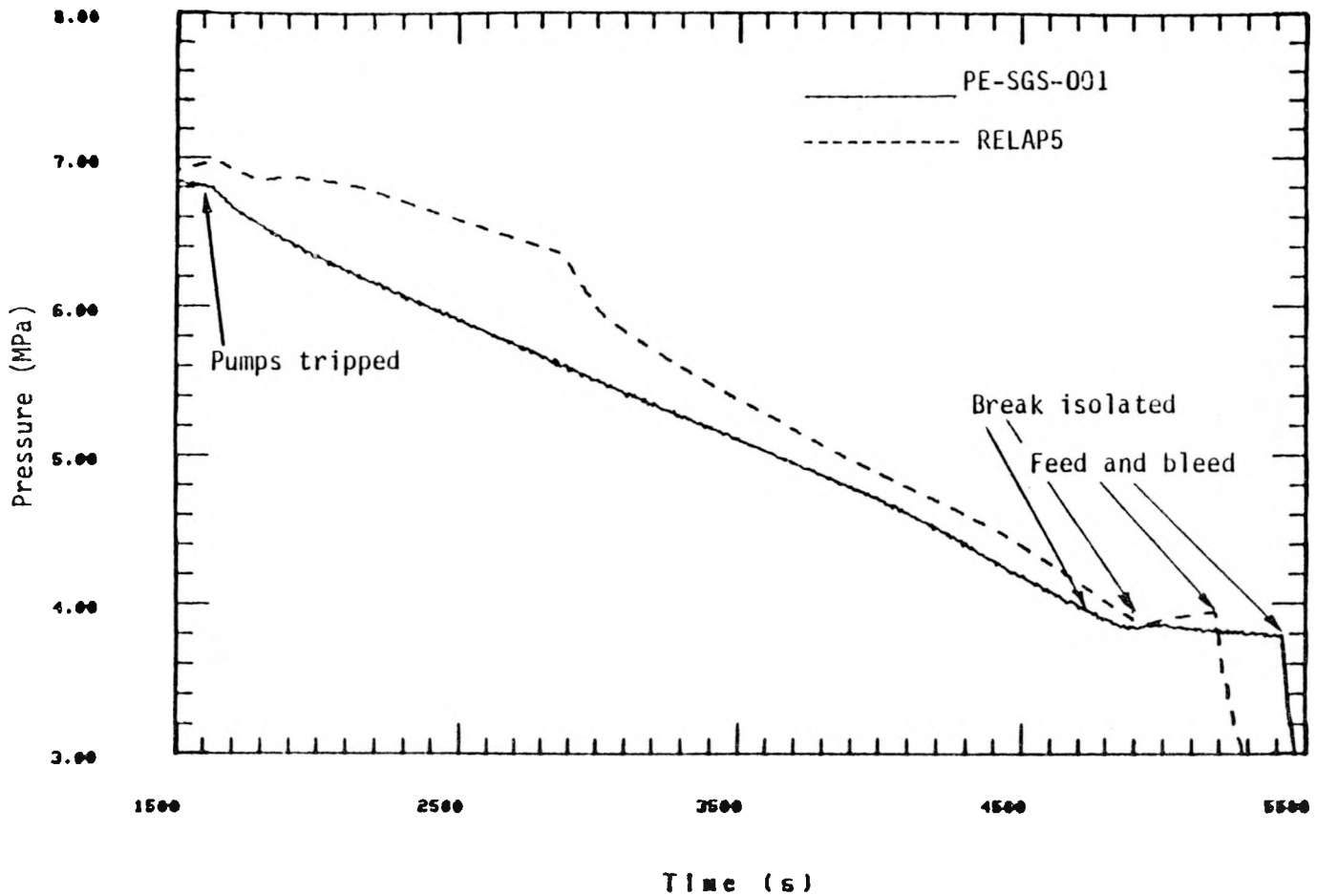


Figure 27. Comparison of pressures in the steam generator secondary side

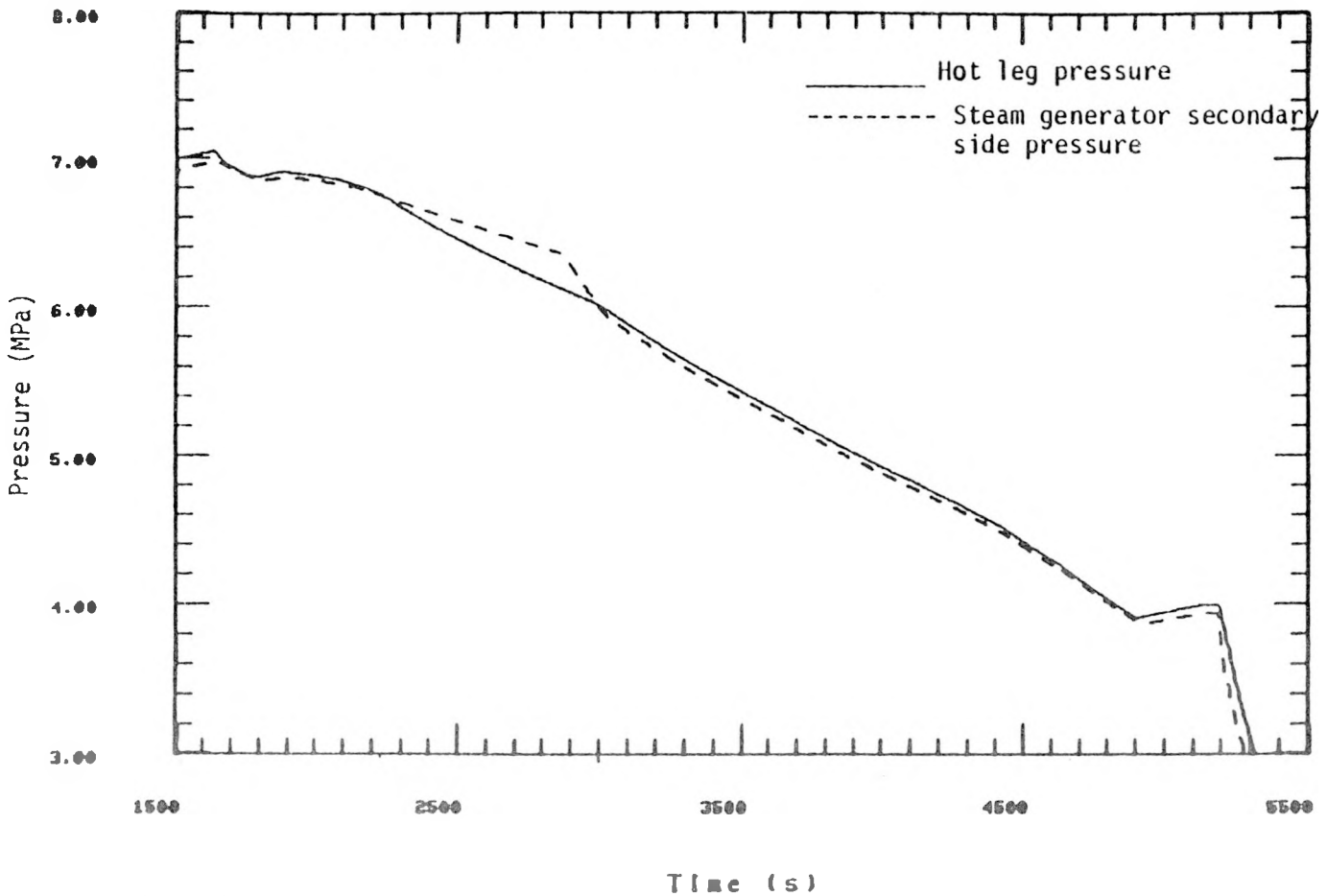


Figure 28. Comparison of calculated pressures in the primary and secondary systems

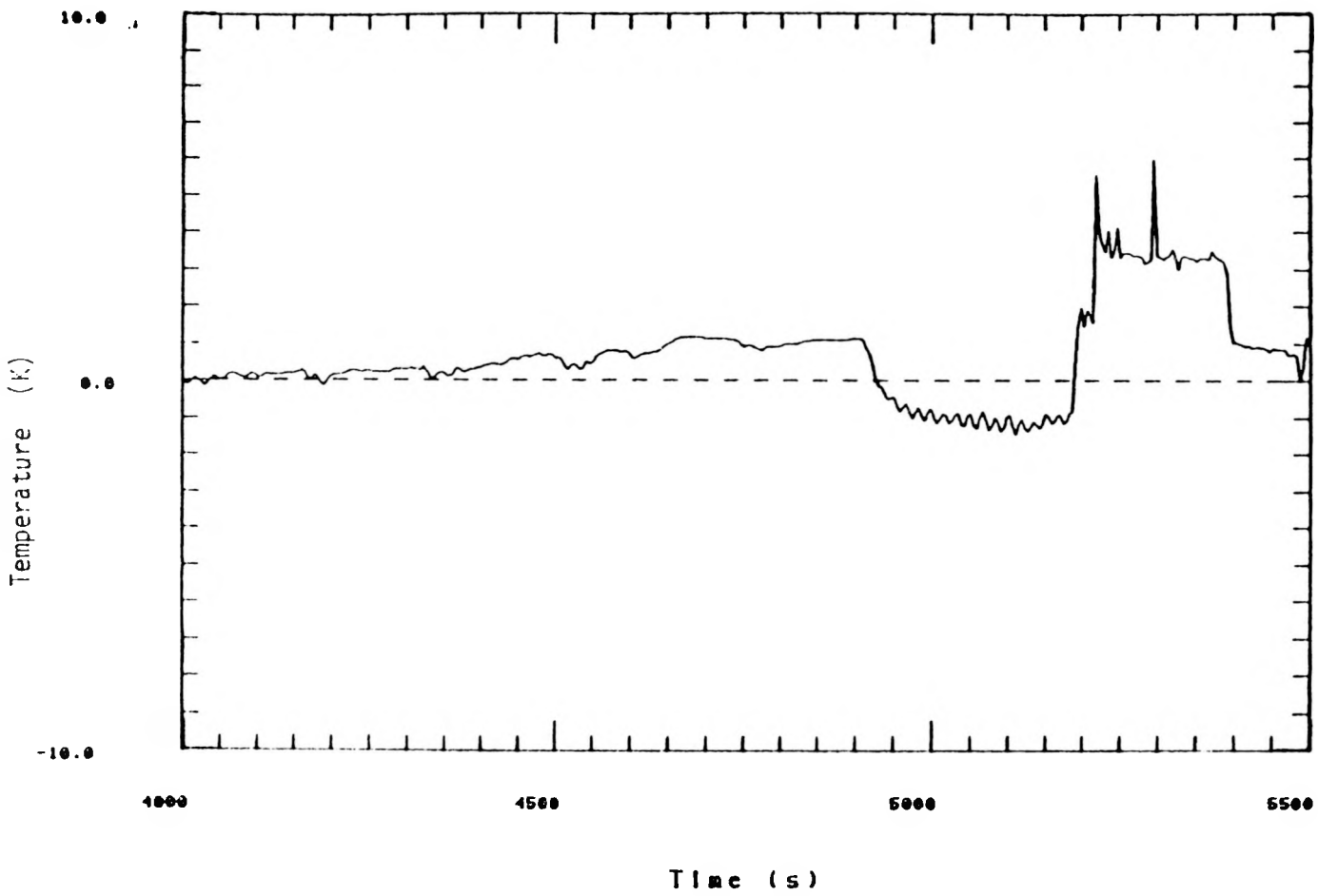


Figure 29. Calculated temperature difference between the primary and secondary systems

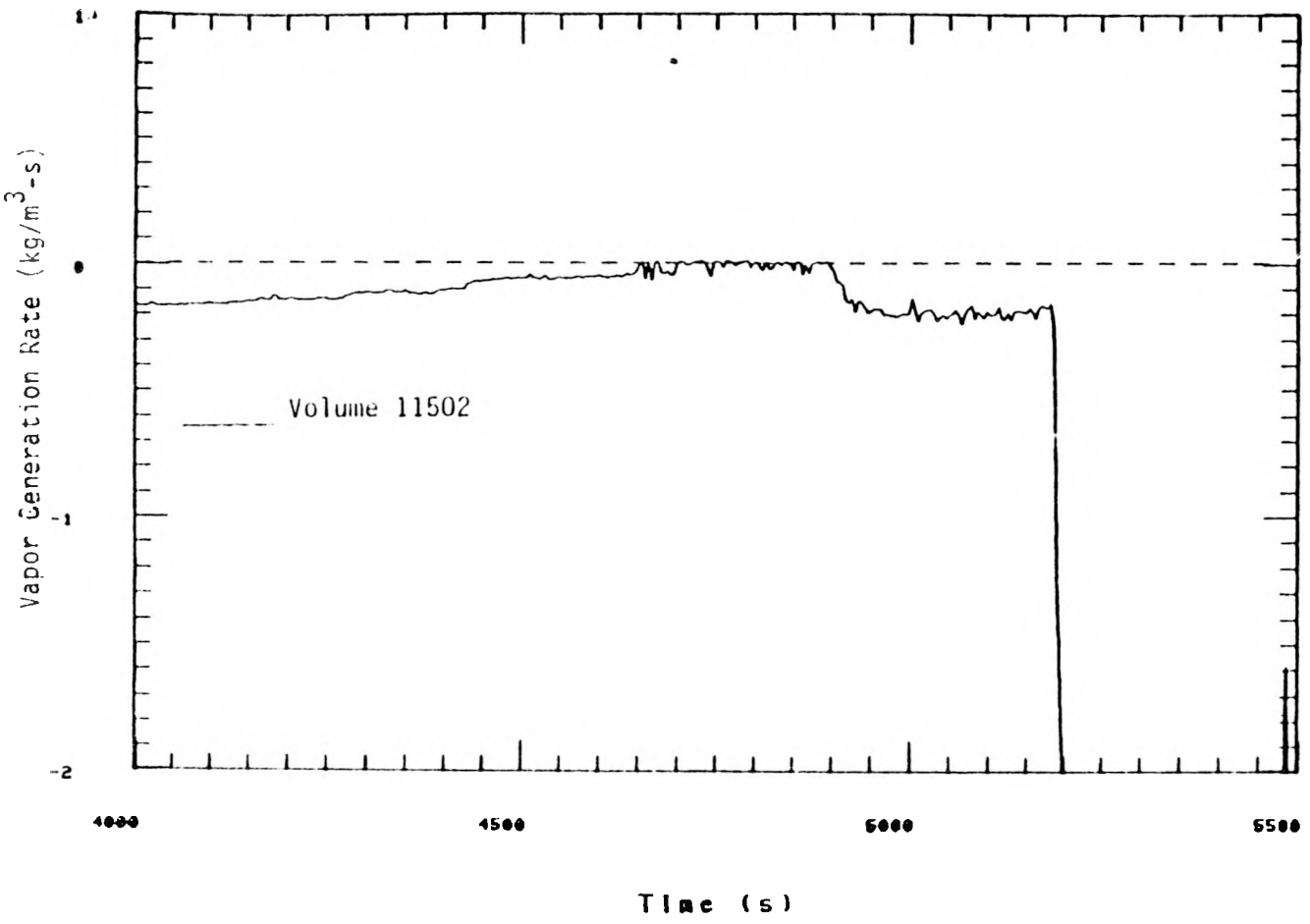


Figure 30. Vapor generation rate in the steam generator uprigth

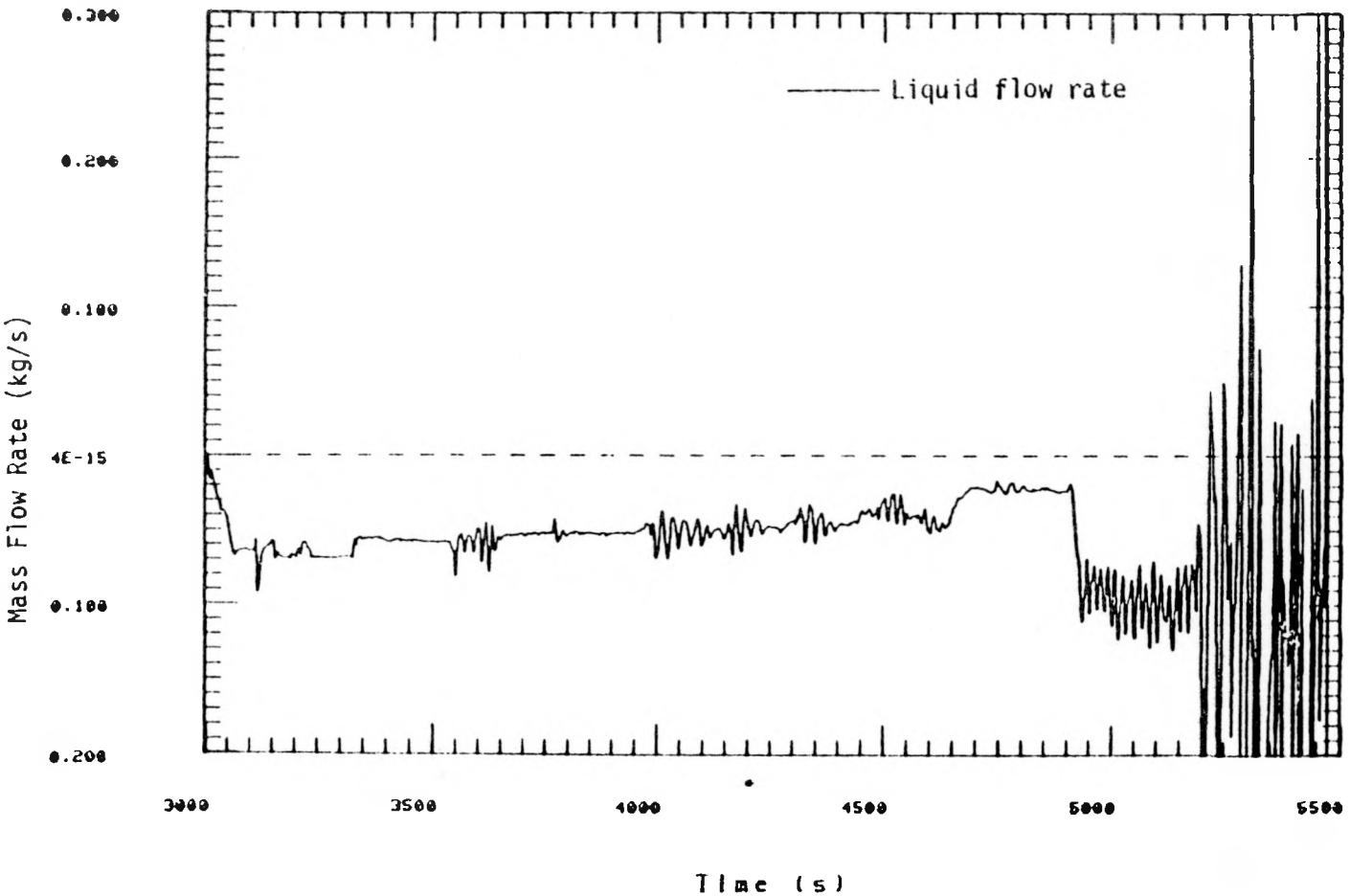


Figure 31. Calculated liquid flow rate in the steam generator inlet plenum

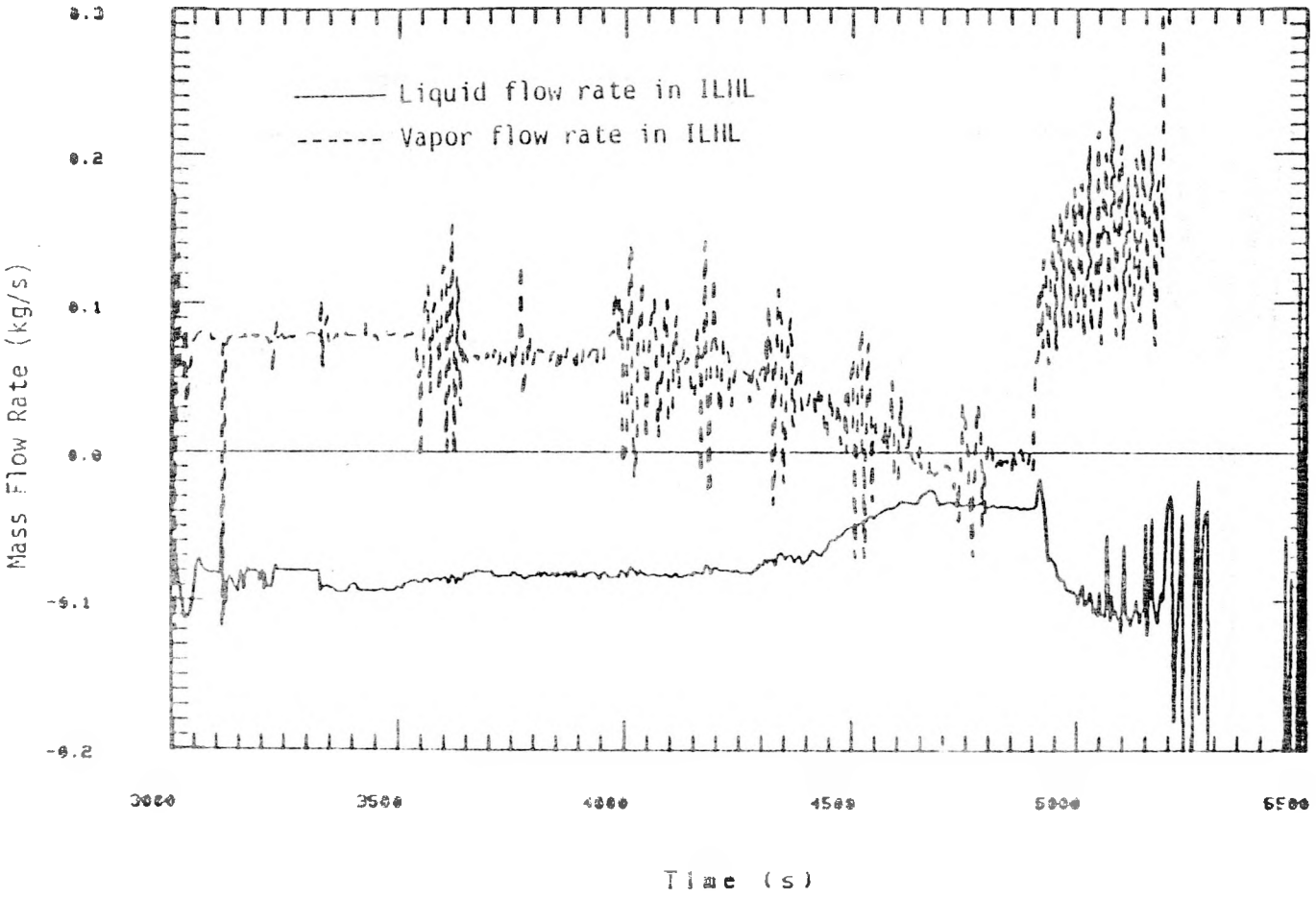


Figure 32. Calculated liquid and vapor flow rates in the intact loop hot leg

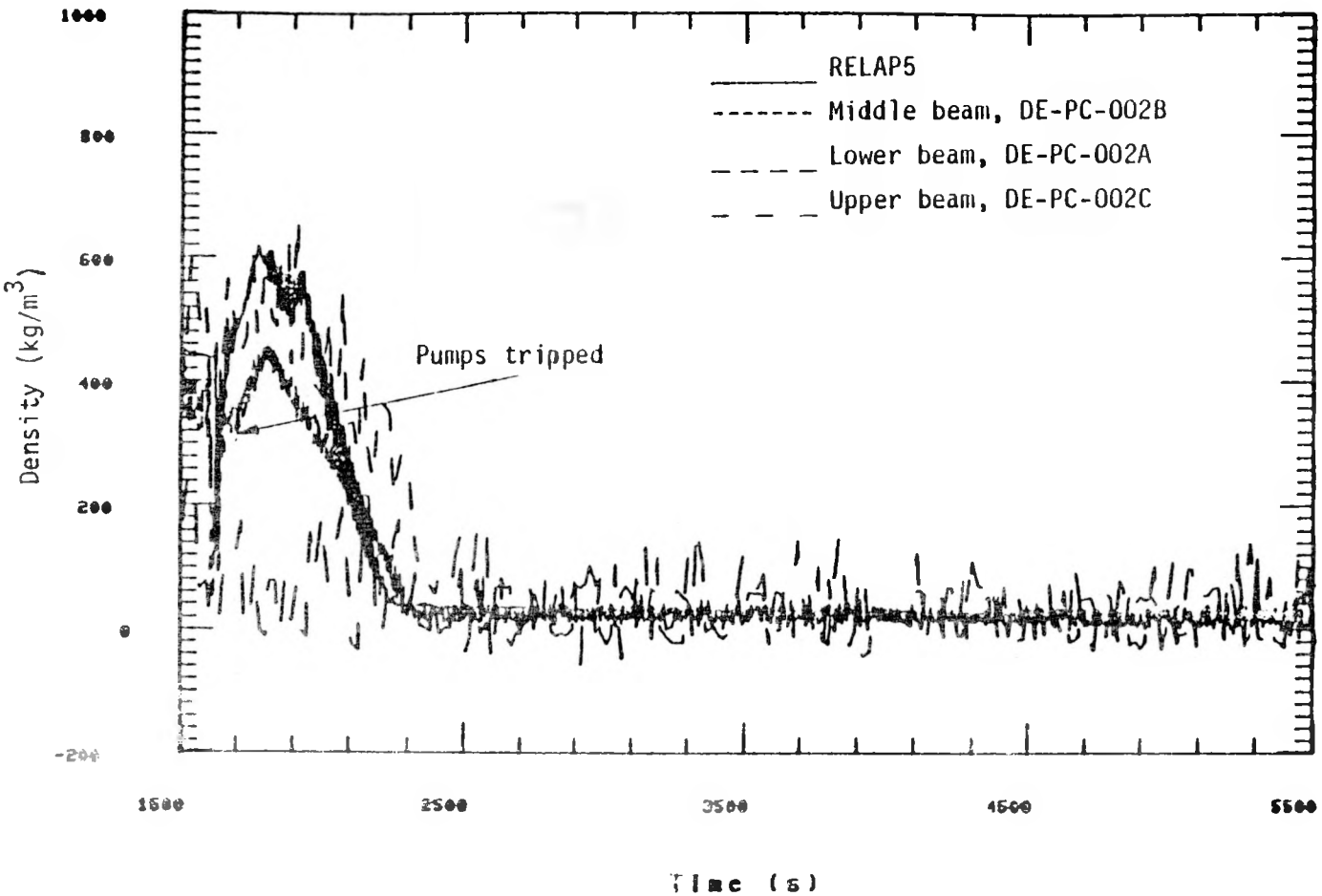


Figure 33. Comparison of densities in the intact loop hot leg

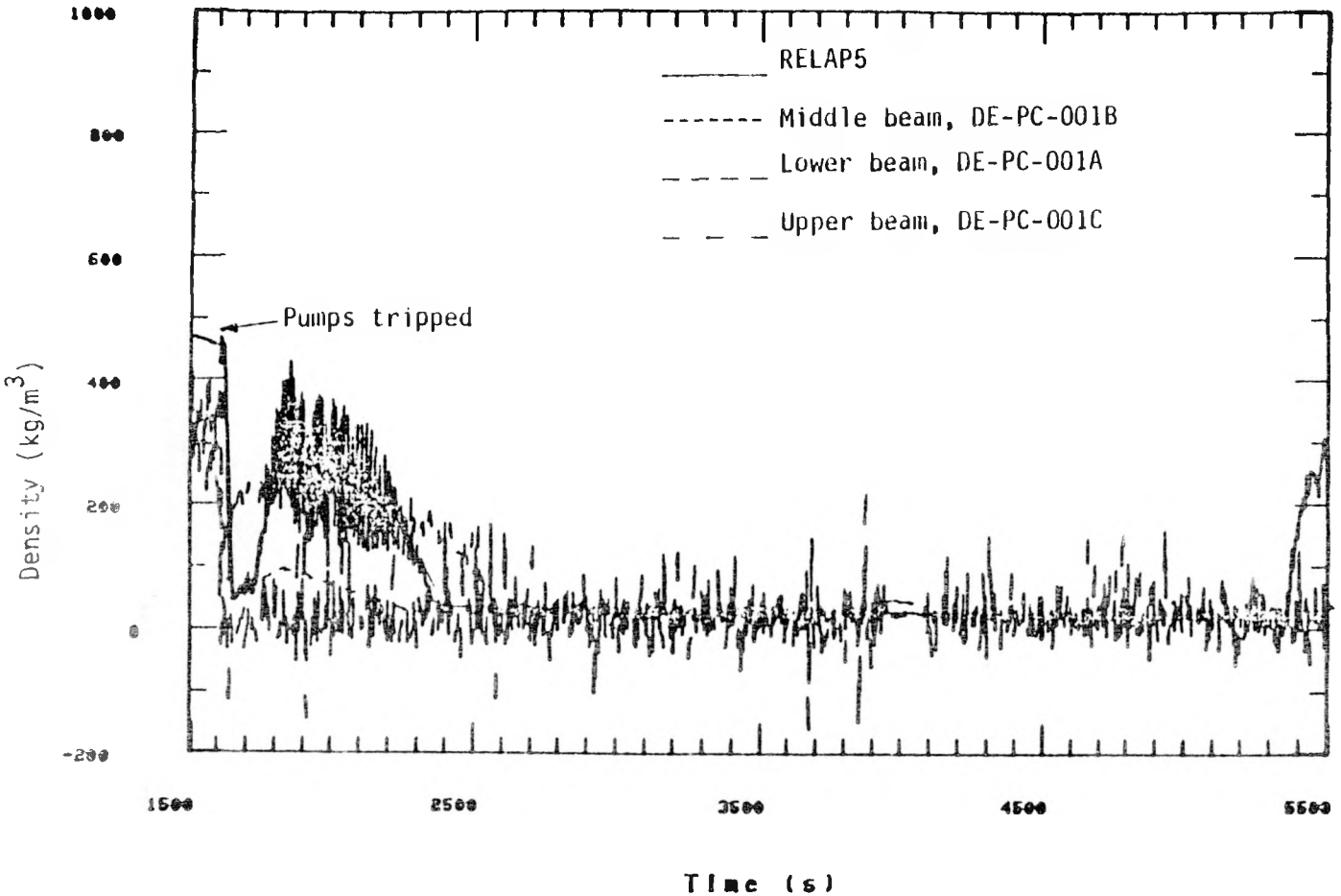


Figure 34. Comparison of densities in the intact loop cold leg

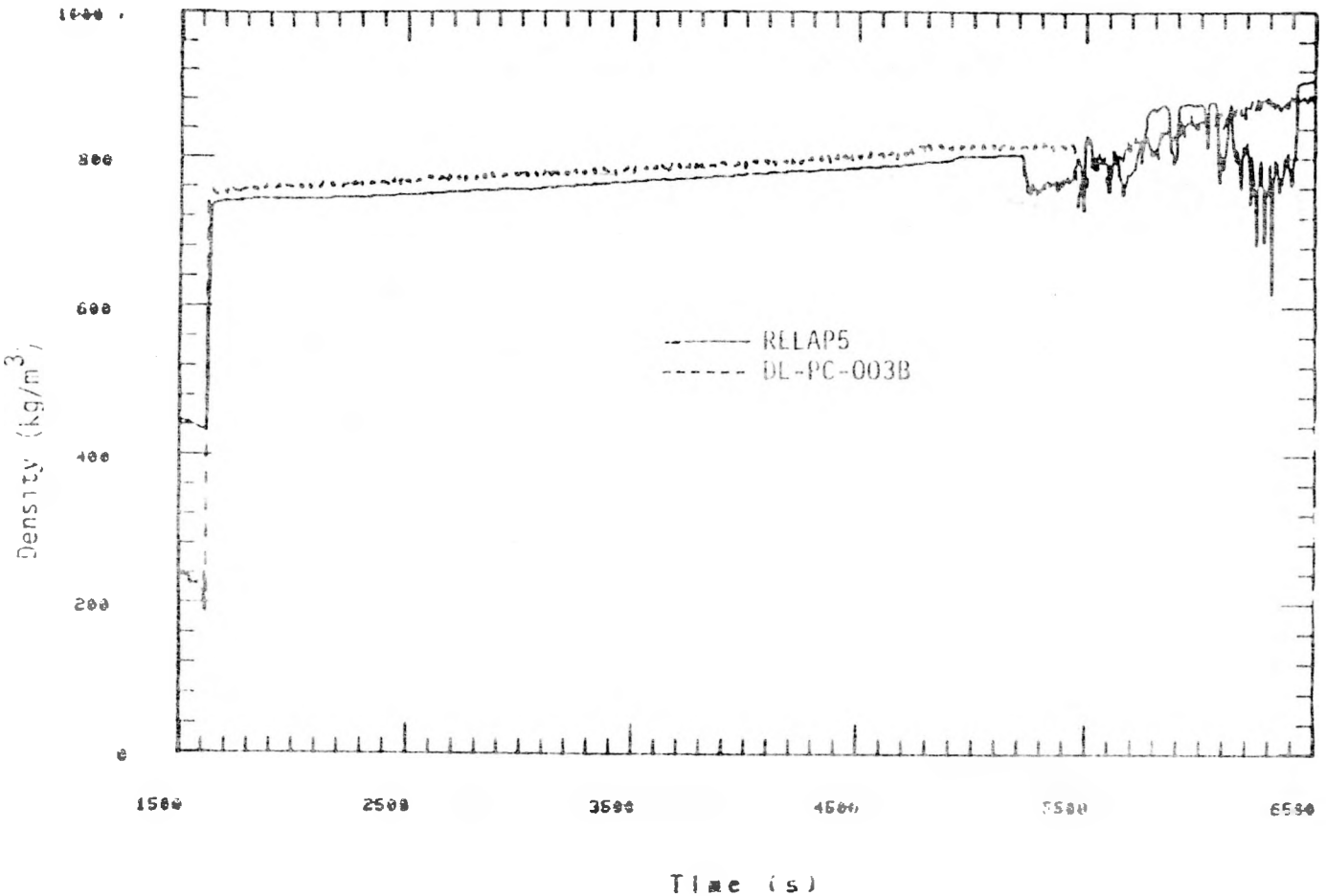


Figure 35. Comparison of densities in the loop seal

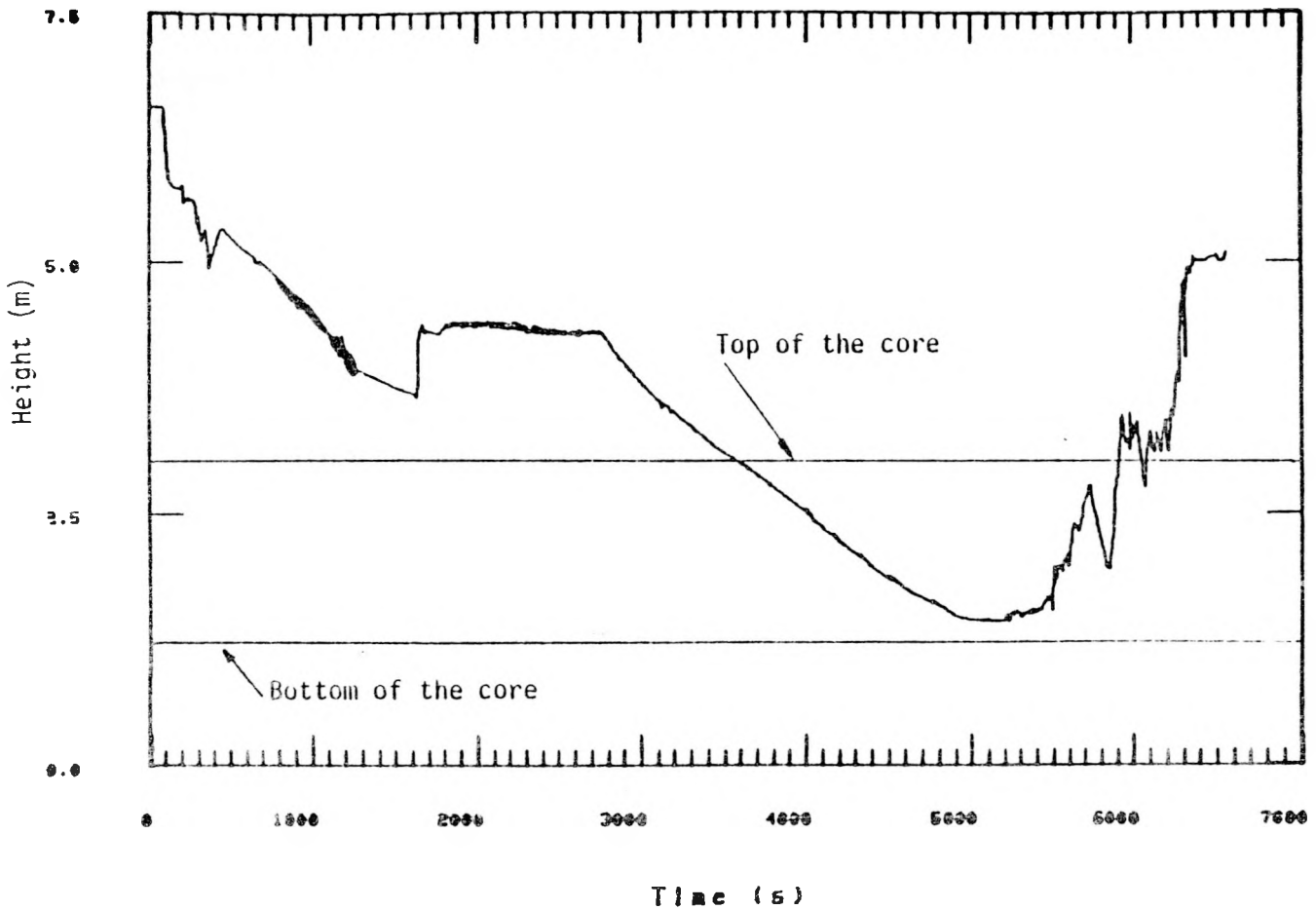


Figure 36 . Calculated collapsed liquid level in the reactor vessel

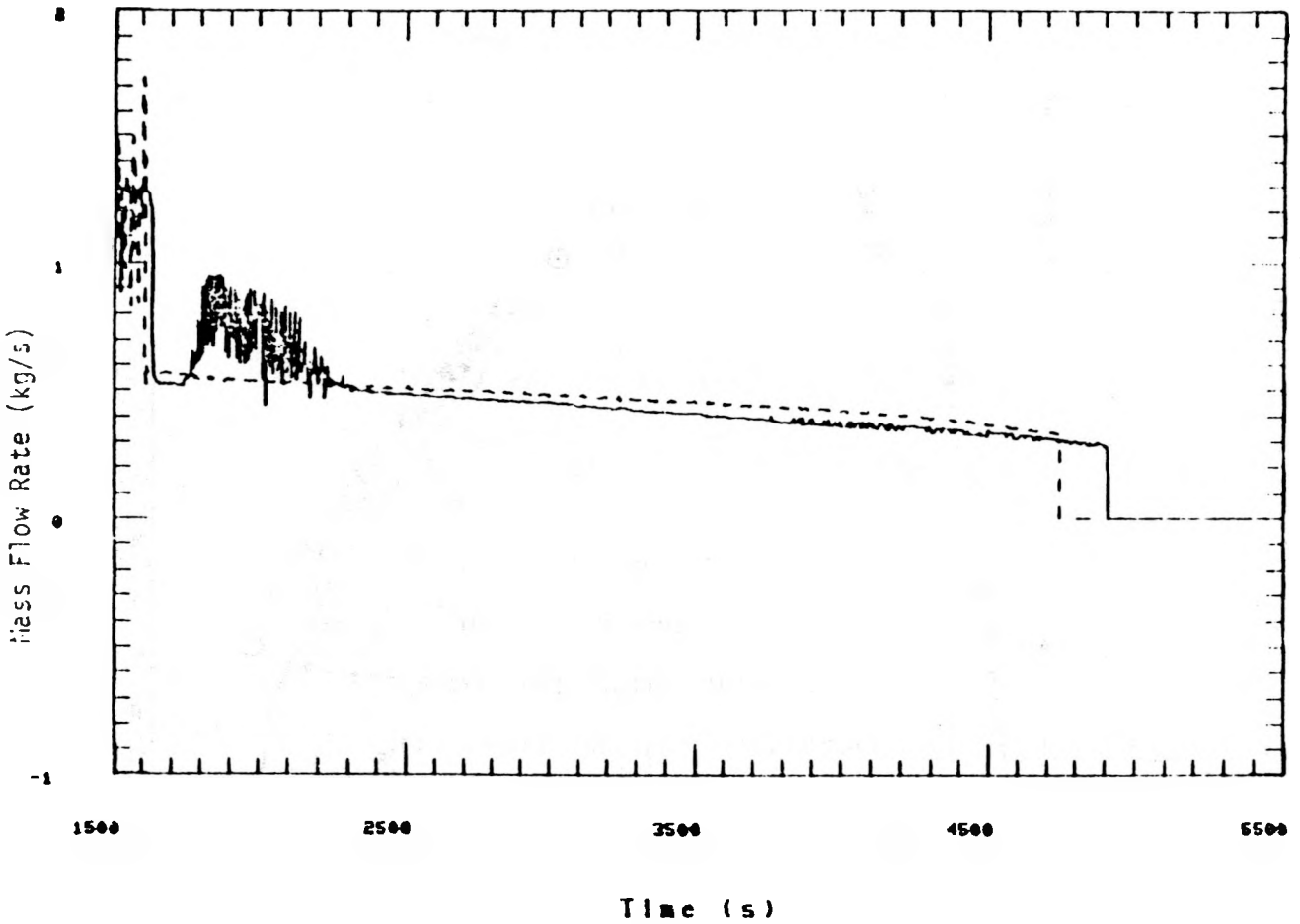


Figure 37. Comparison of break flow rates

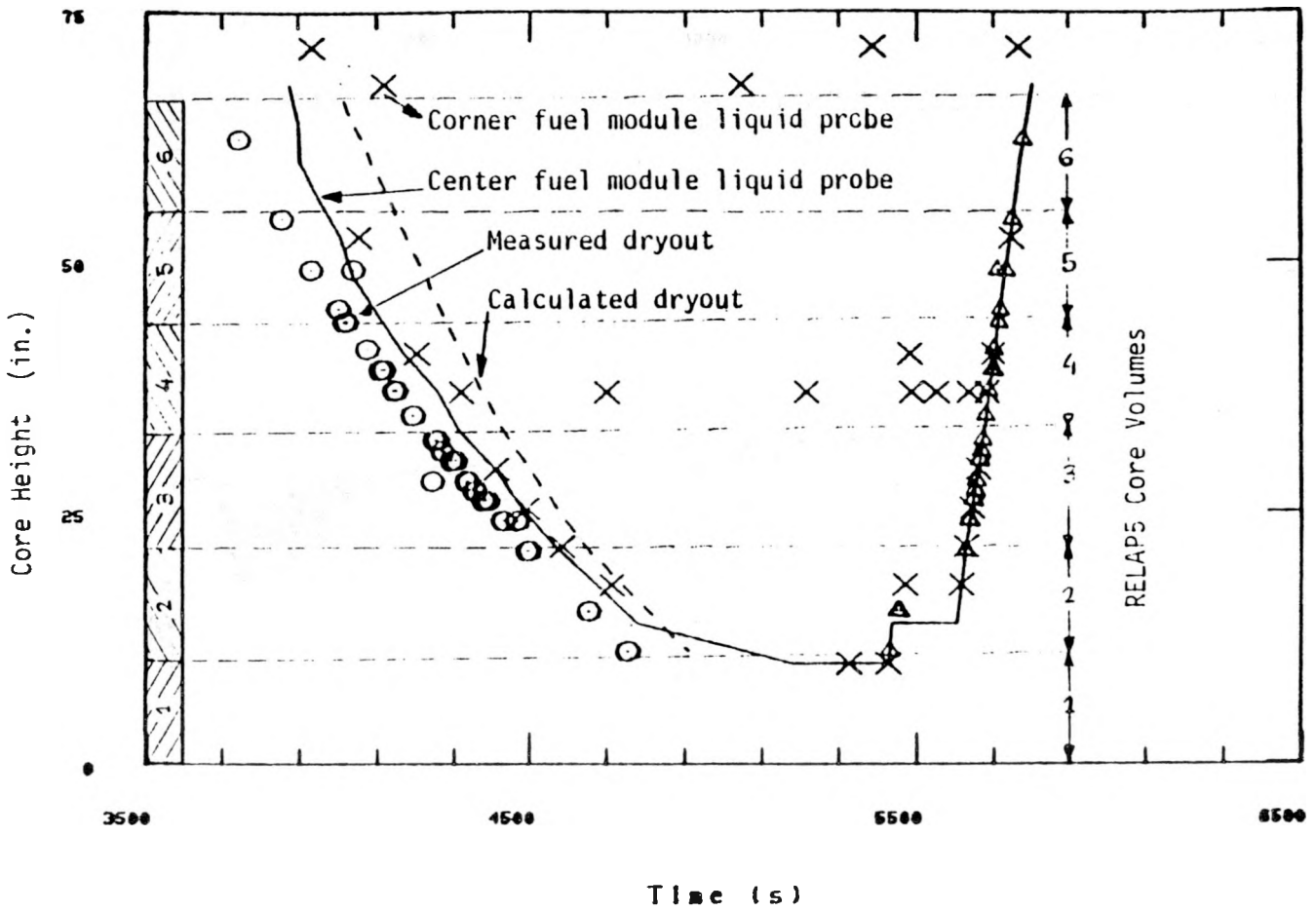


Figure 38. Comparison of dryouts measured and calculated

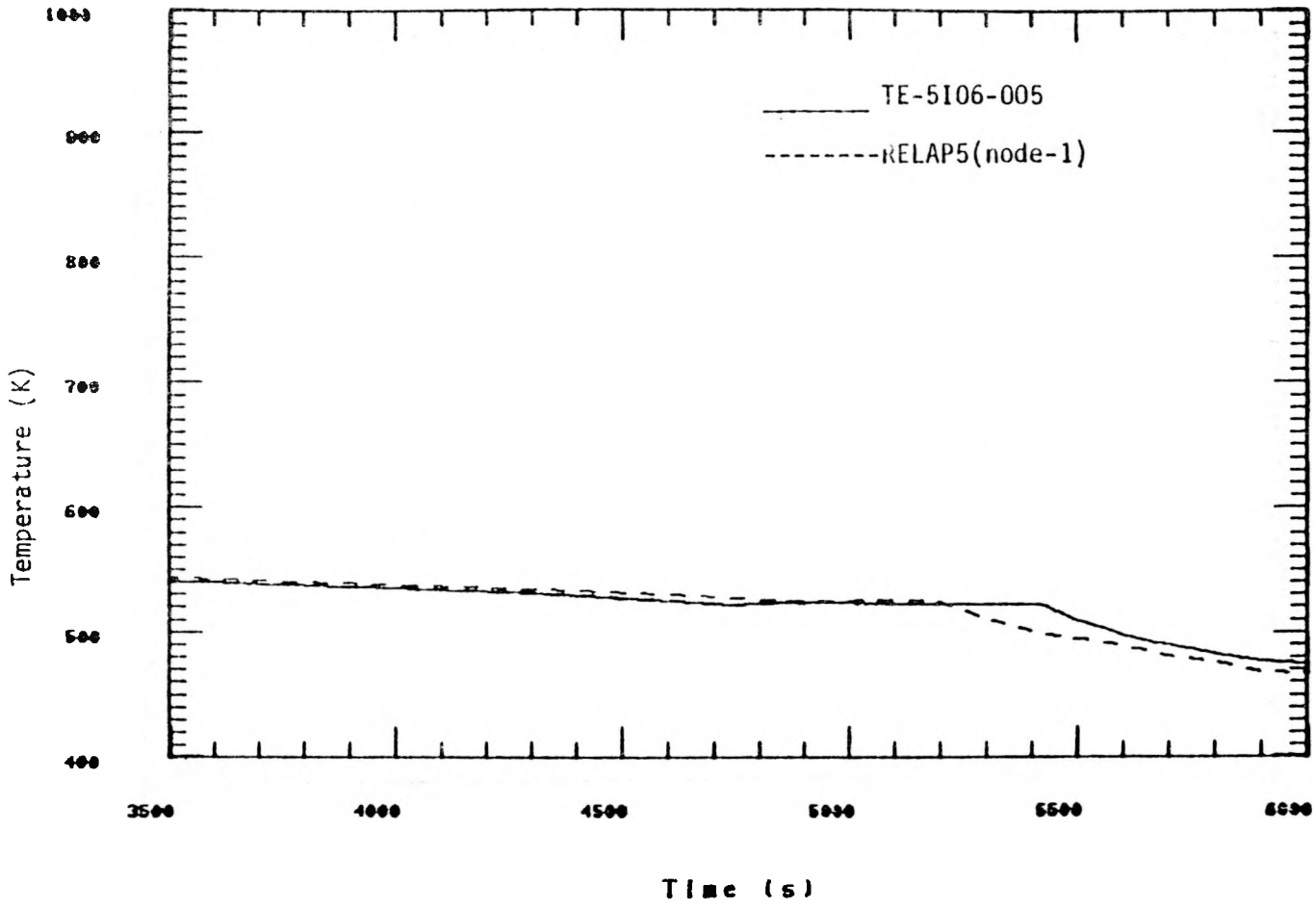


Figure 39. Comparison of cladding temperatures at 12.7 cm elevation

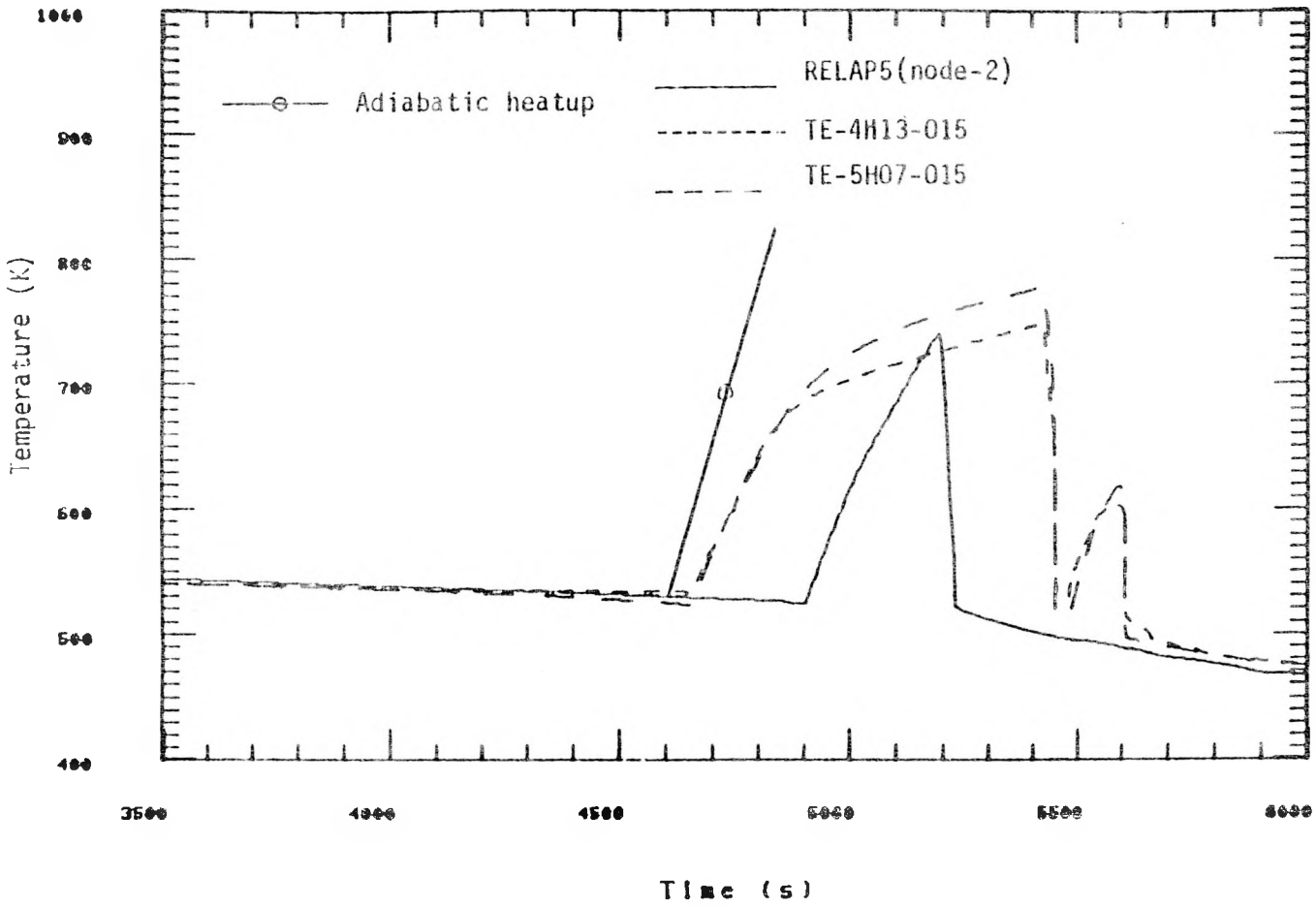


Figure 40. Comparison of fuel cladding temperatures at 38 cm elevation

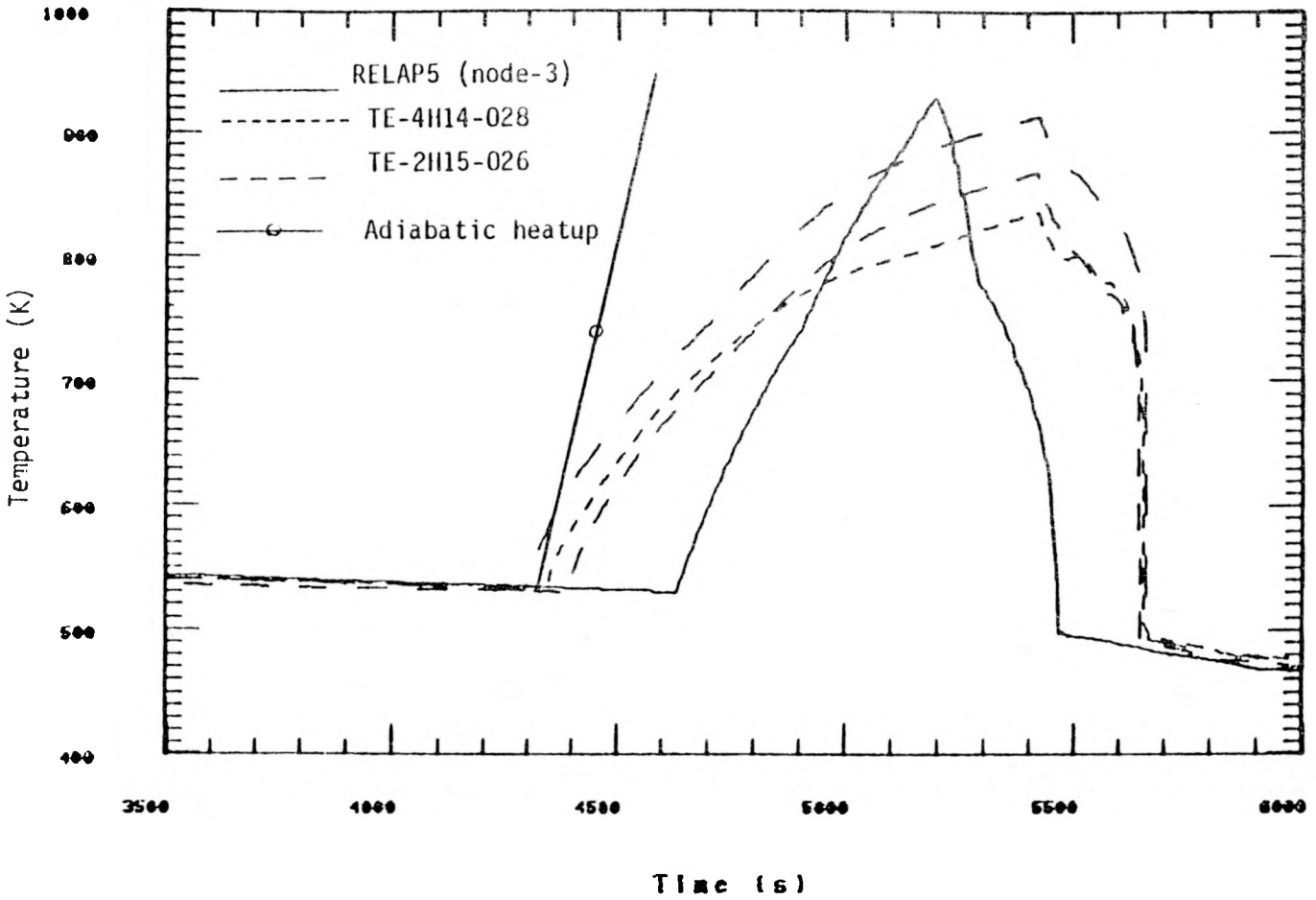


Figure 41. Comparison of fuel cladding temperatures at 69 cm elevation

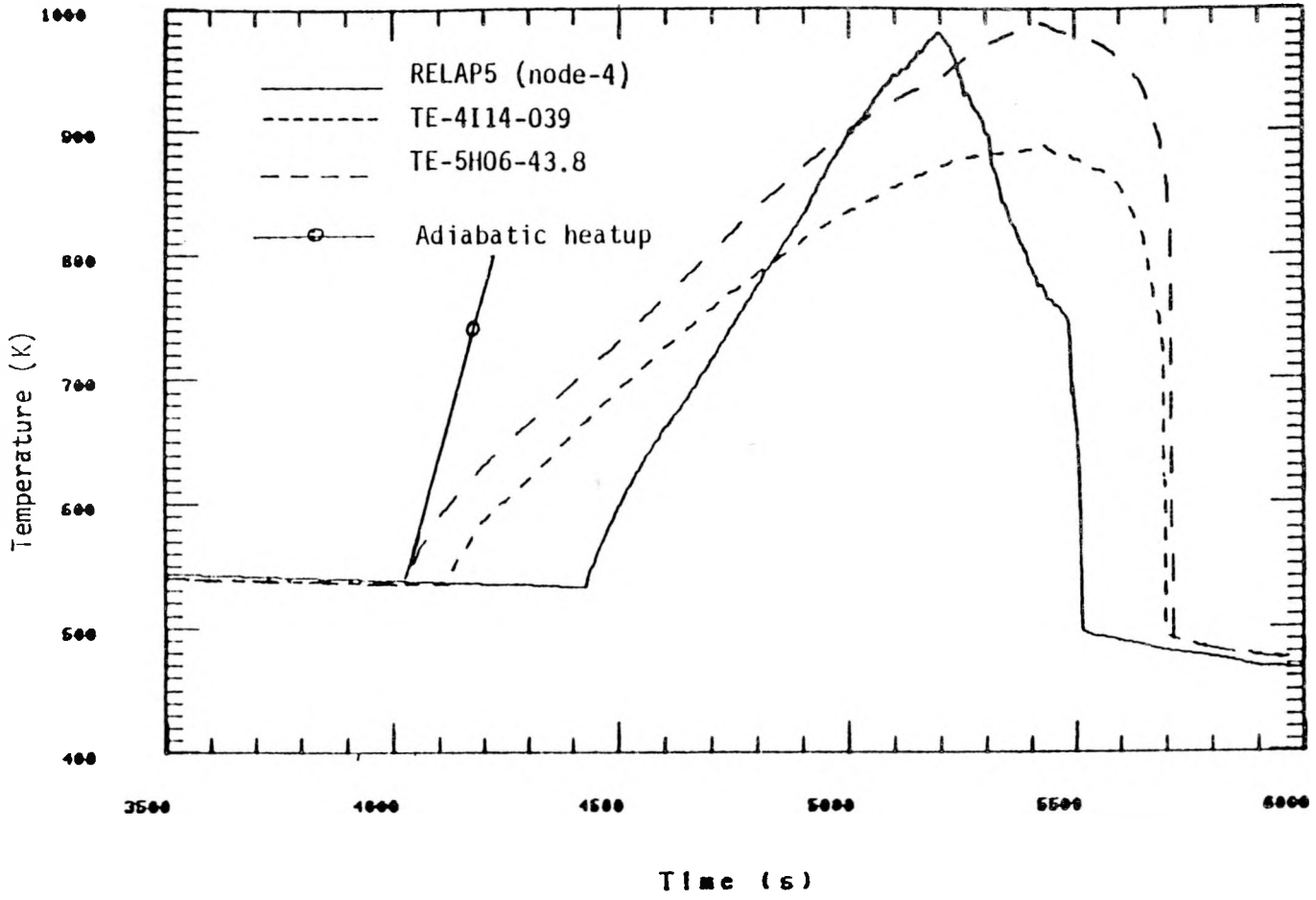


Figure 42. Comparison of fuel cladding temperature at 102 cm elevation

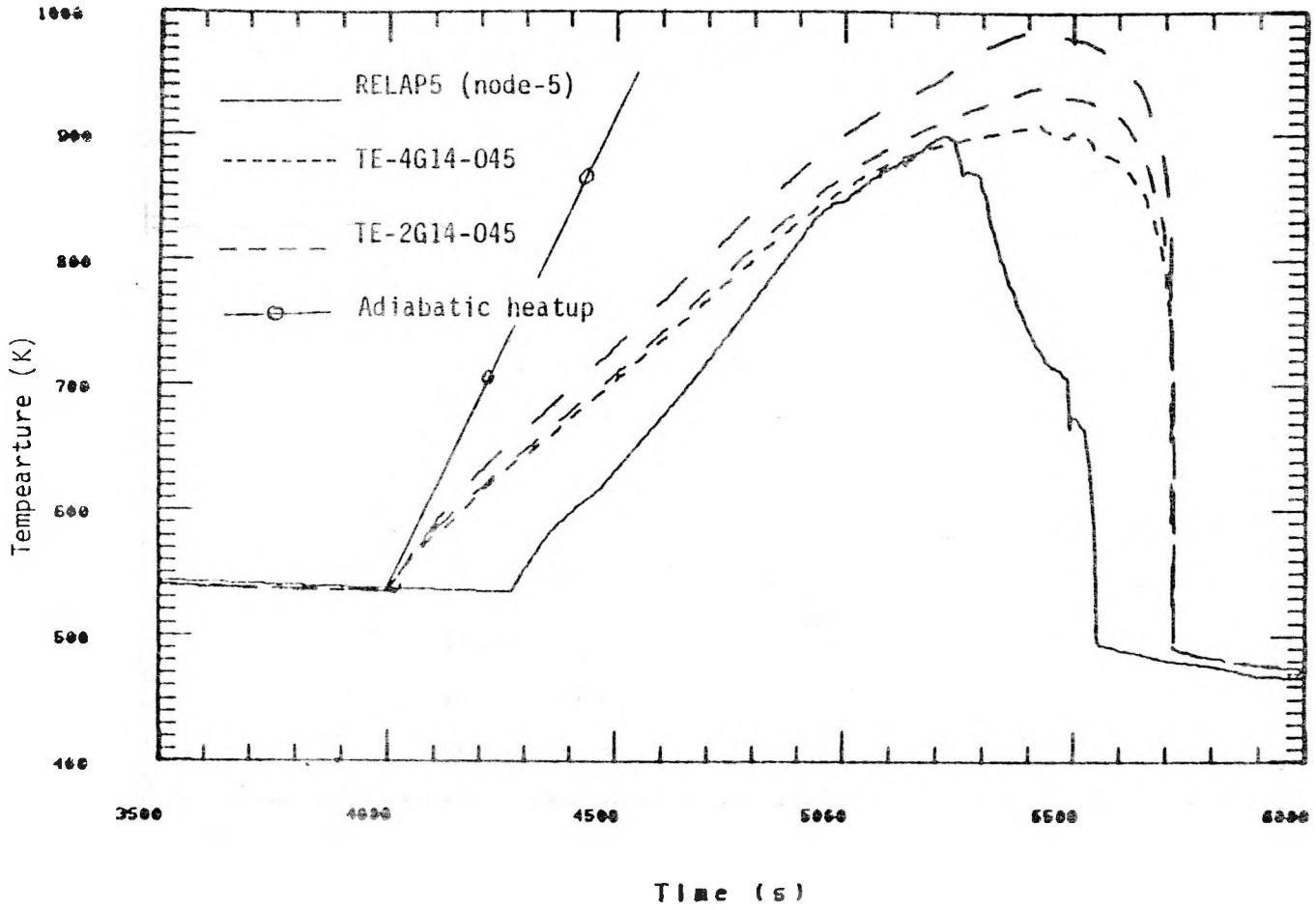


Figure 43. Comparison of fuel cladding temperatures at 114 cm elevation

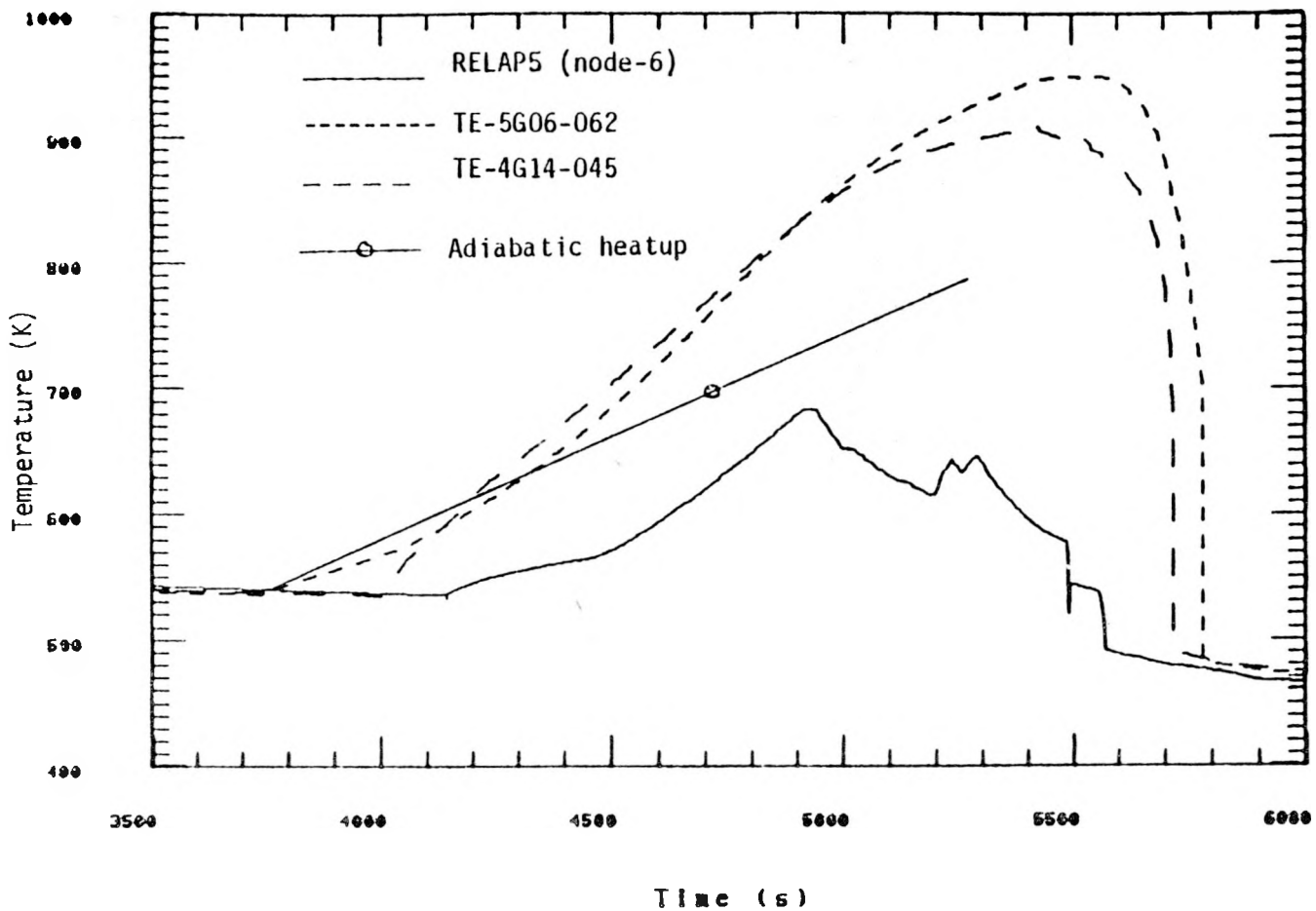


Figure 44. Comparison of fuel cladding temperatures at 157 cm elevation

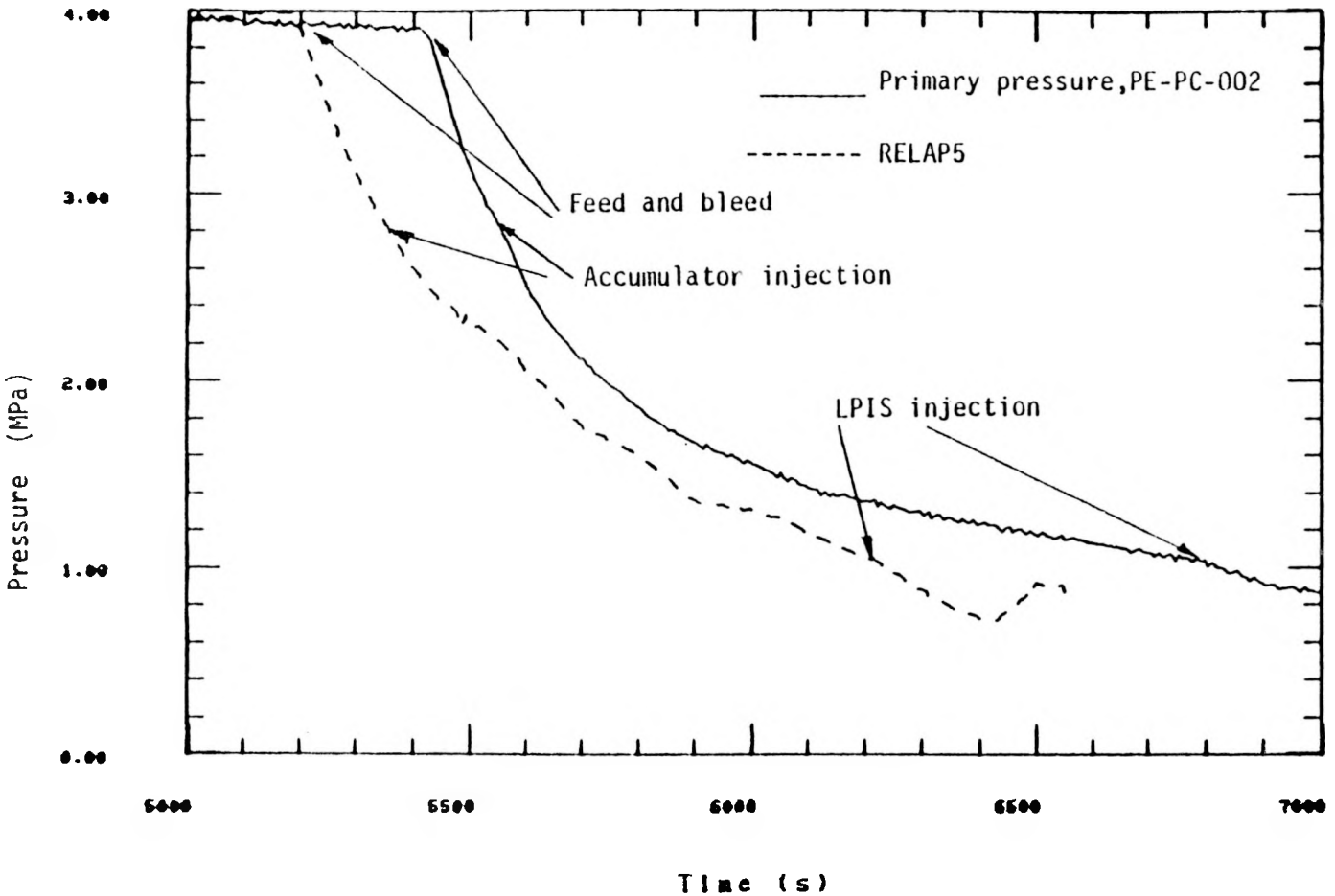


Figure 45. Comparison of pressures in the intact loop hot leg

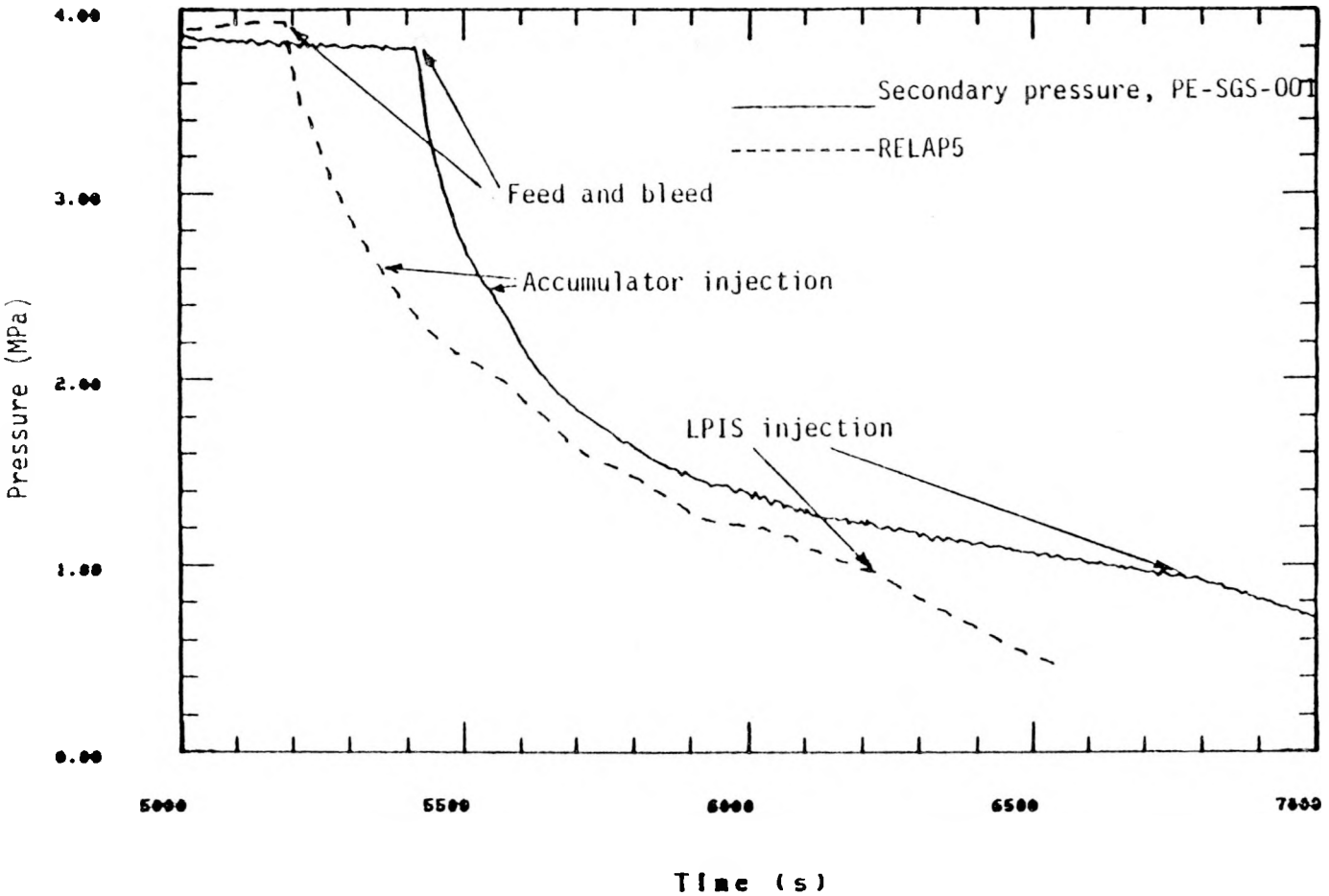


Figure 46. Comparison of pressures in the secondary side

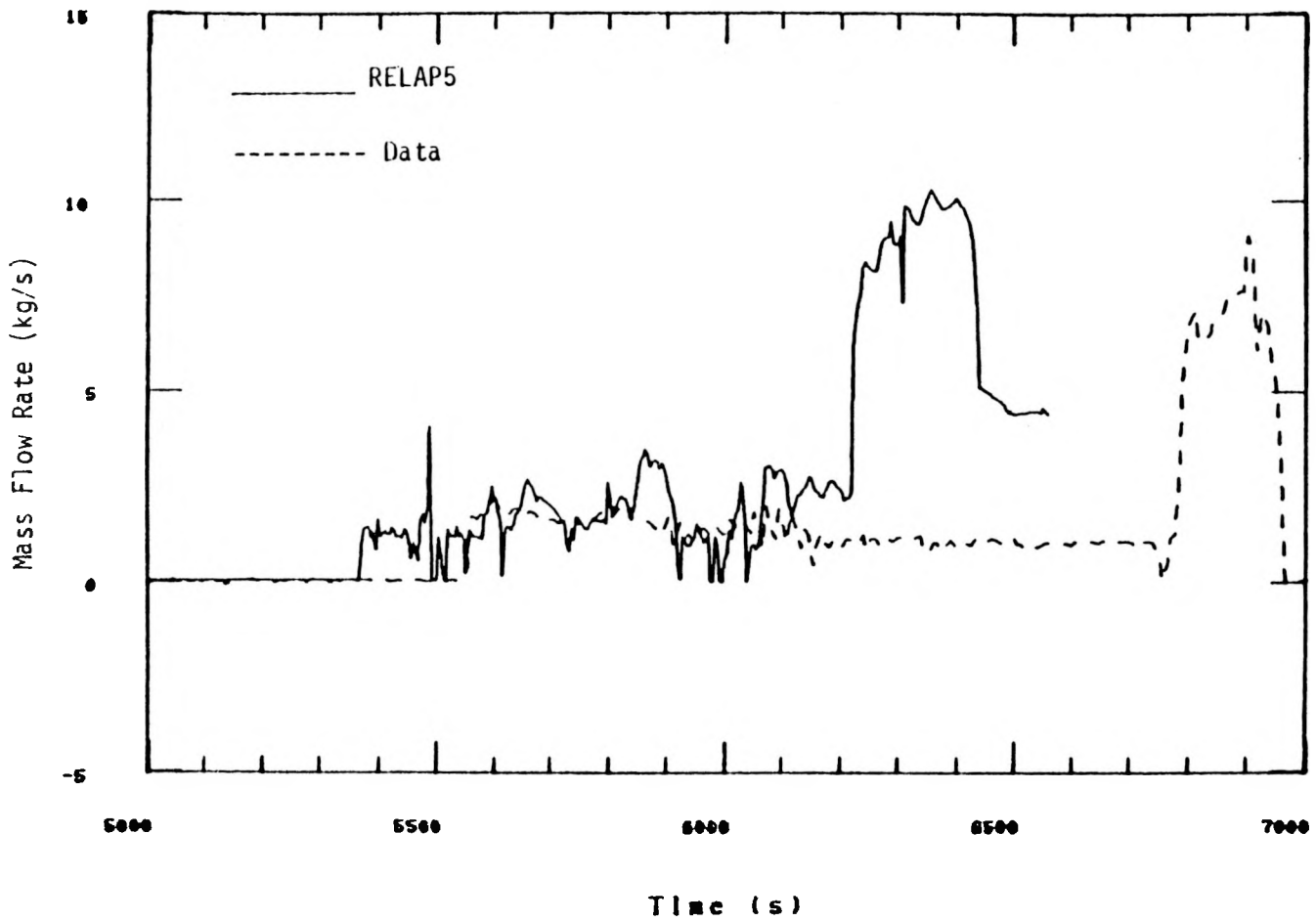


Figure 47. Comparison of ECC injection flow rates

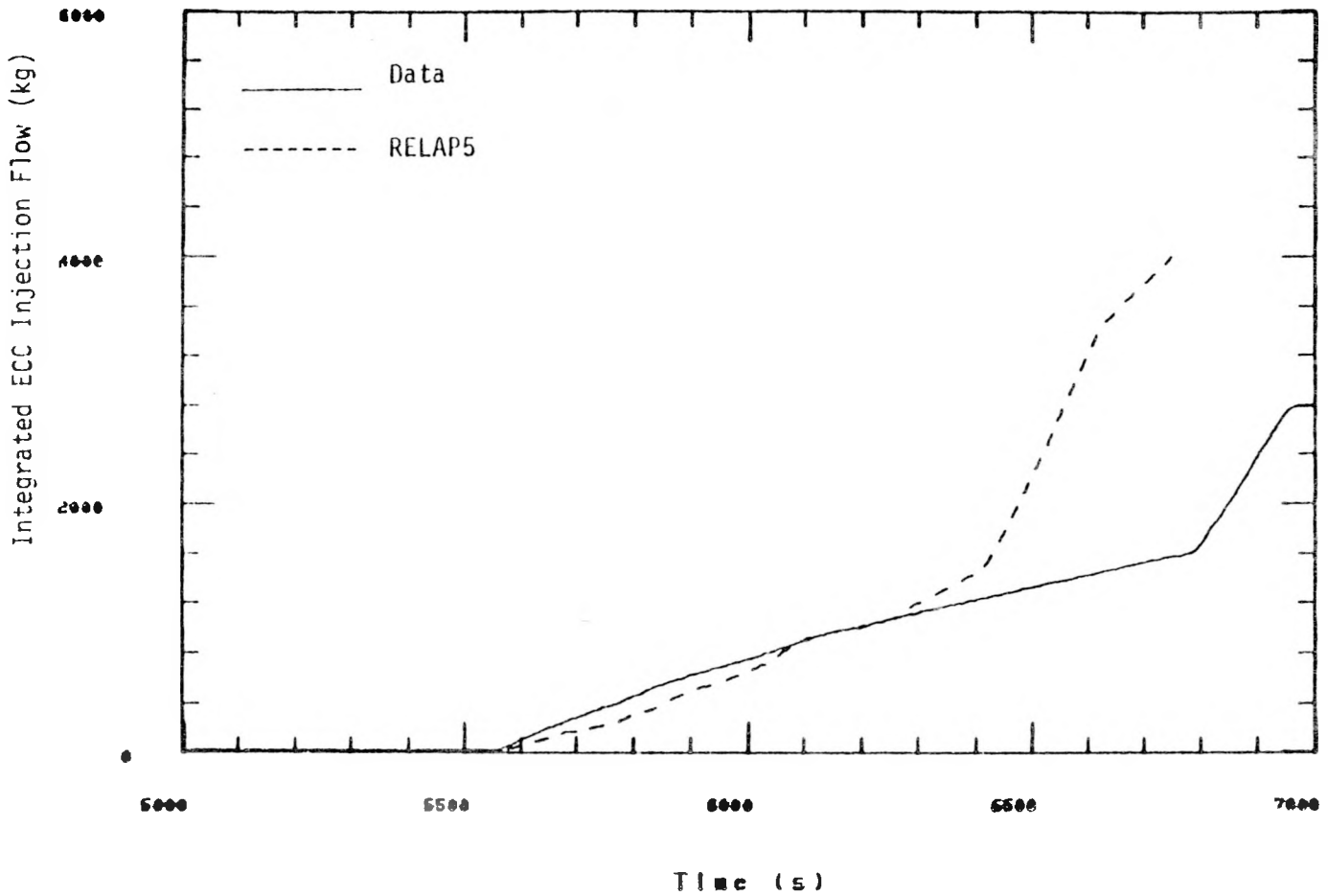


Figure 48. Comparison of integrated ECC injection flows

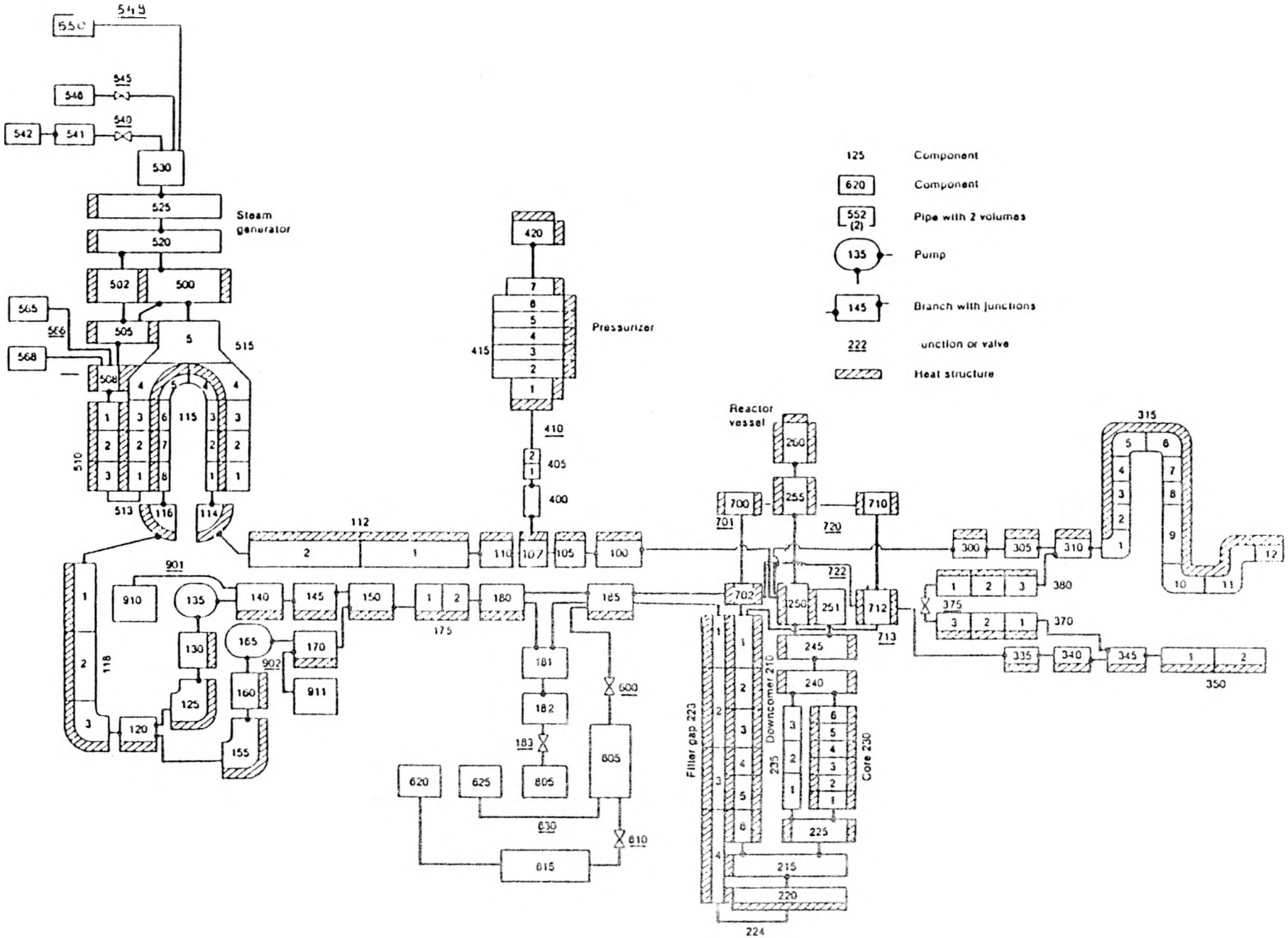


Figure 49 . RELAP5/MOD2 Nodalization for Sensitivity analysis

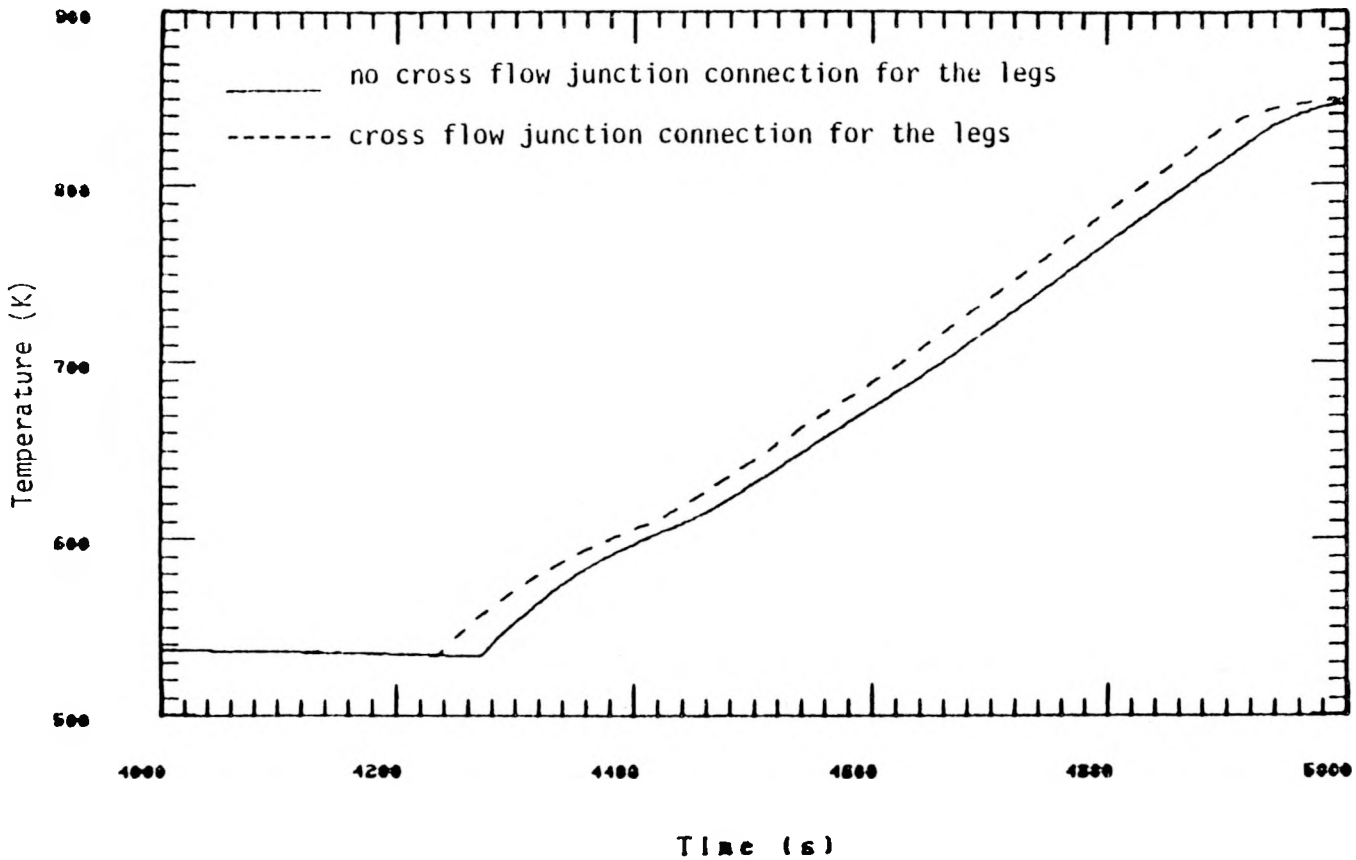


Figure 50. Comparison of fuel cladding tempeartures at level 5

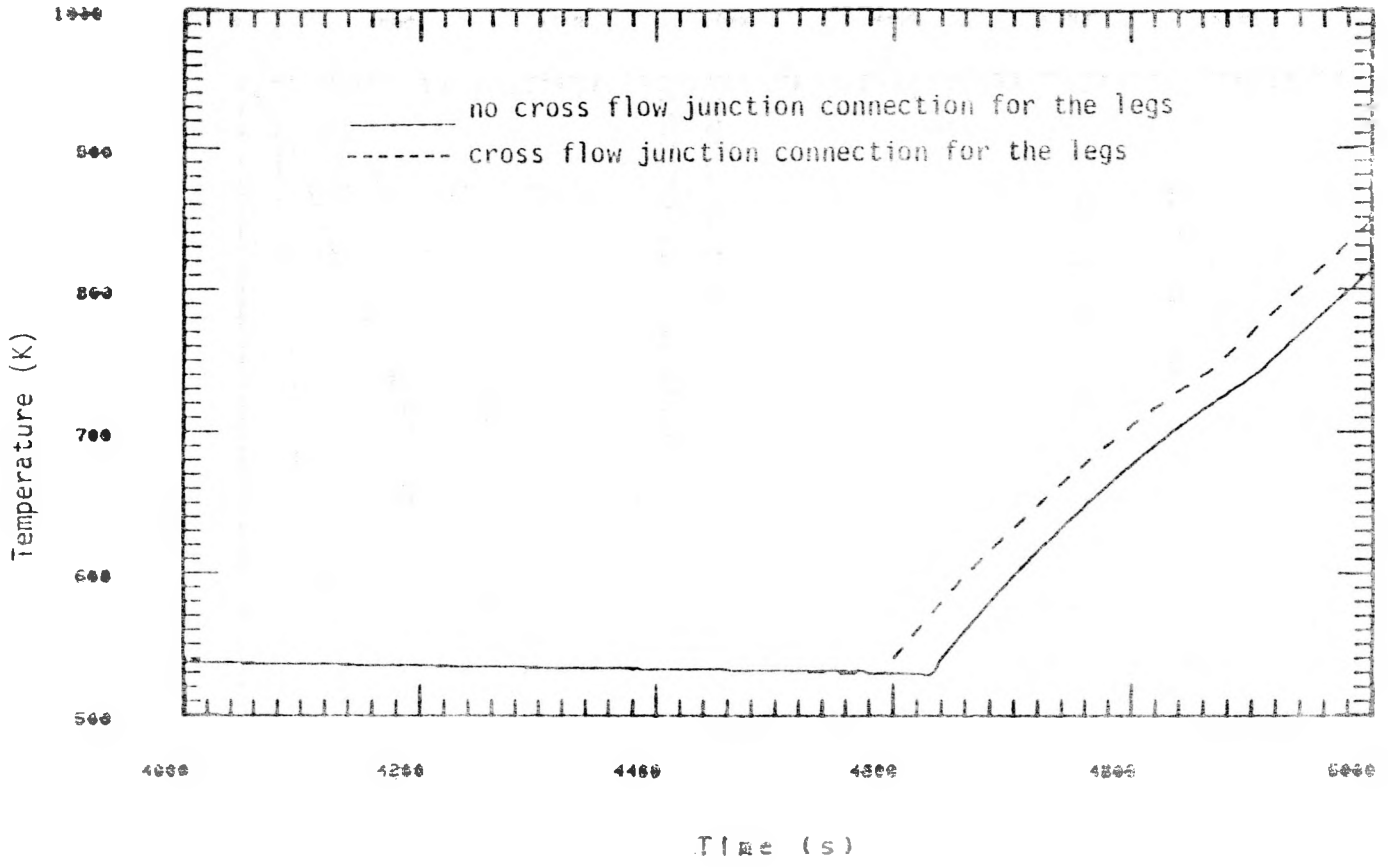


Figure 51. Comparison of fuel cladding tempeartures at level 3

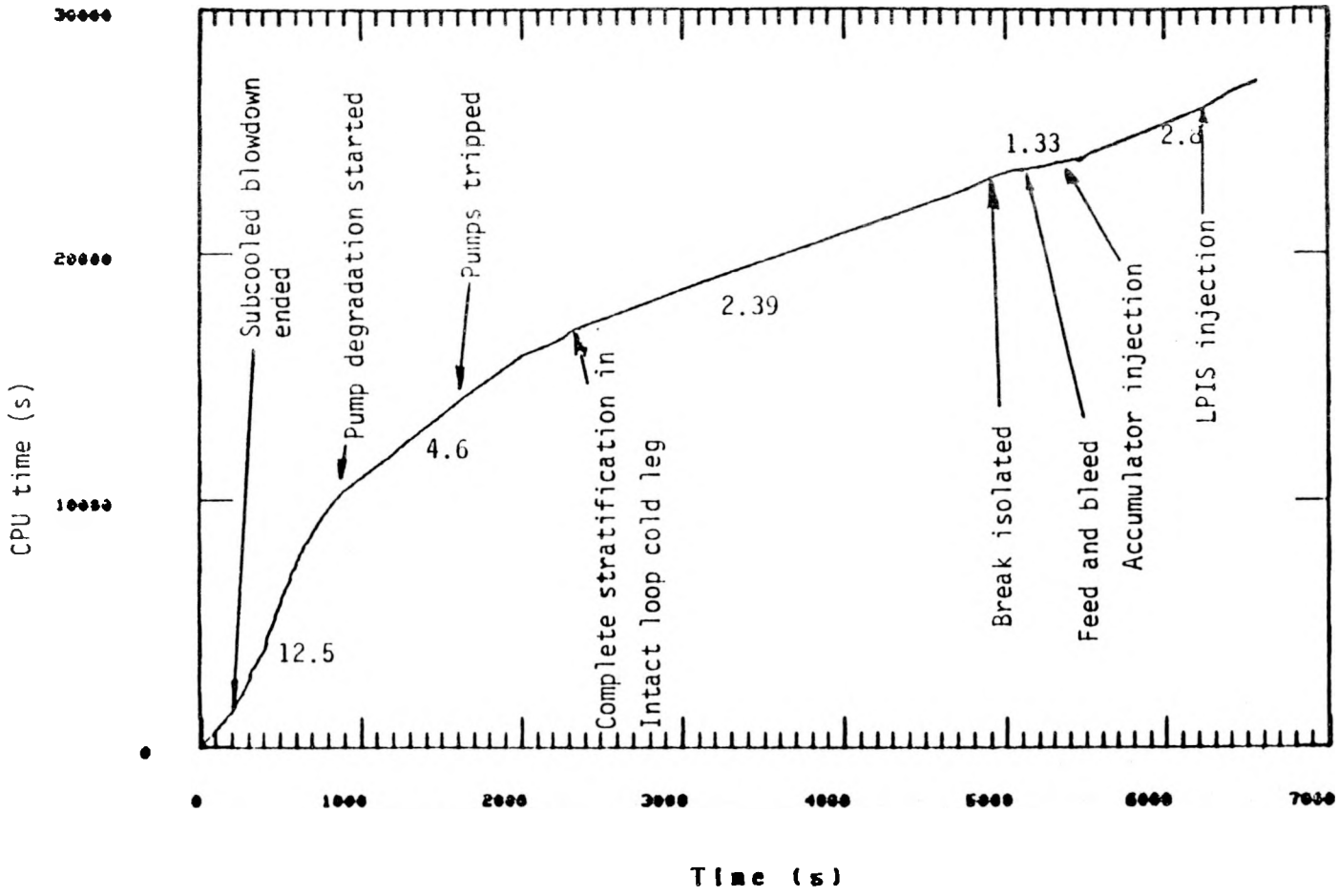


Figure 52 . CPU time versus transient time and required CPU seconds per real second

APPENDIX A

## SYSTEM CONFIGURATION

The LOFT facility was designed to simulate the major components and system responses of a commercial pressurized water reactor (PWR) during a LOCA. The experimental assembly includes five major subsystems which have been instrumented such that system variables can be measured and recorded during a LOCA simulation. The subsystems include the reactor vessel, the intact loop, the broken loop, the blowdown suppression system (BST), and the ECC systems. Complete information on the LOFT systems is provide in Reference A-1 and a discussion of the LOFT scaling philosophy is provided in Reference A-2. details of LOFT measurement capability and its instrumentation can be found in Reference A-1.

The arrangement of the major LOFT components is shown in Figures A-1. The intact loop simulated three loops of a commercial four-loop PWR and contains a steam generator, two primary coolant pumps in parallel, a pressurizer, a Venturi flowmeter, and connecting piping. A spool piece was connected to the intact loop cold leg downstream of the pump discharge. A schematic of the break piping and nozzle configuration is shown in Figure A-2. The break piping provided the break path during the blowdown. This line was closed when the maximum temperature in the core reached 977 K.

The broken loop consists of a hot leg and a cold leg, each of which are connected to the reactor vessel. The broken loop hot leg also contains a simulated steam generator and a simulated pump. These simulators have hydraulic orifice plate assemblies which have similar (passive) resistances to flow as an active steam generator. Both of the legs have quick opening and isolation valves. During Experiment LP-SB-3, these valves remained closed because the break was in the intact loop cold leg

The two LOFT ECC systems are capable of simulating the emergency injection of a commercial PWR. They each consists of an accumulator, a high-pressure injection system, and a low pressure injection system.

During Experiment LP-SB-3, the high pressure injection system was not used. Accumulator "A" was used to inject a volume scaled amount of liquid to represent the liquid volume of three accumulators in the reference three-loop PWR.

The LOFT steam generator, located in the intact loop, is a vertical U-tube design steam generator. The main steam valve is automatically regulates the secondary side pressure within given limits.

The reactor contains 1300 unpressurized fuel rods in five square (15 by 15 assemblies) and four triangular (containing 78 fuel rods) corner fuel modules, shown in Figure A-3 and described in Reference A-1. The center fuel module is highly instrumented. Two of the corner and one of the square assemblies are not instrumented. The fuel rods have an active length of 1.67 m and an outside diameter of 10.72 mm.

## A-1 References


A-1. D. L. Reeder, LOFT System and Test Description, NUREG-CR-0247. TREE-1208, July 1978.

A-2. L. J. Ybarondo et al., Examination of LOFT Scaling, 74-WA-HT-53. Proceeding of the Winter Meeting of American Society of Mechanical Engineers, New York, November 1974, CONF-741104.

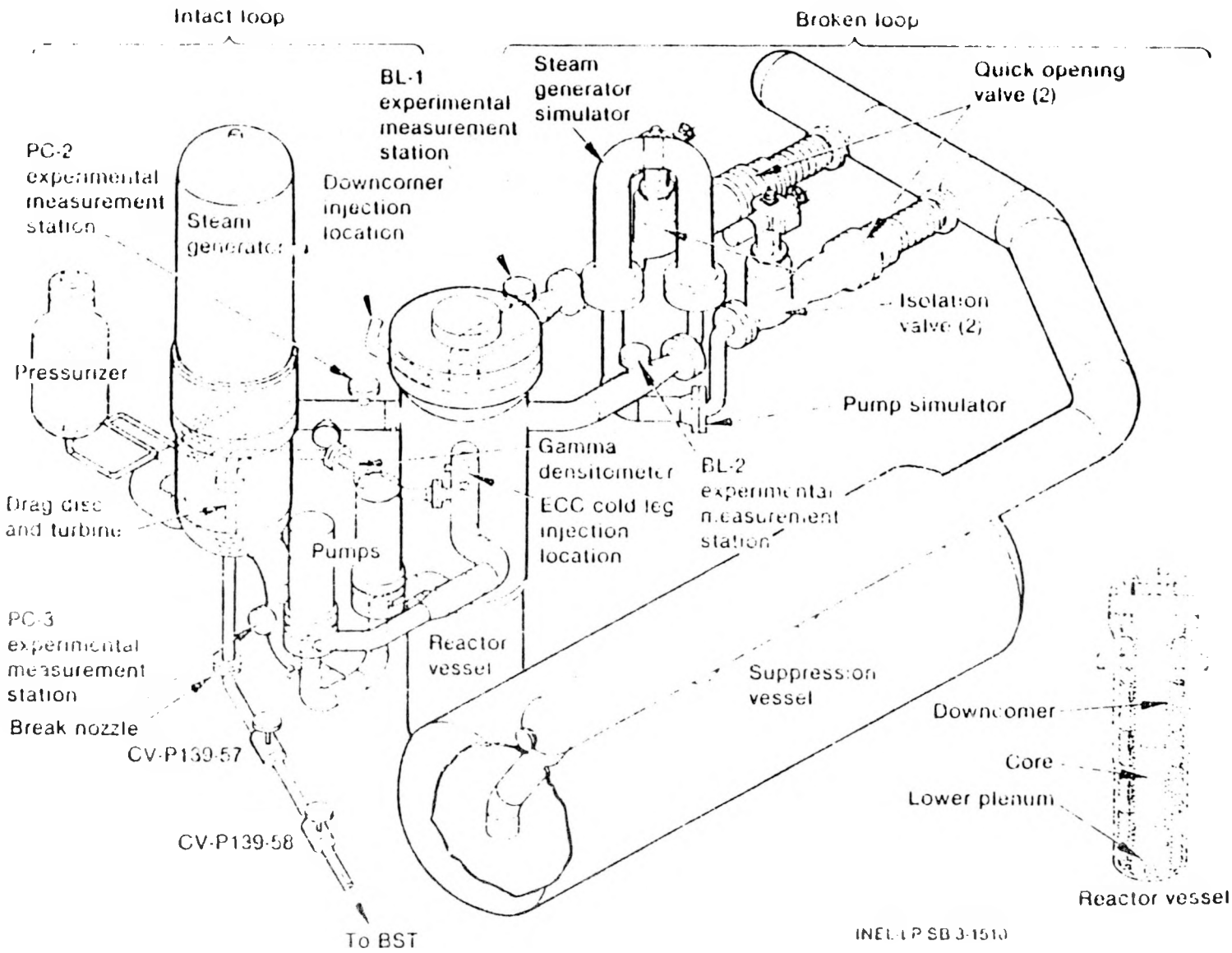


Figure A-1. LOFT configuration for cold leg intact loop small break LP-SB-3

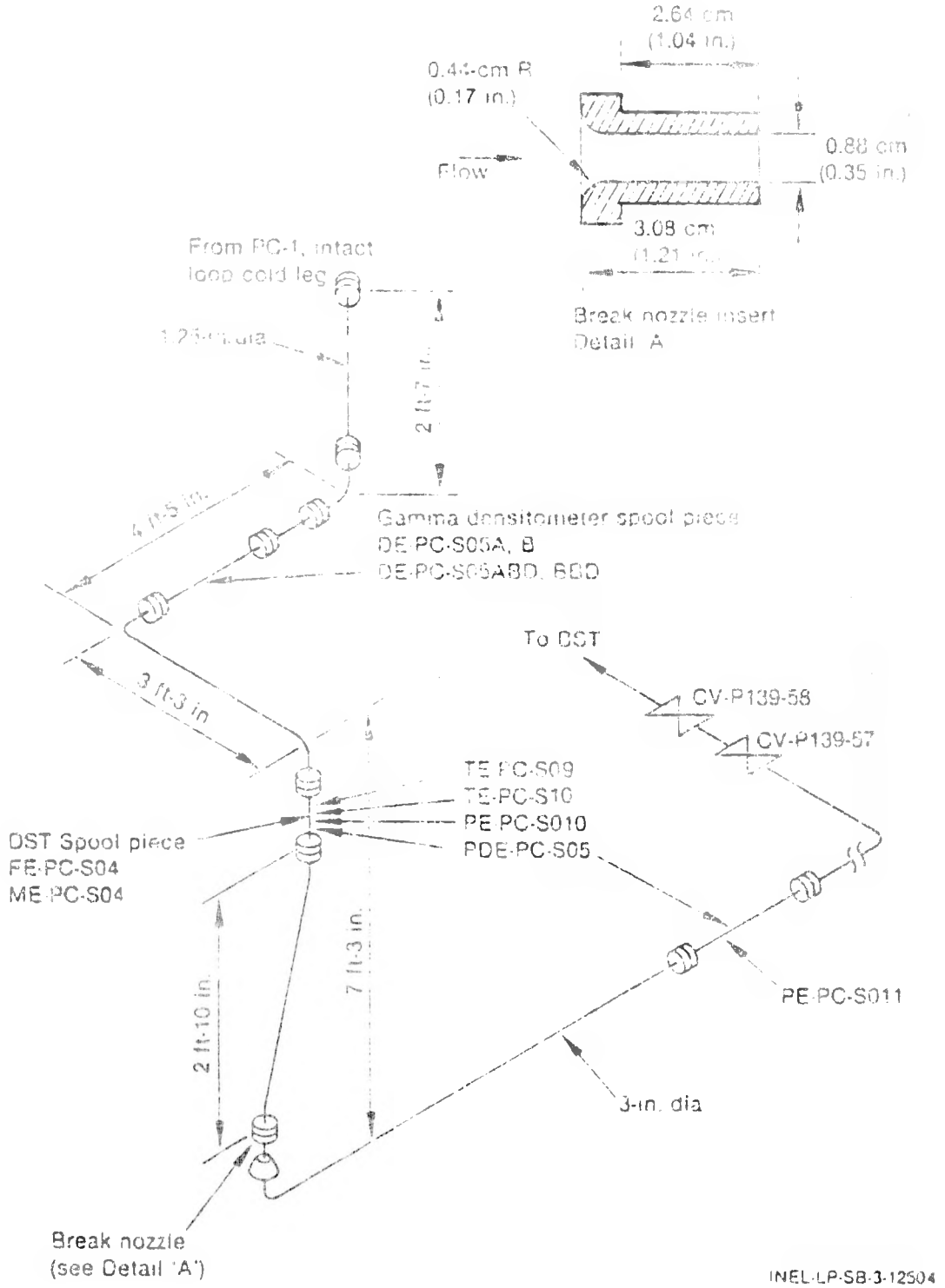


Figure A-2. Experiment break piping instrument configuration.

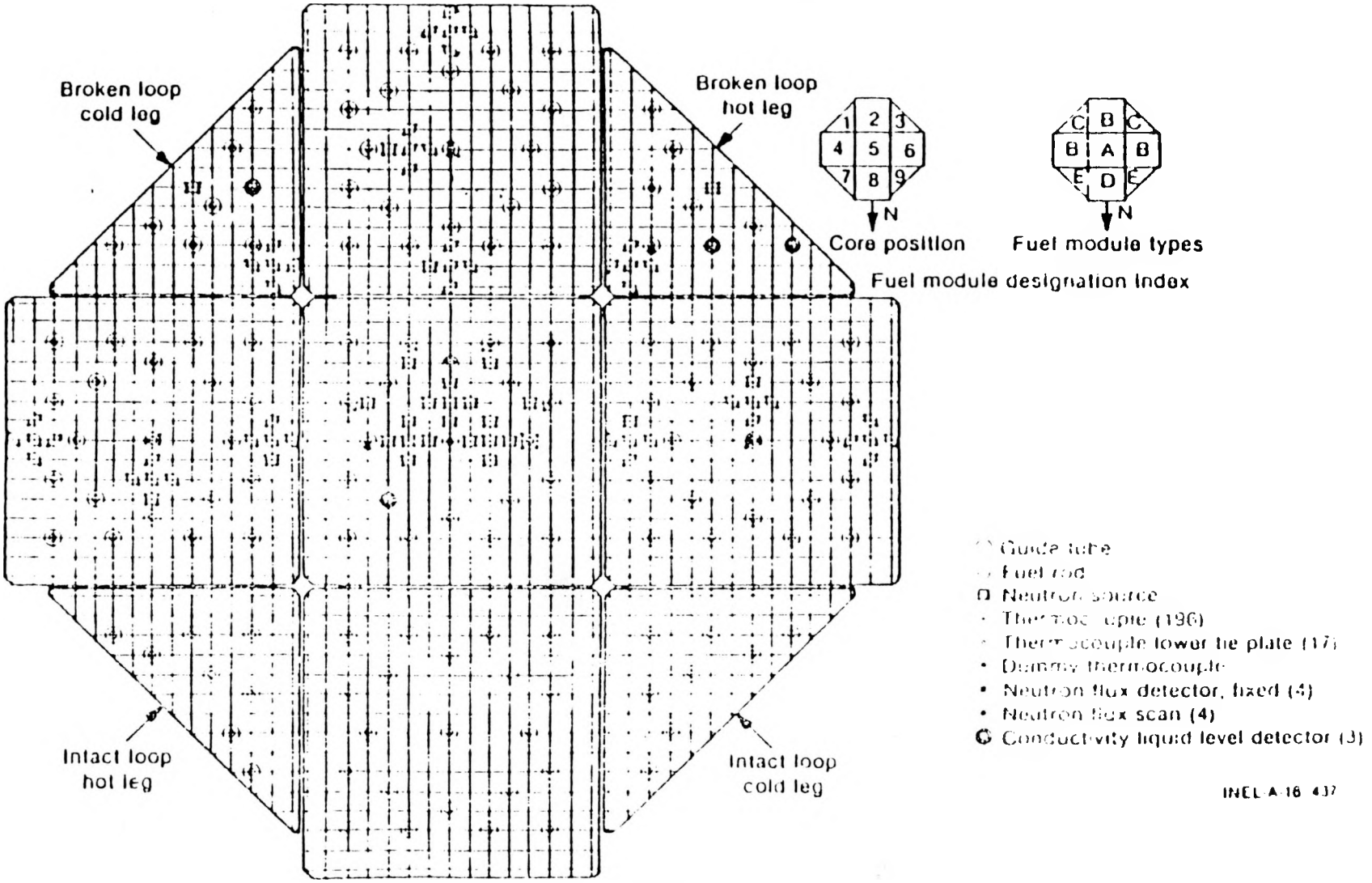


Figure A-3. LOFT Core Configuration and Instrumentation

NRC FORM 335 (2 84) NRCM 1102, 3201, 3202

U.S. NUCLEAR REGULATORY COMMISSION

**BIBLIOGRAPHIC DATA SHEET**

SEE INSTRUCTIONS ON THE REVERSE

1 REPORT NUMBER (Assigned by TIDC, add Vol. No., if any)
NUREG/IA-0018

2 TITLE AND SUBTITLE
RELAP5/MOD2 Assessment, OECD-LOFT Small Break Experiment LP-SB-3

3 LEAVE BLANK

4 DATE REPORT COMPLETED
MONTH: February YEAR: 1986

5 AUTHOR(S)
S. Guntay

6 DATE REPORT ISSUED
MONTH: April YEAR: 1990

7 PERFORMING ORGANIZATION NAME AND MAILING ADDRESS (Include Zip Code)
EIR
CH-5303 Wurenlingen
Switzerland

8 PROJECT/TASK/WORK UNIT NUMBER

9 FIN OR GRANT NUMBER
A6827

10 SPONSORING ORGANIZATION NAME AND MAILING ADDRESS (Include Zip Code)
Office of Nuclear Regulatory Research
U.S. Nuclear Regulatory Commission
Washington, DC 20555

11a TYPE OF REPORT
Technical Report

b PERIOD COVERED (Inclusive dates)

12 SUPPLEMENTARY NOTES

13 ABSTRACT (200 words or less)

An analysis of the experimental results and post-test calculations using RELAP5/MOD2 carried out for OECD-LOFT small break experiment LP-SB-3 are presented. Experiment LP-SB-3 was conducted on March 5, 1984 in the Loss-of-Fluid Test (LOFT) facility located at the Idaho National Engineering Laboratory (INEL). The experiment simulated a small cold leg break, with concurrent loss of high pressure injection system, and cooldown and recovery by feed and bleed of the steam generator secondary side and accumulator injection respectively.

This report documents a short post-test analysis of the experiment emphasizing the results of additional analysis performed during the course of this task. RELAP5/MOD2 input model and results of the post-test calculation are documented. Included in the report is the results of a sensitivity analysis which show the predicted thermal-hydraulic response to a different input model.

14 DOCUMENT ANALYSIS - a KEYWORDS/DESCRIPTORS
RELAP5/MOD2, ICAP Program, Small Break LOCA, LOFT

b IDENTIFIERS/OPEN-ENDED TERMS

15 AVAILABILITY STATEMENT
Unlimited

16 SECURITY CLASSIFICATION
(This page) Unclassified
(This report) Unclassified

17 NUMBER OF PAGES

18 PRICE

UNITED STATES
NUCLEAR REGULATORY COMMISSION
WASHINGTON, D.C. 20555